

Synthesis of Nitrogen-Carbon-Nitrogen-Boron (NCNB) and Nitrogen-Boron-Nitrogen (NBN) Zwitterions via a Multicomponent Reaction



MPhil
(Master of Philosophy)
University of Cardiff

Diem Dong-Min, LEE

Cardiff

2018-2020

Acknowledgements

First of all, I would like to express my sincere gratitude to my supervisor *Prof. Davide Bonifazi*, for providing the opportunity to start my post-graduate studies in an international scientific environment. I will never forget your strong belief in my potential and your bold decision in accepting me into your group. It has been an honour to study under your supervision.

Special thanks to *Dr. Jacopo Dosso*. I am quite lucky to have had your guidance during my BN chemistry training. You have also shown me how to live an exemplary life as a chemist, which will be a good indicator for my future postgraduate life.

Great thanks to *Dr. Grazia Bezzu* for your assistance. Thanks for the helpful comments and for spending your precious time in reading and correcting my thesis.

Tremendous thanks to all the members of the Bonifazi's group who made this unbelievable experience. Firstly, I am thankful to *Dr. Antoine Stopin, Dr. Andrey Berezin, Dr. Cataldo Valentini, Dr. Nicolas Biot, Tommaso Battisti, Olivia Matuszewska, and Jack Fletcher-Charles* for the time they spent and the helps provided. I cannot skip my special colleagues *André Oliveira Sequeira* and *Stavroula-Melina Sakellakou*. You have led me to this moment by providing positive energy and helped me first when I was struggling with the preparation of my abroad placement. I am deeply thankful to *Deborah Romito*, for not only helping with the measurement of crystal structures but also her infinite kindness. Furthermore, to our previous group members *Francesco Fasano, Tanja Miletic* and *Rodolfo Tondo*, the time we spent together cannot be forgotten.

Many thanks to *Prof. A. Jorge Parola*, from the INFUSION program in FCT, Lisbon, Portugal, for having me as a secondment student. Muito obrigado!

Also, my abroad challenge could not have been accomplished without *William Greves, Jonathan Harding, Tom Hardwick, Alex Jones* and *Flo Sutherland Howard* who are my fantastic undergraduate alumni from Cardiff University.

Thank you *Ye-Damm Cho* for your all supports. Ich danke Ihnen noch einmal!

Also special thanks to *Eun-Hee, Kim* and *Wook-Hee, Cho* for always supporting my decisions.

Finally, I would like to pay my special regards to my family *Gi-Jun Lee, Eun-A Kim* and *Seon-Min Lee*. I am thankful for your absolute and invaluable support and encouragement that motivated me throughout this abroad study.

Abbreviations

| | |
|--------------------|-------------------------------------|
| Å | Angstrom |
| AlCl ₃ | Aluminium chloride |
| BCl ₃ | Boron trichloride |
| BBr ₃ | Boron tribromide |
| b.p | Boiling point |
| °C | Degree centigrade (0 °C = 273.16 K) |
| CDCl ₃ | Deuterated chloroform |
| CH ₃ CN | Acetonitrile |
| CHCl ₃ | Chloroform |
| cm | Centimetre |
| CVD | Chemical vapour deposition |
| DCM | Dichloromethane |
| DHPMs | Dihydropyrimidinones |
| DFT | Density Functional Theory |
| eq. | Equivalent |
| ESI | Electrospray ionisation |
| EtOAc | Ethyl acetate |
| fpt | Freeze-pump-thaw |
| h | Hours |
| HBBNC | Hexa-peri-hexabenzoborazinocoronene |
| HBC | Hexa-peri-hexabenzocoronene |
| H ₂ O | Water |

| | |
|-------------------|------------------------------------|
| HOMO | Highest occupied molecular orbital |
| HR-MS | High resolution mass spectrometry |
| Hz | Hertz |
| IR | Infra-red |
| J | Coupling constant |
| K | Kelvin |
| KOH | Potassium hydroxide |
| LR-MS | Low resolution mass spectrometry |
| LUMO | Lowest occupied molecular orbital |
| MCRs | Multicomponent reactions |
| MeOH | Methanol |
| MeLi | Methyl Lithium |
| MesBr | 2-Bromomesitylene |
| MesLi | Mesityl lithium |
| MgSO ₄ | Magnesium sulphate |
| MHz | Mega-hertz |
| μm | Micro-meter |
| min | Minutes |
| mm | Millimetre |
| mp | Melting point |
| MS | Mass spectrometry |
| <i>n</i> -BuLi | <i>n</i> -Butyllithium |
| nm | Nanometre |
| NMR | Nuclear magnetic resonance |

| | |
|--------------------|--|
| NOE | Nuclear overhauser effect |
| NOESY | Nuclear overhauser effect spectroscopy |
| PAH | Polycyclic aromatic hydrocarbon |
| PhBCl ₂ | Phenylboron dichloride |
| PhLi | Phenyl Lithium |
| PhCN | Benzonitrile |
| PrCN | Butyronitrile |
| PXX | <i>peri</i> -Xanthenoxanthene |
| rds | Rate-determining step |
| r.t. | Room temperature |
| THF | Tetrahydrofuran |
| TLC | Thin layer chromatography |
| TMS | Tetramethylsilane |
| UV-Vis | Ultraviolet-visible |

Abstract

Graphene is considered one of the most promising materials in modern industry. However, the absence of a band gap in graphene critically hinders its application in the field of semiconductors. In order to overcome this drawback, extensive research has been undertaken to fabricate graphene-like materials that possess a band gap. In this context, the development of Boron-Nitrogen doped polycyclic aromatic hydrocarbons (PAHs) with the aim of producing graphene-like semiconducting materials is one of the most widely studied areas in organic chemistry. This high interest towards these BN doped molecules derives from the fact that both computational and experimental studies proved BN doping to be an efficient method to finely tune the HOMO-LUMO gap of organic molecules. As a result, various synthetic routes for BN doped PAHs have been researched. Nevertheless, efficient methods for the synthesis of BN doped systems are needed as currently they are obtained in low yields by multi-stage synthetic strategies. Therefore, this project proposes a simpler potential synthetic route for this kind of materials via a multicomponent reaction. (Figure A.1)

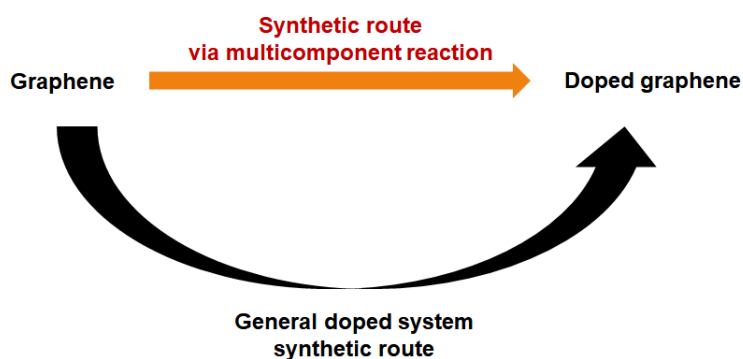
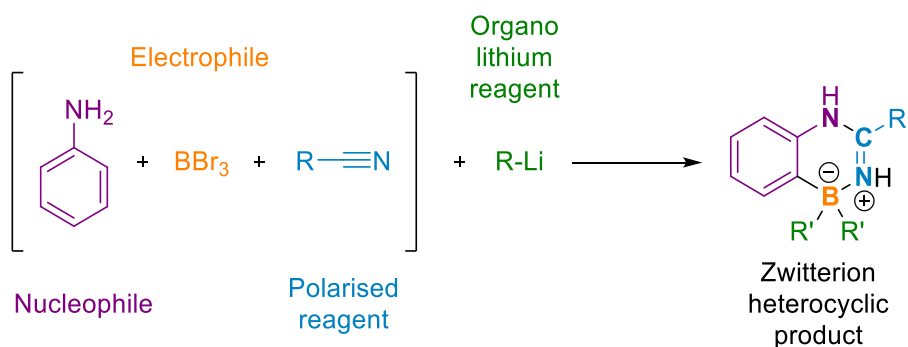


Figure A.1. A new idea for reaching to 'Doped graphene' from 'Graphene' via multicomponent reaction, solving the synthetical challenge of finding a general doped system synthetic route.

The work described in this thesis focuses on the development of a potential new synthetic pathway for BN doped molecules with the final aim of its exploitation for graphene doping. The first chapter delivers a brief introduction

to graphene doping especially focused on the concept of 'BN doping', followed by a short description of some examples of multicomponent reactions such as the Biginelli and Ugi reactions. Finally, the Sugasawa reaction is described as it constitutes a sort of starting point for this work. In chapter 2, through the introduction of a previously studied reaction from the Bonifazi group, we report our investigation of a proposed multicomponent reaction that can help in finding a possible solution for the synthetic challenge of graphene doped systems. Chapter 3 addresses the initial investigation of the feasibility of reagents bearing functional groups such as carbonyl and nitrile for the proposed one-pot process. This chapter then describes how nitrile reagents could take part in the reaction leading to the formation of two different combinations of heteroatoms (NCNB and NBN) in the newly formed heterocycles in the products with a Zwitterion.



Scheme A.1. Optimised the multicomponent synthesis reaction in the thesis.

Chapter 4 presents our attempts to optimise the one-pot synthesis process. In chapter 5, the investigation of the new multicomponent reaction with different starting reagents is summarised. In this summary, three different conditions of reactions are highlighted. Lastly, in chapter 6, all the information of the experimental details is reported to support all the scientific work that was done in this project.

Contents

| | |
|--|------------------------|
| Declaration..... | 오류! 책갈피가 정의되어 있지 않습니다. |
| Acknowledgements..... | III |
| Abbreviations..... | VII |
| Abstract..... | XIII |
| Chapter 1 – Introduction..... | 1 |
| 1.1 General introduction to the doping of graphene..... | 1 |
| 1.1.1 Graphene and graphene doping..... | 1 |
| 1.1.2 Heteroatom doping..... | 1 |
| 1.1.3. Concept of BN doping with HBBNC..... | 2 |
| 1.2. Properties of the BN based materials..... | 4 |
| 1.2.1. BN based unit (Azaborines)..... | 4 |
| 1.2.2. BN based unit (Borazines)..... | 5 |
| 1.3 Synthetical study of BN doping system..... | 6 |
| 1.4. Multicomponent reaction..... | 8 |
| 1.4.1. Ugi reaction..... | 8 |
| 1.4.2. Biginelli reaction..... | 11 |
| 1.5. Sugasawa reaction..... | 13 |
| Chapter 2 – Aim of the project..... | 15 |
| 2.1. Previous research on the multicomponent reaction towards NBO heterocyclic compounds from the Bonifazi group..... | 15 |
| 2.2. Investigations of the reaction conditions to build a new heterocyclic forming multicomponent reaction..... | 17 |
| 2.3. Study of the new multicomponent reaction..... | 18 |
| Chapter 3 First stage: Initial investigation on feasible functional groups for the proposed one-pot process synthesis..... | 19 |
| 3.1. Investigation of ketones (cyclohexanone) as the potential polarised heteroatom source in the reaction..... | 21 |
| 3.2. Investigation of nitriles (benzotrile) as the potential polarised heteroatom source in the reaction..... | 23 |
| 3.3. Investigation of aldehydes (3-perylenecarboxaldehyde) as the potential | |

| | |
|---|----|
| polarised heteroatom source in the reaction..... | 27 |
| 3.4. Overall results and conclusion..... | 29 |
| Chapter 4 - Second stage: Building-on previous results and the one-pot synthesis process modification | 31 |
| 4.1. A retrosynthetic pathway for the proposed multicomponent reaction. | 32 |
| 4.2. Multicomponent reaction modification | 33 |
| 4.3. Overall results and conclusion..... | 40 |
| Chapter 5 – Third stage: Exploration of the multicomponent reaction..... | 41 |
| 5.1. Exploring the reaction with different amino nucleophiles | 41 |
| 5.2. Exploring the reaction with different types of nitrile substituted reagents | 44 |
| 5.3. Exploring the reaction with different types of lithiation reagents | 47 |
| 5.4. Conclusion of the exploration stage | 55 |
| References..... | 58 |
| Chapter 6 - Experimental section..... | 62 |
| 6.1. General remarks..... | 62 |
| 6.1.1 Instrumentation..... | 62 |
| 6.1.2 Material and methods | 63 |
| 6.2. Experiment details | 65 |
| 6.2.1. Synthesis of the diphenyl diazaborinine 7a or 7b | 65 |
| 6.2.2. Synthesis of the phenyl diazaborininol 8c or 8d | 66 |
| 6.2.3. Synthesis of the dibutyl phenyl dihydro diazaborinine 11b | 67 |
| 6.2.4. Synthesis of the dibutyl methyl dihydro diazaborinine 13 | 68 |
| 6.2.5. Synthesis of the dibutyl methyl dihydro naphthodiazaborinine 20a or 20b | 69 |
| 6.2.6. Synthesis of the dibutyl propyl dihydro diazaborinine 21a or 21b.. | 70 |
| 6.2.7. Synthesis of the trimethyl dihydro diazaborinine 22 | 71 |
| 6.2.8. Synthesis of the methyl diphenyl dihydro diazaborinine 23 | 72 |

| | |
|---|----|
| 6.3. NMR-HRMS spectroscopic characterization (^1H , ^{13}C , ^{11}B , LRMS, HRMS) | 73 |
| 6.4. X-ray data | 88 |

Chapter 1 – Introduction

1.1 General introduction to the doping of graphene

1.1.1 Graphene and graphene doping

Graphene is an exceptionally attractive material due to its unique physical properties and the variety of potential applications in catalysis, electronics, energy conversion and storage.^{1,2} Nevertheless, the lack of an intrinsic band gap in graphene limits its application as a semiconductor.³ In order to overcome this drawback, extensive research has been undertaken to fabricate graphene-like materials that possess a band gap and a widely explored way is the graphene doping. This graphene doping can be classified into two different types: electrical and chemical doping.⁴ Electrical doping is applied by converting the gate voltages of graphene devices. The change in the gate voltage generates an electrostatic potential difference between the graphene and the gate electrode. The produced electrostatic potential increases the amount of charge carriers and modifies the band structures in the graphene materials by changing the Fermi level.^{4,5} While electrical doping is a physical process that does not change the lattice structure, chemical doping is applied by heteroatom substitution or adsorption of organic and inorganic molecules into graphene layers.⁶ In particular, the substitution of carbon atoms with heteroatoms in the pristine graphene will generate both electronic and structural distortions, resulting in a significant modification of the graphene's properties.⁷

1.1.2 Heteroatom doping

Heteroatom doping is a very exciting method as it allows researchers to design graphene-like materials and tune their properties depending on the type of dopants. Studies on heteroatom doping have taken on two different approaches. Most of the research has explored using only one type of element as a dopant. For example, we can consider the heteroatom doping of a polycyclic aromatic hydrocarbon (PAH) such as PXX (*peri*-Xanthenoxanthene), where the CH in positions 6 and 12 of anthanthrene have been replaced with O atoms (Figure 1.1)

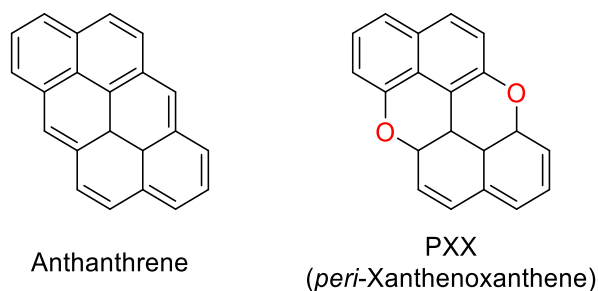


Figure 1.1. Structures of Anthanthrene and its O doped PXX.

This O-doping in PAHs has been evaluated as a versatile tool that can control various chemical properties such as the stability and self-assembly behaviours of the corresponding molecules.⁸ However, the heteroatom doping does not necessarily imply the use of a single element as the dopant like in PXX. One can also simultaneously employ different types of atoms to generate new properties or create synergistic effects. For example, B (boron) and N (nitrogen) can be used together as dopants due to their similar size and because they have opposite effects in graphene. For instance, boron, a group III element, when sp^2 hybridised will be stable in the planar structure of graphene made of carbon lattices even though the B-C bond length is different from that of C-C bonds. Nitrogen, a Group V element, has a similar bond length (C-N (1.41 Å) to that of C-C (1.42 Å)) bonds in graphene and forms planar structures, but can only form three bonds. Pyrrolic N, therefore, disrupts the planar structure of graphene due to its morphology as it prefers to be part of 5 membered rings. Furthermore, the B-N and C-C bonds are stronger than the separated B-C and N-C bonds due to the polarisation on the BN bond favouring BN co-doping.

1.1.3. Concept of BN doping with HBBNC

As can be seen in figure 1.2, an increasing number of BN sites in graphene leads to the opening of the band gap generating a semiconductor and that in the extreme case represented by h-BN where all the atoms are boron and nitrogen the band gap is so large that this material is an insulator.

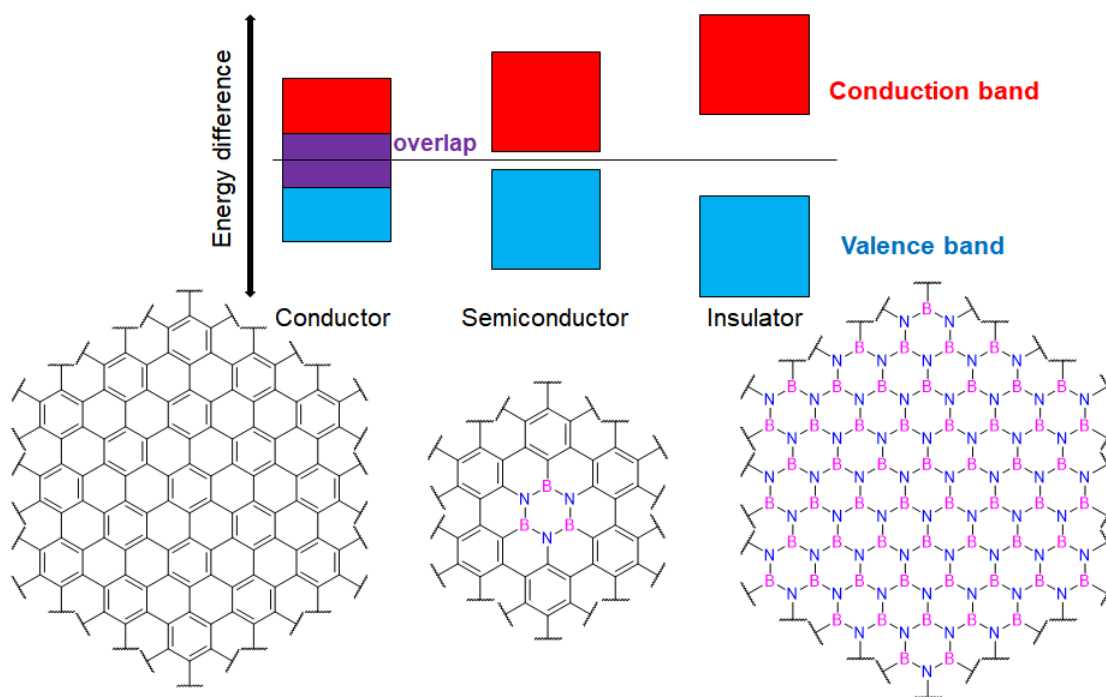


Figure 1.2. An energy bandgap diagram of a conductor (graphene), semiconductor (BN doped graphene) and an insulator (boron nitride h-BN).

Taking this into consideration, the graphene doping with borazine units should allow one to achieve semiconducting behaviour through an increase in the HOMO-LUMO gap of the BN doped material (Figure 1.2). In addition, due to the fact that B-N bonds are isostructural with C-C double bonds, this new BN doped graphene retains the pristine material morphology while also becoming a semiconductor.^{9,10} Therefore, the doping with BN systems is considered an effective strategy for opening a band gap in mono-atomic graphene layers and has potential to reach an important target by overcoming problems in the applications of graphene as a semiconductor. Hexa-*peri*-hexabenzoborazino-coronene (HBBNC **2**, Figure 1.3) is a good example in the application of BN doping of carbon materials. The HBBNC was firstly isolated through pyrolysis of a borazine precursor by Bettinger and co-workers.¹¹ Their research caused a significant change to the field, as it was the first example of a molecule of hybrid nanographene featuring controlled BN doping patterns.

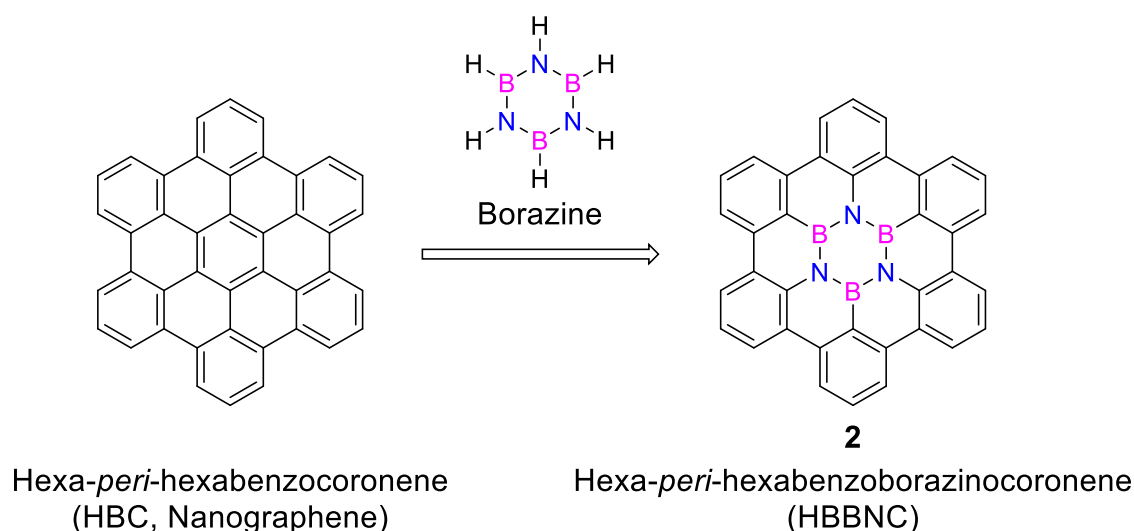


Figure 1.3. Application of borazine into graphene (HBC) to form HBBNC.

In 2017, Bonifazi and co-workers reported the synthesis of the first soluble hexa-*peri*-hexabenzoborazinocoronene (HBBNC) and its photochemical properties. The hexa-*peri*-hexabenzoborazinocoronene (HBBNC) obtained in a 5% yield from hexa-fluoroborazine by means of a C-F bond cyclisation triggered by carborane stabilised silylium ions.^{12,13} However, considering the low yield of this reaction and the high cost of the involved carborane reagent, the development of an easier pathway towards HBBNC derivatives still remains a major challenge to be addressed.

1.2. Properties of the BN based materials

1.2.1. BN based unit (Azaborines)

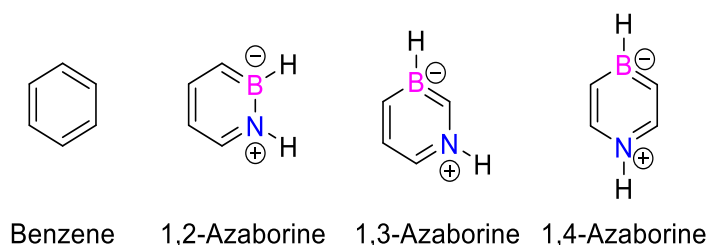


Figure 1.4. Structures of benzene and different types of azaborines.

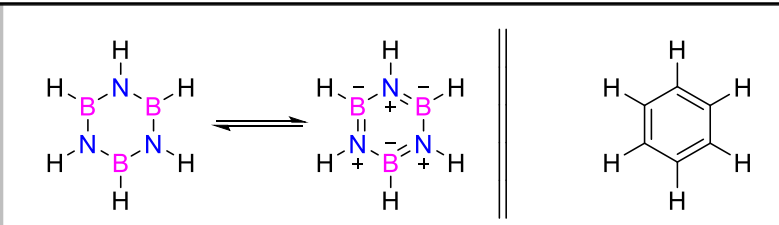
In the 1950s and 60s, Dewar and co-workers synthesised aromatic systems substituted with B-N units, increasing the interest in azaborine chemistry (Figure

1.4).¹⁴ Since Dewar and co-workers invented the azaborine chemistry, the isoelectronic relationship between C-C and B-N units has been explored. As a result of this research in azaborines, the BN doping system was founded.

1.2.2. BN based unit (Borazines)

Borazine ($B_3N_3H_6$, molecule 1, Table 1.1) is a heterocyclic ring containing only boron and nitrogen that was synthesised for the first time by Stock and Pohland in 1926.¹⁵ Borazine has been often referred to as an 'inorganic benzene' due to the fact it shares a number of structural similarities with benzene (Table 1.1).^{9,16}

Table 1.1. A comparison of the structural properties between borazine and benzene.^{17,18}

| | | |
|---|---|---|
| |  | |
| | Borazine 1 | Benzene |
| Structure | Planar hexagonal | |
| Bond length | 1.44 Å | 1.40 Å |
| Difference in electronegativity on bond | 1 ($\because 3(N) - 2(B) = 1$) | 0 ($\because 2.5(C) - 2.5(C) = 0$) |

Both molecules have a planar hexagonal structure and similar calculated bond lengths of 1.44 Å and 1.40 Å for borazine and benzene respectively.^{17,18} Furthermore, when considering the resonance form of borazine, the number of π -electrons is the same as that of benzene.¹⁹ Because of its similar structural and electronic properties with benzene and the polar character of its bonds, borazine constitutes a potentially crucial unit in organic chemistry. The borazine bonds are composed of atoms which have different electronegativities. This difference results in a partial π -character of the bond that is strongly polarised towards nitrogen atom through an electron donation from its lone pairs towards the electrophilic boron centres.

1.3 Synthetical study of BN doping system

Remarkably, a number of BN substituted polycyclic aromatic molecules have been prepared during the last decade; thus, different synthetic routes have been explored to substitute C-C bonds with B-N bonds more effectively.^{3,20} In particular, this can be seen when looking at the construction of BN doped nanographenes that essentially can be done by two quite opposite approaches. The first one is a ‘top-down’ approach which was introduced by Ajayan and co-workers who used chemical vapour deposition (CVD) to form BN doped nanographenes. (Figure 1.5)²¹

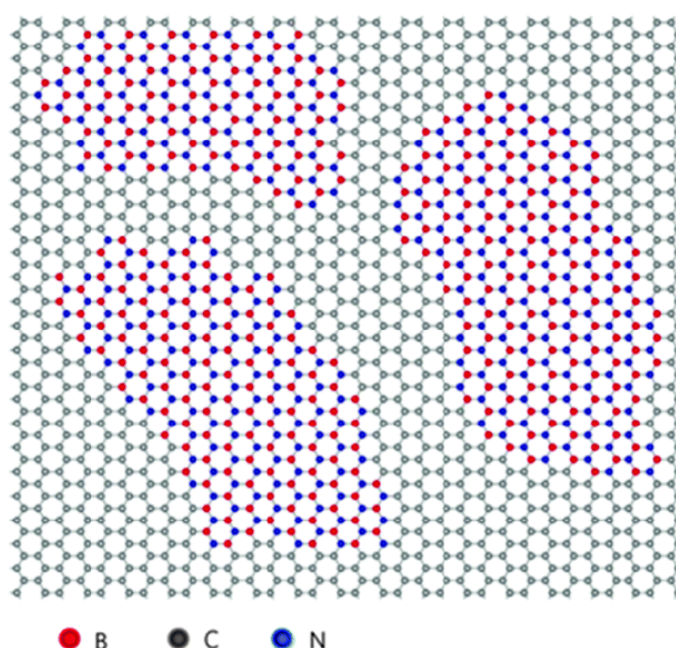
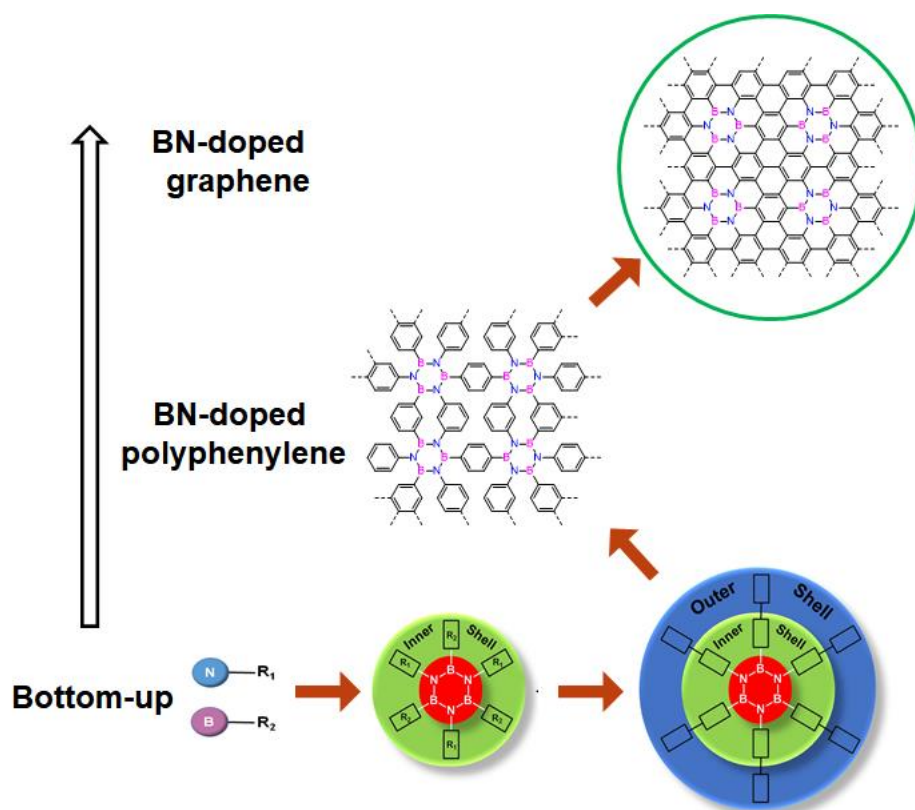


Figure 1.5. Atomic model of the BN doped graphene by using the CVD method.²¹

They reported that methane and ammonia borane were used as the carbon and BN precursors. To do this they inserted methane and ammonia borane into the reaction chamber, which was then annealed at 600 °C for 20 min under an Ar/H₂ flow and then gradually heated up to 900-1000 °C. As a result, the growth of *h*-BN graphene films was successfully carried out on metal substrates. Furthermore, they noticed that the BN-doping range could be scaled between 10% and 100% by controlling experimental conditions such as temperature, reaction time and the ratio of carbon and BN precursors. By using this system Ajayan *et al.* demonstrated that the electronic properties of BN substituted

graphene could be controlled by tuning the BN doping percentage.²¹ Nevertheless, their top-down approach still included limitations for the precise structural designing of the BN doped systems. Not only did the material consist of segregated boron nitride and graphene islands on the metal substrate but the edges of the *h*-BN graphene films were also terminated with impurities.²² These referred limitations inhibited the achievement of atomic precision and consequently resulted in low predictability of the electronic properties of these novel materials as the proportion and location of BN doping has significant effects on the mobility of the charge carriers.²³

On the other hand, a ‘bottom-up’ method (Scheme 1.1) represents the opposite alternative where the atomic/molecular components are designed and synthesised first and then assembled to develop the potential nanographene system.



Scheme 1.1. The synthetic strategy of BN doped graphene with a bottom-up approach.

This method allows for precise control of both the doping position and percentage; hence it can tackle the problems of the top-down approach. Although the bottom-up approach has a crucial disadvantage, it has not yet been developed in modern chemistry. This stepwise method requires a

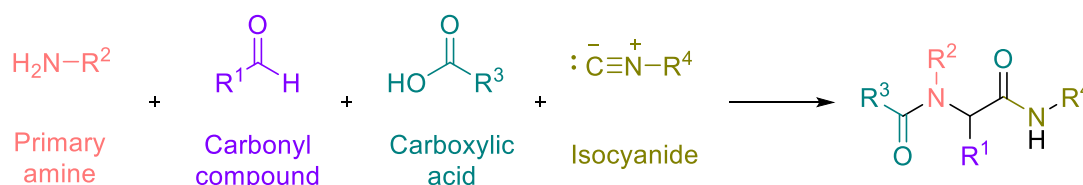
significant synthetic effort and a large amount of time. Furthermore, high yielding steps are required to achieve an efficient synthesis of the final material. Nonetheless, it still remains an attractive option due to its specific strength and potential application.

1.4. Multicomponent reaction

Multicomponent reactions (MCRs) are defined as synthetic protocols that combine three or more substrates. This MCRs create highly functionalised organic molecules under highly regio- and stereoselective conditions.²⁴ They are considered important reactions in modern chemistry as new heterocyclic compounds can be synthesised in a single step. From this point of view, we consider MCRs to be the official synthetic root for solving the synthetic challenge problem in the 'bottom-up' approach. Leading towards the synthesis of BN molecules that can be then assembled to form doped graphene materials. Therefore, in this section, we would like to explore the Ugi and Biginelli reactions as general examples of MCRs to highlight the defining properties and potential of this kind of strategy.

1.4.1. Ugi reaction

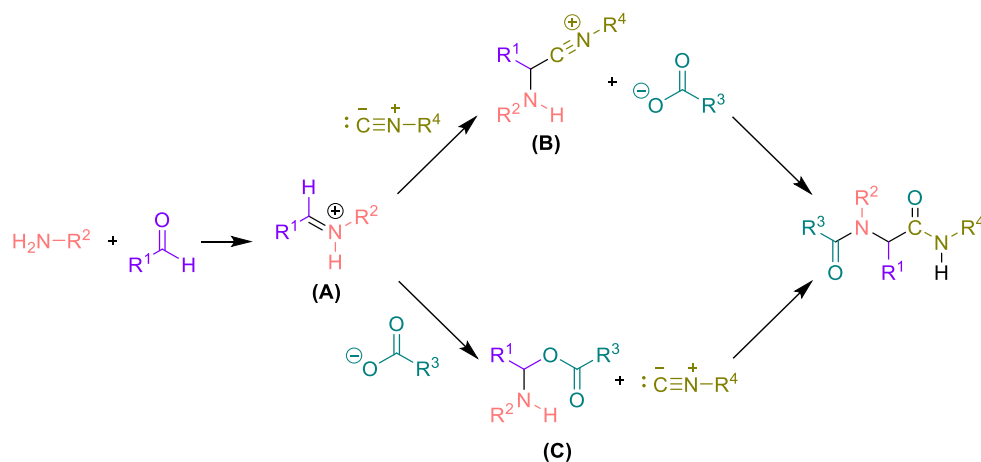
The Ugi reaction was reported by Ivar Ugi in 1959.²⁵ He discovered a one-pot process reaction involving four different components: a carbonyl, a primary amine, a carboxylic acid and an isocyanide to form α -aminoacyl amide derivatives. (Scheme 1.2).



Scheme 1.2. General scheme of the Ugi reaction.

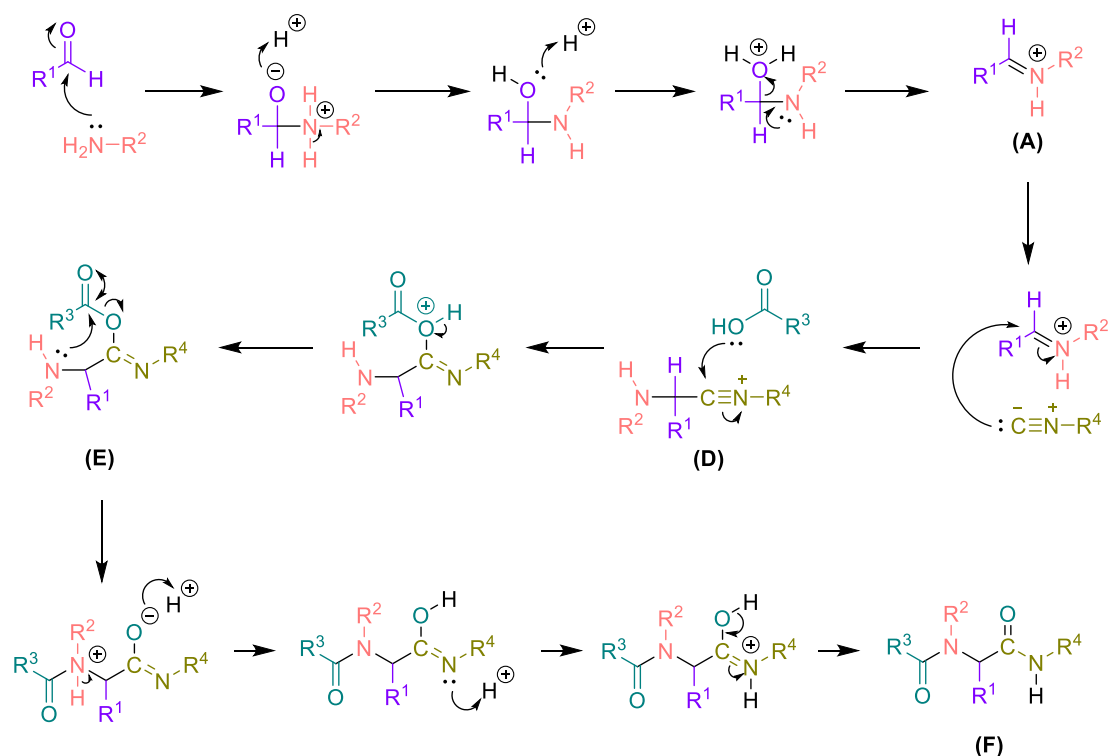
The Ugi reaction is classified as an isocyanide-based multicomponent reaction.²⁶ These kinds of reactions have been developed only within the last 20 years due to the limited accessibility of isocyanide materials and poor

knowledge of the mechanism prior to 2000.²⁷ Two possible pathways for it have been postulated and are shown below in scheme 1.3.²⁸



Scheme 1.3. Two possible pathways for the Ugi reaction.²⁸

Both pathways share the preparation of iminium ion (A). After that, the addition of either isocyanide or carboxylic acid produces different intermediates labelled here as (B) and (C) respectively. However, according to an experimental analysis by Ugi and Hack in 2012, the intermediate (B) formation pathway appears to be the correct one whereas the intermediate (C) formation pathway is considered unlikely to occur.²⁹ According to the proposed mechanism that leads to intermediate (B), the iminium ion (A, Scheme 1.4) is produced by a condensation reaction between a primary amine and a carbonyl compound with the generation of one equivalent of water. Nucleophilic addition of the isocyanide to the carbon of the iminium ion leads to the formation of a nitrilium ion intermediate (D). After that, a lone pair on the oxygen atom of the carboxylic acid attacks the carbon atom of the nitrilium ion to form the intermediate (E), which by the Mumm rearrangement forms the α -aminoacyl amide derivative (F) concluding the Ugi reaction.³⁰

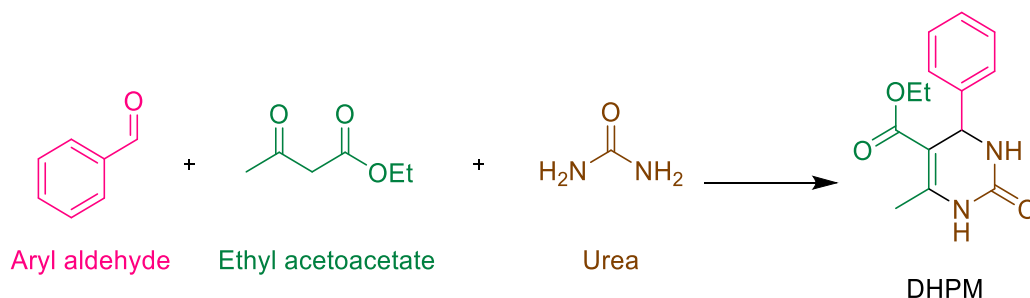


Scheme 1.4. Proposed mechanism for the Ugi reaction.³⁰

In terms of application, the Ugi reaction is a very crucial synthesis as it allows for a wide variety of substitution patterns in the products through the introduction of only simple modifications in the starting materials.³¹ Therefore, the Ugi reaction has been prominently used in the field of pharmaceutical chemistry and can be a starting point to develop new chemical reactions based on previous results allowing for the production of various new target drugs.³² This advantage is not only limited to the synthesis of drugs, but it can also be applied to natural products, as searching for an efficient synthetic route for their complex structures is also a significant challenge.³³ The development of synthetic libraries can help in reducing the use of time-consuming multi-step processes as well as leading to more efficient synthetic methods with greater output yields. Furthermore various modified Ugi reactions have been developed, with most of the modifications of Ugi products involving cyclisation to form diverse heterocyclic scaffolds.³⁴

1.4.2. Biginelli reaction

In 1893, Pietro Biginelli reported an acid-catalysed three component organic synthesis between an aldehyde, ethyl acetoacetate and urea to form dihydropyrimidone (DHPM) derivatives (Scheme 1.5).³⁵

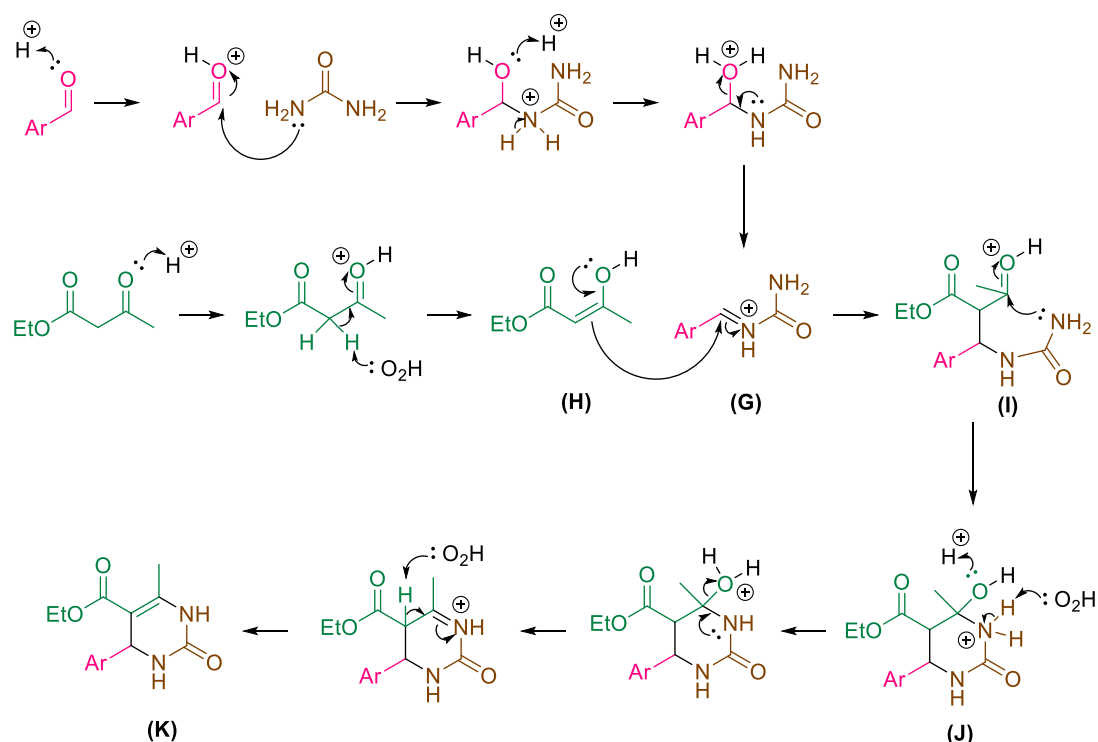


Scheme 1.5. Overview of Biginelli reaction.

Table 1.2. Three proposed routes of the Biginelli reaction.

| Route | Reagents | Intermediates | The third component |
|-------------------|----------|---------------|---------------------|
| Iminium Route | + | | |
| Enamine Route | + | | |
| Knoevenagel Route | + | | |

Since Biginelli published his reaction, several different mechanisms have been suggested such as the iminium route³⁶, the enamine route³⁷ and the Knoevenagel route³⁸ (Table 1.2). The detailed mechanism for the iminium pathway is shown in scheme 1.6. The aryl aldehyde is protonated due to the acidic conditions leading to a nucleophilic attack from the amino group of the urea.



Scheme 1.6. Iminium route mechanism for the Biginelli reaction.³⁶

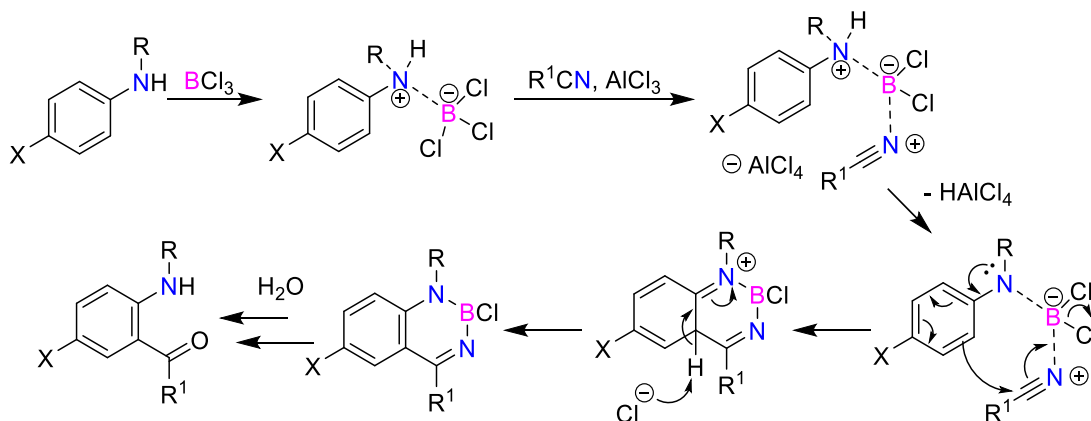
As a result of proton transfer the alcohol is protonated and loses a molecule of water, leading to the formation of an *N*-acyliminium ion intermediate (**G**). In acidic conditions the enolic form of the β -keto-ester acetoacetate (**H**) attacks the *N*-acyliminium ion intermediate to form intermediate (**I**). Another nucleophilic attack from the free amine group of the urea to the ketone carbonyl follows forming a cyclic intermediate (**J**). This cyclic intermediate is then transformed to final pyrimidone product (**K**) by loss of a molecule of water and proton transfer steps.³⁶

MCRs have been recognised to be among the most efficient tools in modern synthetic chemistry since they contribute to both saving synthetic steps and providing higher yields of the target molecules.³⁹ In addition, through the

Biginelli reaction, heterocyclic compounds can be produced with a one-pot process. However, it was also found that in the Biginelli reaction, different intermediates could be formed, with the addition order among starting reagents leading to different products.⁴⁰ Therefore, we have to consider that the fragments deriving from the starting materials could be incorporated in the final product in different combinations and different products can be obtained when we use the MCRs in synthetic chemistry.

1.5. Sugasawa reaction

The Friedel-Crafts acylation is a key organic reaction for the preparation of a variety of aromatic compounds. However, Friedel-Crafts acylation of anilines is inherently difficult due to deactivation of the resulting aromatic system by a reaction between the amino group and the Lewis acid. As a solution, a new synthetic method for *ortho*-acylation of anilines was introduced by Sugasawa in 1978. In 1994, Sugasawa proposed a new reaction which produces a nitrogen-boron-nitrogen (NBN) heteroatom ring intermediate from aniline, a nitrile reagent and two Lewis acids (BCl_3 and AlCl_3).⁴¹ This reaction was identified as a multicomponent reaction by Douglas *et al.*, who showed that the order of reactants addition was not critical to the formation of the product.⁴² Also, from further research on the Sugasawa reaction it was found that the yield of the product is affected by both the temperature⁴³ and the solvent⁴⁴ used for the reaction. In addition, Douglas *et al.* proposed a mechanism for the Sugasawa reaction by studying NMR spectra of various intermediates (Scheme 1.7).⁴³



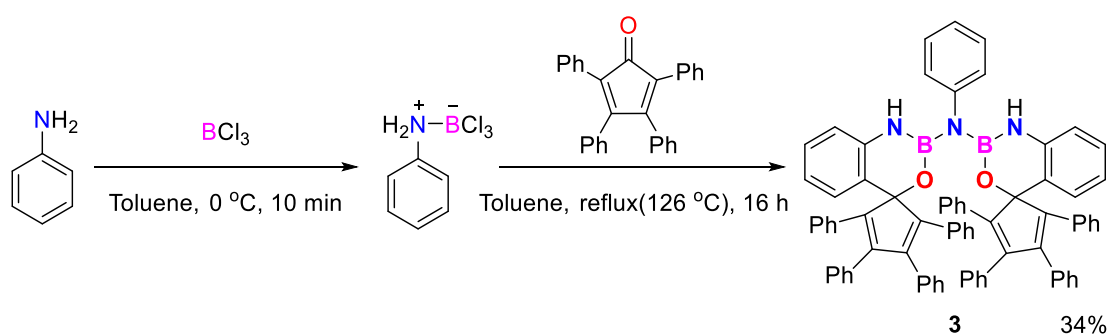
Scheme 1.7. Proposed Sugasawa reaction mechanism from A.W. Douglas.⁴²

In the reaction, a nitrile was used as an *ortho*-acylating reagent in the presence of BCl_3 and AlCl_3 . In detail, the aniline derivative reacts first with BCl_3 , as this is the stronger Lewis acid, to form a Lewis acid-base adduct. The latter then forms a “super-complex” with the nitrile, as a chloride ion is transferred from boron to AlCl_3 . After that, a cyclisation reaction occurs, forming a NBN containing heterocyclic intermediate. We took inspiration from the Sugasawa reaction, to design a potential multicomponent reaction where aniline and nitrile could be used as N bearing precursor for the formation of NBN heterocyclic compounds.

Chapter 2 – Aim of the project

2.1. Previous research on the multicomponent reaction towards NBO heterocyclic compounds from the Bonifazi group

The research group of *Prof. Bonifazi* has explored amino-borane chemistry. *Francesco Fasano* and *Maria Mercedes Lorenzo Garcia* (Cardiff University, Wales) found that NBO containing heterocycles can be formed by reacting aniline with BCl_3 and ketone derivatives (Scheme 2.1 and Scheme 2.2, Unpublished data).



Scheme 2.1. The reaction of aniline with BCl_3 and tetraphenyl cyclopentadienone.

The structure of product **3** confirmed by single-crystal X-ray diffraction analysis. (Figure 2.1)

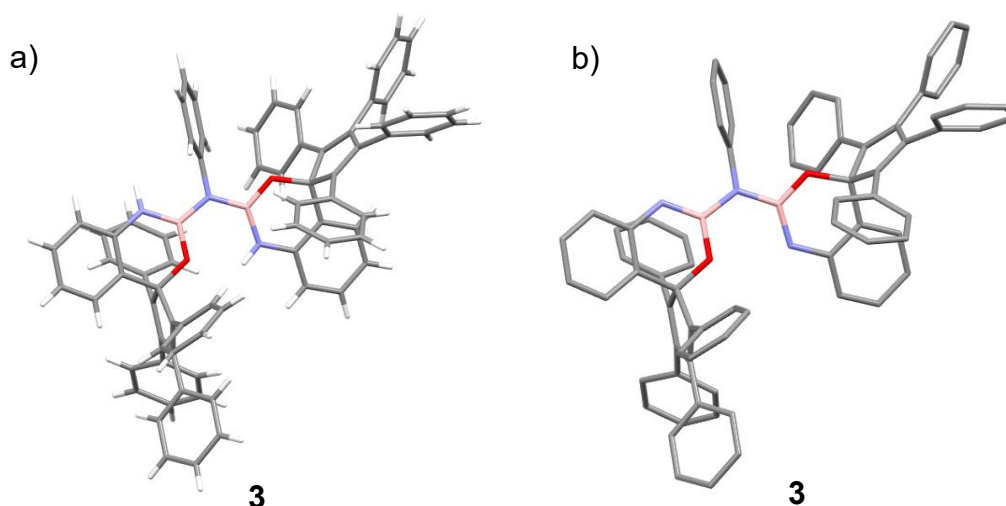
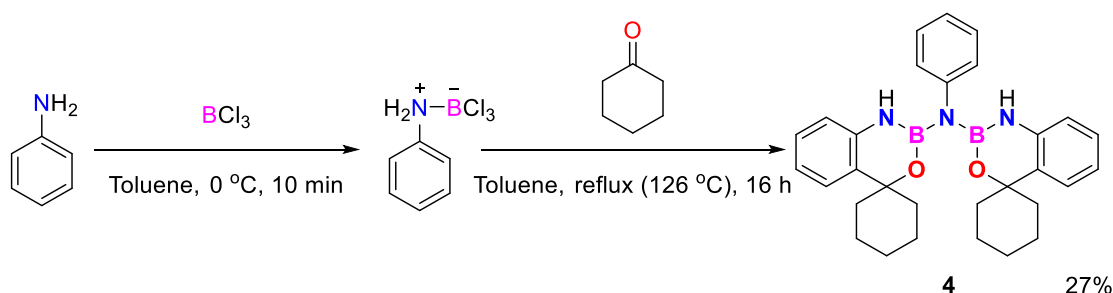


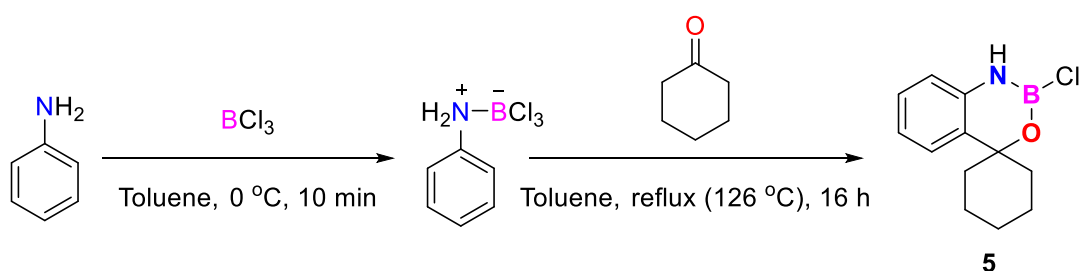
Figure 2.1. a) A capped sticks style representation of the molecular crystal structure of the product **3**. b) A capped sticks style representation of the molecular crystal structure of product **3** without hydrogen. Space group $P21/n$, R-Factor = 8.96%.

In addition, this reaction also occurred when the ketone was added prior to BCl_3 , proving that it is a one-pot process leading to the same product independent of the order of addition of the starting materials. The same protocol was used for the reaction of aniline with BCl_3 and cyclohexanone to afford the NBO heterocyclic derivative **4** with a 27% yield (Scheme 2.2).



Scheme 2.2. The reaction of aniline with BCl_3 and cyclohexanone.

An interesting point from these reactions is that both products contain two NBO heterocycles in the product. This is due to the reaction of aniline with two equivalents of BCl_3 forming two heterocycles. These can go on to further react with two more molecules of the aniline and two equivalents of the ketone and closing the rings. The products of these reactions are different from those that could be expected from a reaction proceeding in a similar manner to the Sugasawa reaction. For the Sugasawa mechanism an aniline molecule reacts with one equivalent of BCl_3 , and one ketone molecule, resulting in the formation of a single NBO heterocycle at its side (such as **5** in scheme 2.3). They are, however, still encouraging as they show a similar outcome.



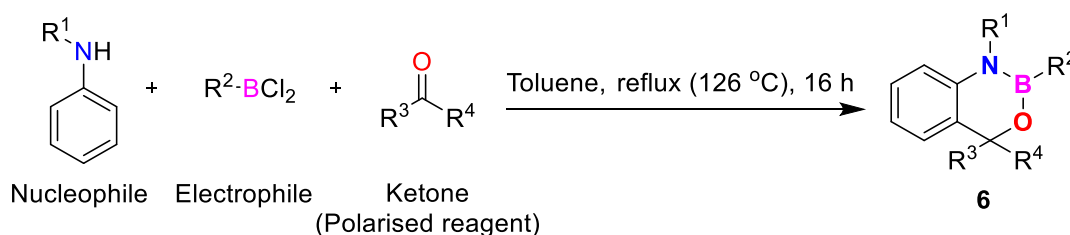
Scheme 2.3. Scheme of expected target product **5** from cyclohexanone.

Therefore, we decided to explore the potential application of this method as a multicomponent reaction to obtain compounds with a single NBO cycle such as **5** (Scheme 2.3). There are three reasons why we would like to form single NBO

products rather than one containing two NBO cycles products such as **3** and **4**. First of all, one single heterocycle in the product can allow a better understanding of its properties compared to the complicated OBNBO combination; this is a necessity before we can think of applying this chemistry to obtain molecules which can be ultimately used to produce doped graphene. Secondly, as the two oxygen atoms in products **3** or **4** are not connected, it could destroy the hexagonal lattice in a PAH or graphene when applied in the doping system. Thirdly, the presence of the chloride on the boron would allow further functionalisation in the following step, allowing for the introduction of different functionalities, for instance by the use of lithiated organometallic nucleophiles. Therefore, starting from this previous research, we want to focus our investigation on the proposed multicomponent reaction to find the conditions that lead to single heterocyclic products, such as **5**, for further potential application to prepare molecular graphene.

2.2. Investigations of the reaction conditions to build a new heterocyclic forming multicomponent reaction

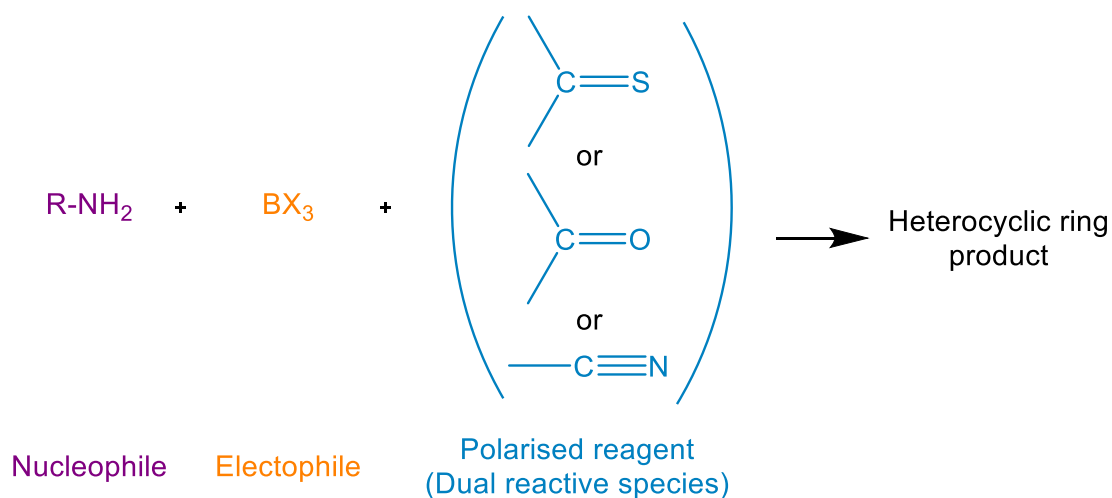
Building on the previous draft from our group, we propose to investigate the general multicomponent target reaction shown in scheme 2.3, as a new route to form heterocyclic compounds **6** containing boron, nitrogen and oxygen atoms.



Scheme 2.3. Reaction scheme of the target multicomponent reaction.

This target reaction involves an aniline (or substituted anilines) as a nucleophile and BCl_3 or substituted dichloroboranes as an electrophile. Along with ketones, other reagents containing a carbonyl group, such as aldehydes, or nitriles have been selected as the polarised reagent, so that potentially either NBO or NBN containing heterocycles could be formed.

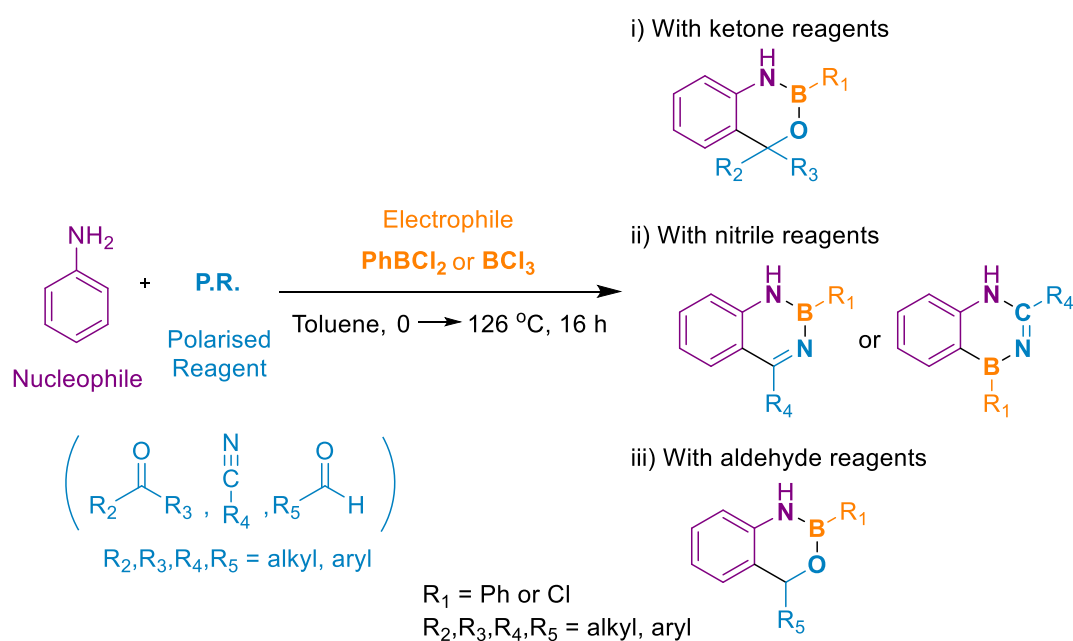
2.3. Study of the new multicomponent reaction



Scheme 2.4. Hypothesis for this project.

Based on *Chapters 2.1* and *2.2*, we can build the hypothesis shown above in scheme 2.4. Containing a nucleophile, electrophile and polarised reagent, it has the potential to generate a heteroatom-containing cyclic product. This reaction will be carried out as a one-pot process. Therefore, for the first step, we aimed to establish whether the selected functional groups led to the successful formation of the expected products in the proposed multicomponent reaction. Then we wanted to investigate the scope of the reaction by using different nucleophiles and electrophiles.

Chapter 3 First stage: Initial investigation on feasible functional groups for the proposed one-pot process synthesis.



Scheme 3.1. The one-pot process reaction for the preliminary investigation on feasible functional groups.

As mentioned in chapter 2.3, This stage was designed to investigate the reactivity of different functional groups in the proposed multicomponent reaction. Therefore, the attention was focused on understanding the reactivity of the selected functional groups in the proposed reaction conditions to establish whether they worked as a polarised heteroatom source and whether the heteroatom source leads to the expected products (Scheme 3.1).

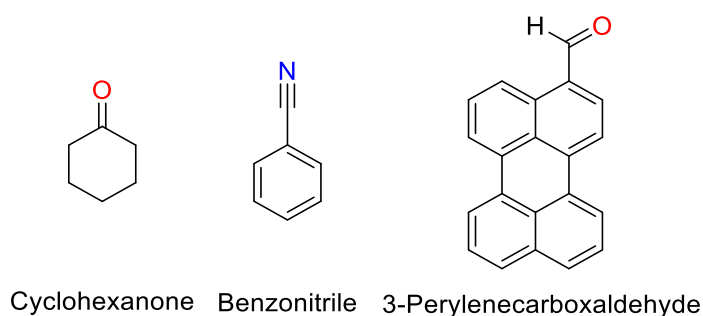


Figure 3.1. Selected reagents for the first screening of functional groups reactivity in the proposed multicomponent reaction.

To be considered good candidates as the polarised reagent source for our reaction, the selected reagents needed to bear functional groups that could not only react with a Lewis acid such as PhBCl_2 and BCl_3 , but also form NBO, NBN containing heterocycles. Based on these conditions, carbonyl and nitrile functional groups have been selected, alongside three representative reagents: Cyclohexanone, benzonitrile and 3-perylenecarboxaldehyde, chosen for our preliminary investigation (Figure 3.1). The selected reagents were investigated under the envisaged conditions in our designed one-pot synthesis with the given Lewis acids and base.

Before moving onto the investigation of what molecules could work as third components and a heteroatom source, we have to consider the possibility of formation of heterocycles with a different order of heteroatoms in their structure. As mentioned in section 1.4.2, a different reaction order among starting reagents could produce different intermediates. This diversity could generate a different relative position of the heteroatoms in the final ring. Therefore, it must be considered that this could also happen with our proposed reaction. Especially when nitrile derivatives are employed, as they can easily react with the electrophilic Lewis acids. This can be explained looking at the different possible pathways of the reaction outlined in table 3.1. In our case, when nitrile derivatives are employed as a polarised heteroatom source, two different combinations of heteroatoms in the heterocyclic product could be obtained. As shown above, if aniline reacts with the Lewis acid (BCl_3 or PhBCl_2) firstly, then the nitrile derivative reacts with the obtained intermediate. After intramolecular cyclisation and a NBN containing cycle is formed.

Table 3.1. Possible pathways for the proposed one-pot process with the nitrile reagents showing the different heteroatom combinations in the product.

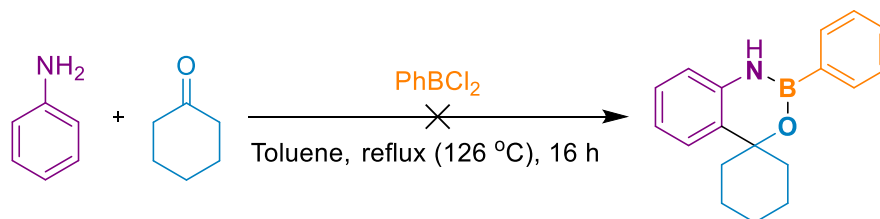
| | Initial reaction | Intermediate and second reaction | | Product |
|---|------------------|----------------------------------|---|---------|
| Pathway A (1,2-azaborine : Sugasawa like pathway) | | | → | |
| Pathway B (1,4-azaborine) | | | | |

On the other hand, if the nitrile derivative reacts with the Lewis acid (BCl_3 or PhBCl_2) forming a Lewis adduct that subsequently undergoes a nucleophilic attack by aniline, a NCNB containing ring is formed. In our study, we need to take this aspect into consideration and try to establish whether one or both products are formed from our reaction, and possibly understand what conditions favour the formation of one over the other.

3.1. Investigation of ketones (cyclohexanone) as the potential polarised heteroatom source in the reaction

As mentioned above, previous experiments by *Dr. Fasano* showed that cyclohexanone reacts with BCl_3 and aniline in a one-pot reaction forming product **4**, containing two NBO heterocycles, demonstrating the potential of the ketone group as a good candidate for our designed reaction (Scheme 2.2). From this experiment, it could be observed that aniline reacts with two equivalents of BCl_3 , and each boron reacts with a further aniline molecule and with cyclohexanone to form a final product containing two NBO heterocycles. Therefore, since we wanted to have only one heterocycle in our targeted product, PhBCl_2 was used instead of BCl_3 in the reaction with cyclohexanone to

avoid the formation of the second heterocycle (Scheme 3.2). The reaction was performed under the same experimental conditions as developed by *Francesco*.



Scheme 3.2. The reaction of the cyclohexanone with PhBCl₂ and aniline.

However, after the reaction, only a small amount of resulting mixture could be collected. Due to the low yield column chromatography did not result in complete separation during the purification step. The ¹H NMR, ¹³C NMR, ¹¹B NMR and MS of the roughly purified product were measured. Unfortunately, as shown below, the ¹H NMR spectrum did not show any evidence of the formation of the desired NBO bonding system.

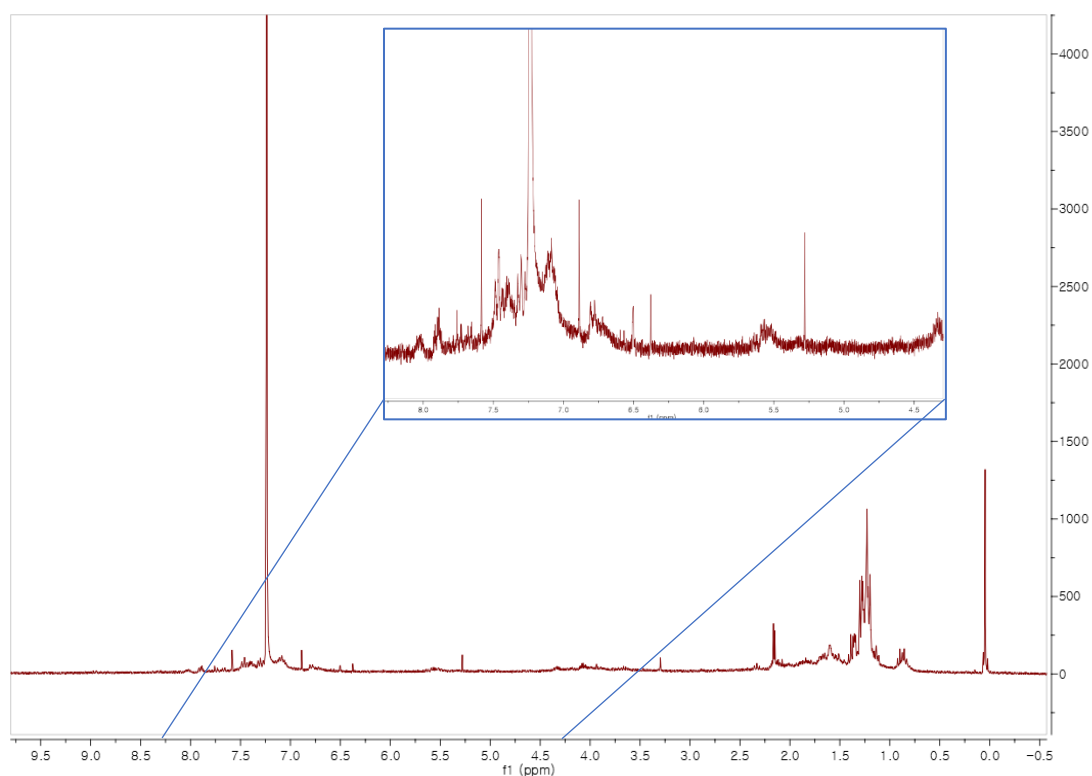


Figure 3.2. ¹H NMR data of the product resulting from the reaction scheme 3.2.

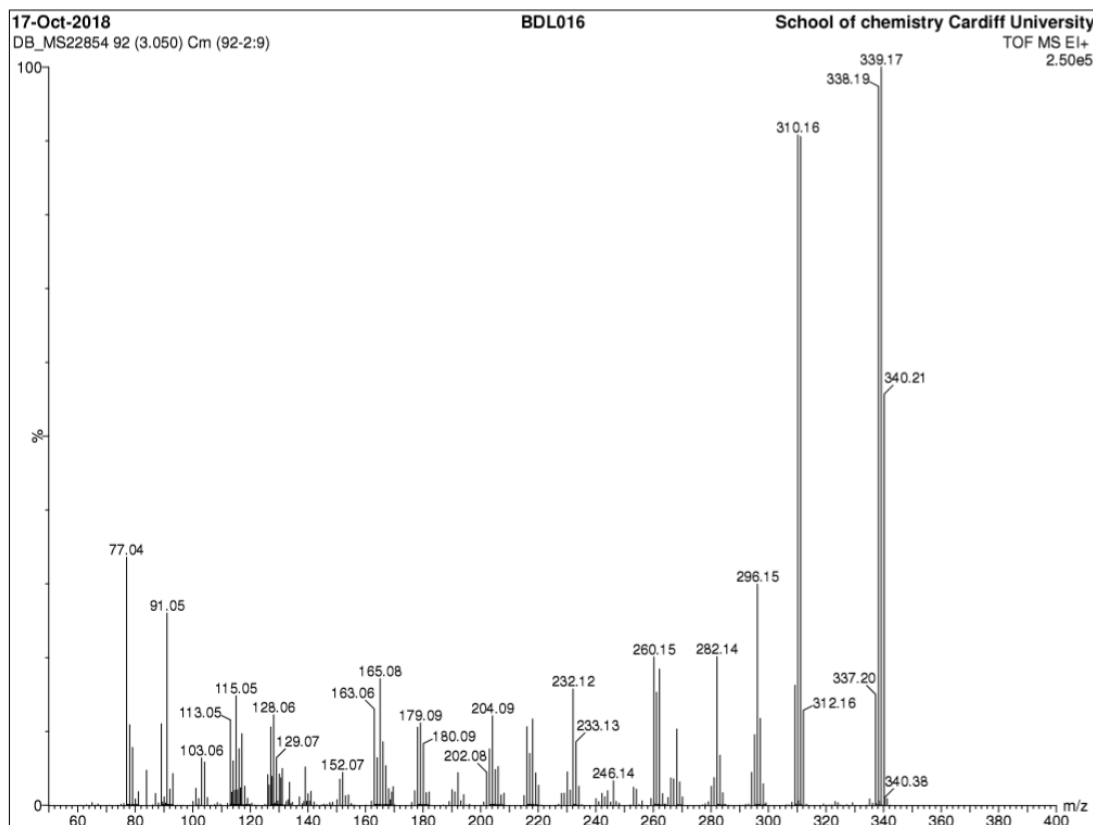
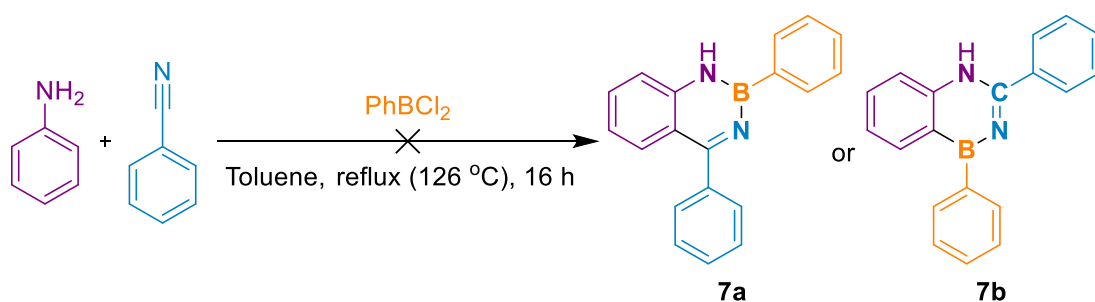


Figure 3.3. Mass spectrometry data from the product resulting from reaction scheme 3.2.

Furthermore, the resulting product could not be analysed as the quantity was too low. Therefore, it was decided to conclude this part of the research as it appears that ketone bearing reagents do not undergo the desired multicomponent reaction.

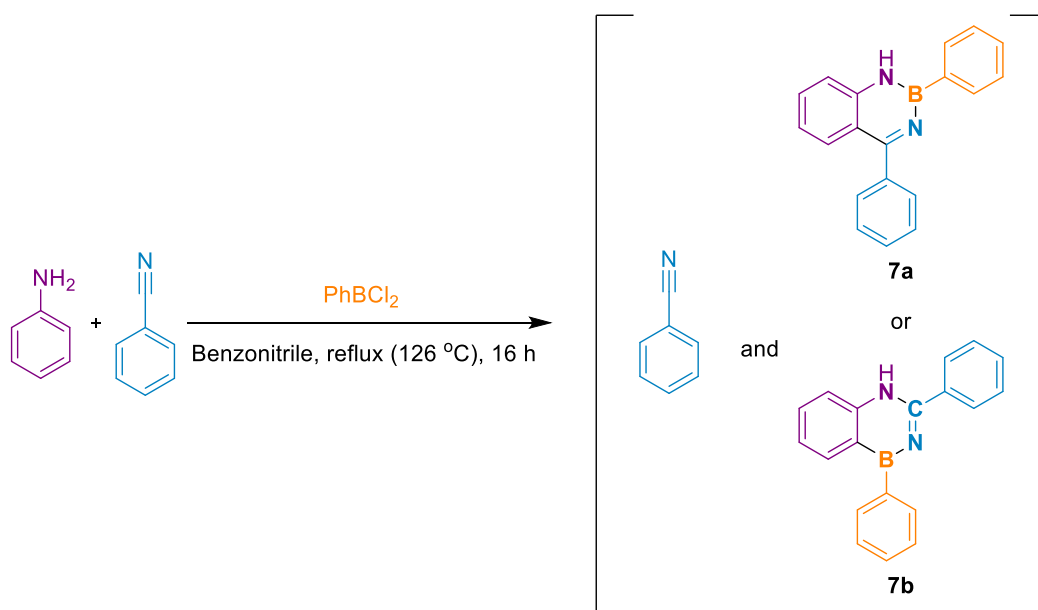
3.2. Investigation of nitriles (benzotrile) as the potential polarised heteroatom source in the reaction

In order to ascertain whether nitrile derivatives take part in the multicomponent reaction and form the desired heterocyclic compound, benzotrile was tested under the same conditions used for the previous cyclohexanone investigation. As mentioned above, the possibility of obtaining two different heterocyclic compounds with the NBN or NCNB sequence in their newly formed ring was also considered. First of all, benzotrile was reacted with aniline and PhBCl_2 under the same reaction conditions as above in scheme 3.2.



Scheme 3.3. The reaction of benzonitrile with PhBCl_2 and aniline in toluene.

Unfortunately, thin layer chromatography (TLC) analysis showed only aniline and benzonitrile in the resulting final mixture and no other spots indicating the possible formation of the expected diphenyl diazaborinine heterocyclic ring **7a** or **7b** were observed. In a second attempt, we considered using benzonitrile as the solvent instead of toluene, since a large excess of benzonitrile could push the reaction forward. Furthermore, benzonitrile is more polar than toluene so should favour solubility of the reagents.⁴⁵ As a result, the reaction shown in scheme 3.4 was carried out.



Scheme 3.4. Reactivity experiment of the benzonitrile with PhBCl_2 in the benzonitrile solvent.

After the reaction, the excess of benzonitrile was removed by distillation and purification of the product was attempted via column chromatography. However, in the ^1H and ^{13}C NMR spectra of the resulting purified material the peaks corresponding to benzonitrile showed that it was the main component of the

isolated fraction, with very dominant peaks and practically no other peaks being visible. Nevertheless, this product was analysed by ^{11}B NMR and showed a small peak at 29.64 ppm, which can be attributed to either product **7a** or **7b** of the scheme 3.4 reaction. The MS spectrum of this product was also measured, and the result showed a peak corresponding to the mass of the isomers diphenyl diazaborinine **7a** or **7b** (Figure 3.4).

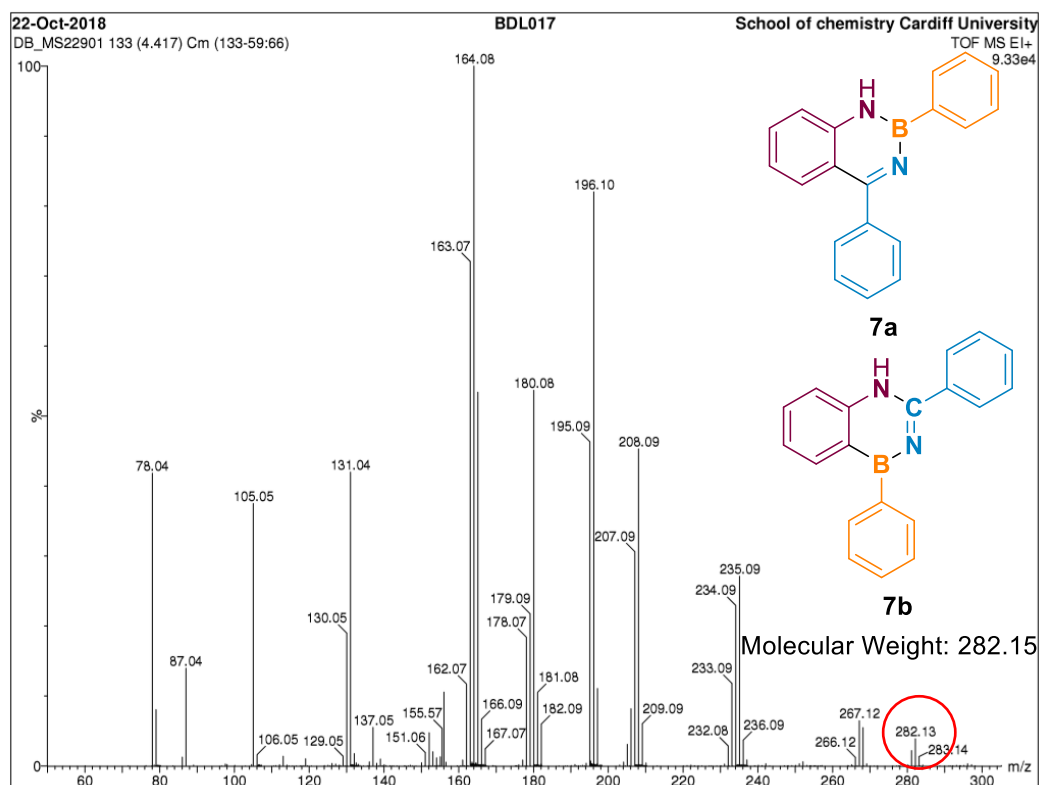
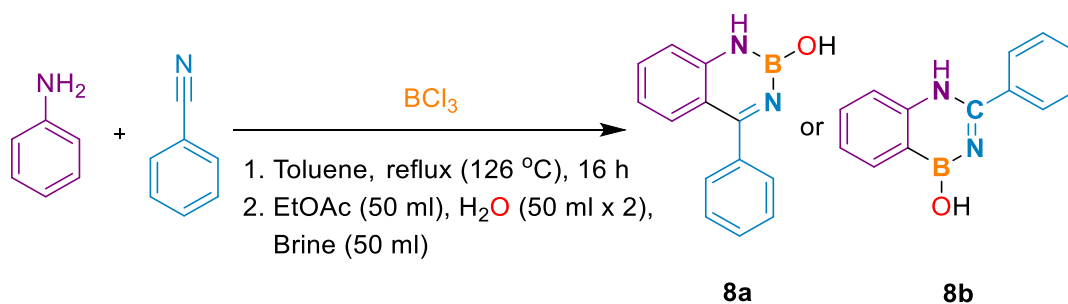


Figure 3.4. Mass spectrometry of the product from the reaction in scheme 3.4.

A similar experiment was then carried out using BCl_3 instead of PhBCl_2 with a toluene solvent and the same reaction conditions as scheme 3.3. (Scheme 3.5)



Scheme 3.5. Planned synthesis for diazaborinine **8a** or **8b**.

This resulted in analogous observations to those made for the reaction with PhBCl_2 . Column chromatography was attempted, but none of the obtained fractions showed clear evidence of the presence of NBN or NCNB products by ^1H and ^{13}C NMR. However, for one of the fractions a peak at 18.93 ppm could be observed in the ^{11}B NMR spectrum, corresponding to the B-N bond. The MS spectrum of this fraction also showed a peak which could indicate the formation of the possible products (Figure 3.5).

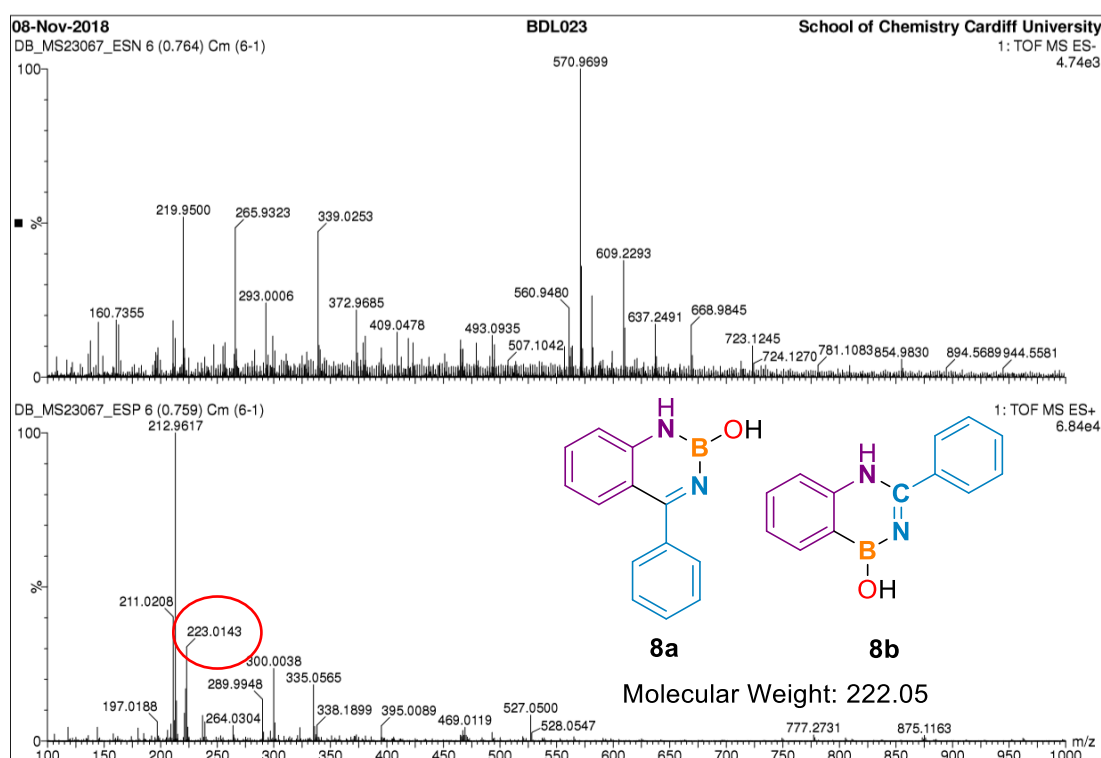


Figure 3.5. Mass spectrum of the hydrolysed diazaborinine **8a** or **8b**.

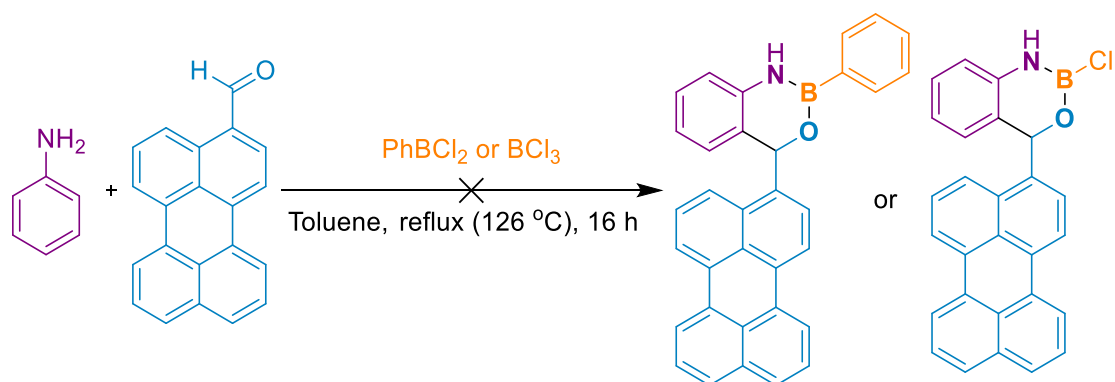
Indeed, the peak at 223.01 m/z $[\text{M}+1\text{H}]^+$ corresponds to the mass of isomers diazaborininol **8a** or **8b**, which contain a ring with the NBN or NCNB sequence. These molecules could form as a result of hydrolysis of diazaborinine **8a** or **8b** with the water used during the reaction work up.

Considering these results, four significant facts can be inferred. First of all, although ^1H and ^{13}C NMR data could not prove the formation of diazaborinine **7a** and/or **7b**, or **8a** and/or **8b**, this could be confirmed by ^{11}B NMR and MS. Secondly, the formation of the heterocyclic product seems to be more favoured when benzonitrile was used as a solvent when compared to toluene. Thirdly,

before purification of the product from the resulting final mixture, the benzonitrile solvent needs to be completely removed by distillation, as otherwise it cannot be separated by column chromatography from the product. However, in this stage, we could not confirm the actual structure of the product. Therefore, we were unable to determine whether either both or only one of the two possible heterocycles were obtained. The ^{11}B NMR and MS results only confirm that the potential heterocyclic ring formation had occurred. As the main purpose of our research at this stage was finding out the appropriate third heteroatom source for the formation of heterocyclic ring product, the determination of the product's structure showing the combination of heteroatoms will be discussed later.

From these preliminary results, we could conclude that the use of nitrile containing reagents in multicomponent reactions is promising. Therefore, it is worth investigating these derivatives to extend the scope beyond the formation of NBN or NCNB heterocyclic compounds.

3.3. Investigation of aldehydes (3-perylenecarboxaldehyde) as the potential polarised heteroatom source in the reaction



Scheme 3.6. The reaction of 3-perylenecarboxaldehyde with BCl_3 and aniline in toluene.

3-Perylenecarboxaldehyde was chosen as a representative aldehyde derivative for the investigation since it is non-volatile and easy to dry and therefore use under the anhydrous conditions required by these kinds of reactions. In addition, 3-perylenecarboxaldehyde is red so this could help in the product purification via column chromatography. This aldehyde was tested using the same conditions as the ones employed for the ketone and nitrile

containing reagents (Scheme 3.6). After the reaction, TLC measurement processed with the reaction crude and the result has been replicated in figure 3.6.

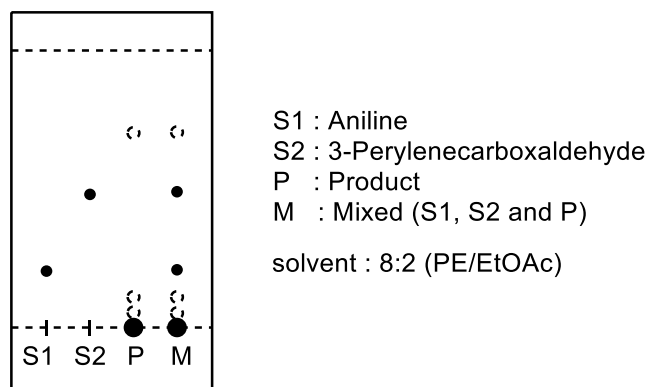


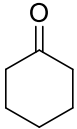
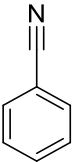
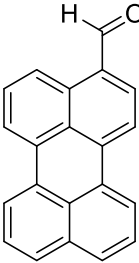
Figure 3.6. The TLC result of the scheme 3.6 reaction crude.

From this TLC result, two conclusions can be drawn. First, there has been a complete consumption of the starting materials. Secondly, a major product could be observed very near the baseline, as shown above in figure 3.8. This observation indicates that the major product has a non-polar character, due to the use of a polar solvent for this measurement. However, the spot located on the baseline could not be eluted from the silica gel column, even when a high polarity solvent was used (100% EtOAc). This analysis does not correlate with the expected structure as the product contains polar bonds consisting of boron, nitrogen and oxygen atoms. The same results were observed even when the reaction was repeated. Since these results were not encouraging the research on aldehydes was stopped, and the investigation continued with the more promising nitriles reagents.

3.4. Overall results and conclusion.

Three functional group candidates were investigated for the production of heterocyclic compounds via a one-pot multicomponent reaction. (Table 3.2)

Table 3.2. A summary of the results in chapter 3.

| Functional group types | Ketone | Nitrile | Aldehyde |
|----------------------------|---|--|---|
| Reagent used |  |  |  |
| Heterocyclic ring produced | No | Yes | No |

The ketones reactivity has been explored in the reaction by using cyclohexanone as a representative reagent. The target was to produce a NBO heterocycle on only one side of the aniline. However, the reaction failed to produce the expected NBO containing heterocycles. According to the results in chapter 3, PhCN showed potential in the production of the heterocyclic product. Therefore, PhCN was selected as a representative polarised reagent in the multicomponent reaction. This showed promising results as by employing a carefully designed method, the formation of heterocycles with either NBN or NCNB could be observed. This result was confirmed by MS data for both the diphenyl diazaborinine heterocyclic ring **7a** (or **7b**) and the phenyl hydrolysed diazaborinine **8a** (or **8b**) (Figure 3.7).

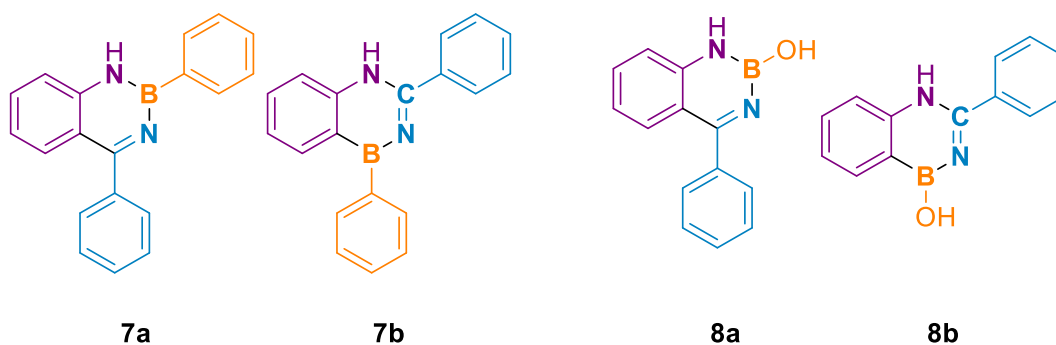


Figure 3.7. Obtained heterocyclic products using the PhCN reagent.

3-phenylenecarboxaldehyde was selected as the representative to investigate the reactivity of aldehydes in the multicomponent reaction; however, no desired NBO bonding system could be isolated by column chromatography from the reaction product mixture. In light of these results, we focused our efforts on syntheses involving nitrile derivatives; looking to obtain NBN or NCNB heterocyclic compounds via a multicomponent reaction.

Chapter 4 - Second stage: Building-on previous results and the one-pot synthesis process modification

In our preliminary investigation it was discovered that benzonitrile could be used successfully in our proposed multicomponent reaction to obtain heterocyclic NBN or NCNB compounds. Although the formation of diazaborinine **7a** (or **7b**) and diphenyl diazaborinine **8a** (or **8b**) could be inferred by analysis of the spectrometry data, their exact structures could not be confirmed. Therefore, as described in this chapter, the one-pot synthesis process was modified in order to confirm the nature of the obtained heterocyclic compounds and to try to increase the reaction yield. In particular, two changes were implemented: the addition of mesitylene as a substituent on the boron position and the use of BBr_3 as the Lewis acid.

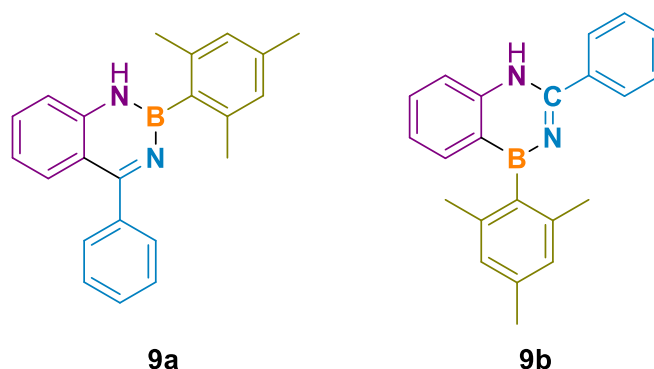
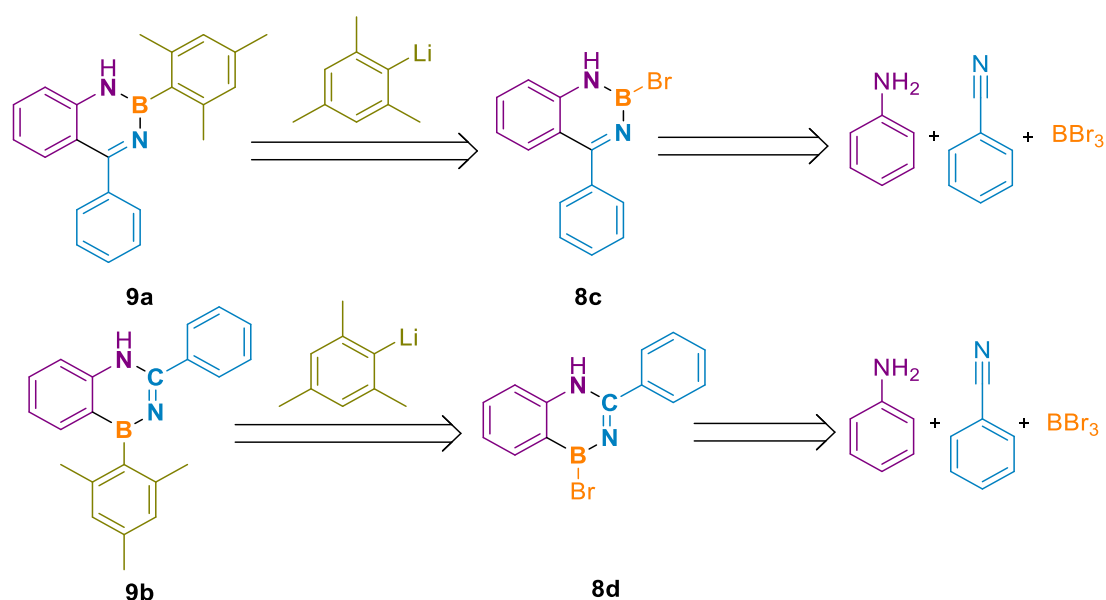


Figure 4.1. Two structures showing the two different possible positions of mesitylene in the potential reaction product, mesityl diazaborinine **9a** and **9b**.

It was decided to use mesitylene as the substituent as this can help to identify which of the two possible different rings forms during the reaction. Due to the presence of the mesitylene group, we can use NOE or NOESY to understand which NBN or NCNB isomer is obtained. As they allow us to find which protons are close in space to those of the *o*-methyl groups. Furthermore, the *o*-methyl groups in the mesitylene shield the boron atom from nucleophilic attack and potential hydrolysis. Therefore, we decided to synthesise mesityl diazaborinine **9a** or **9b** (Figure 4.1) by quenching our multicomponent reaction. For the

quenching, we used a freshly prepared lithium derivative of mesitylene, obtained from MesBr by lithium-halogen exchange with *n*-BuLi. We also decided to use BBr₃ in place of BCl₃ with the aim of achieving a high yield of the diazaborinine formation. When considering the trend of Lewis acid characters, BBr₃ is more acidic and electrophilic than BCl₃. In addition, bromine is a better leaving group than chlorine. Therefore, this change should be favourable in processing the lithium-halogen exchange.

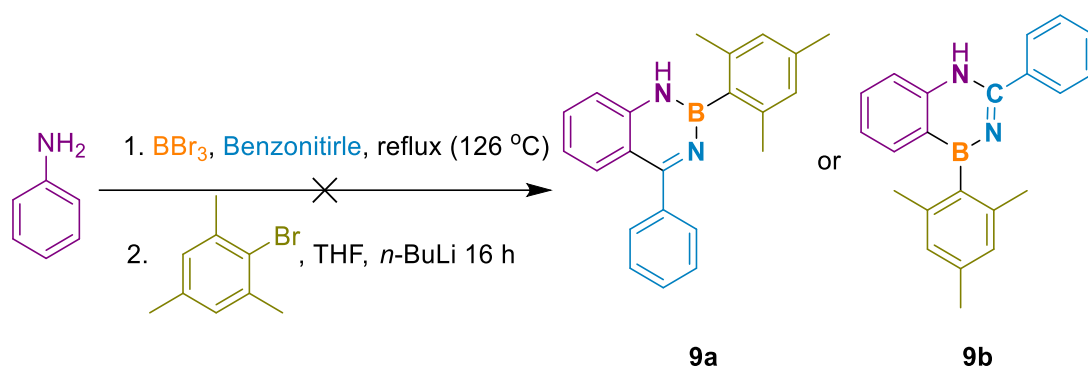
4.1. A retrosynthetic pathway for the proposed multicomponent reaction.



Scheme 4.1. A retrosynthetic pathway of the NBN heterocyclic compound **9a** and **9b**.

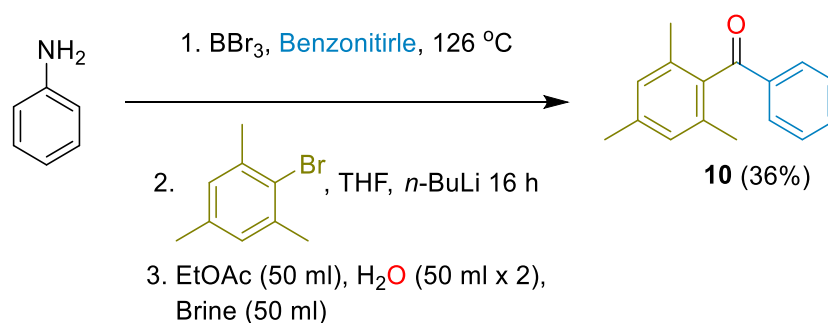
According to scheme 4.1, a multicomponent reaction between aniline, benzonitrile and BCl₃ could produce either diazaborinine precursor **8c** or **8d**. Then, MesLi, prepared using a lithium-halogen exchange by reacting *n*-BuLi with MesBr, substitutes the chloride on the boron atom of the diazaborinine precursor **8c** or **8d** leading to mesityl diazaborinine **9a** or **9b**.

4.2. Multicomponent reaction modification



Scheme 4.2. The modified reaction scheme for the proposed synthesis of mesityl phenyl diazaborinine **9a** and **9b**.

The modified reaction has been tested under the conditions outlined in scheme 4.2. In detail, anhydrous aniline and BBr_3 were added to the dried benzonitrile solvent. This solution was then refluxed for 16 hours at 126 °C. The excess of benzonitrile solvent was then removed by distillation, MesBr and 1 eq. of $n\text{-BuLi}$ were added to the reaction mixture and stirring continued for 16 hours at room temperature. A TLC of the crude showed one major product along with two more faint spots. Only the major product could be isolated by silica gel column chromatography. However, instead of the expected mesityl phenyl diazaborinine **9a** or **9b**, the isolated product was mesityl(phenyl)-methanone **10** (Scheme 4.3). The structure of the actual product was determined by ^1H NMR, ^{13}C NMR and mass spectrometry (Figures 4.2, 4.3, 4.4).



Scheme 4.3. The reaction leading to the formation of mesityl-(phenyl)methanone **10**.

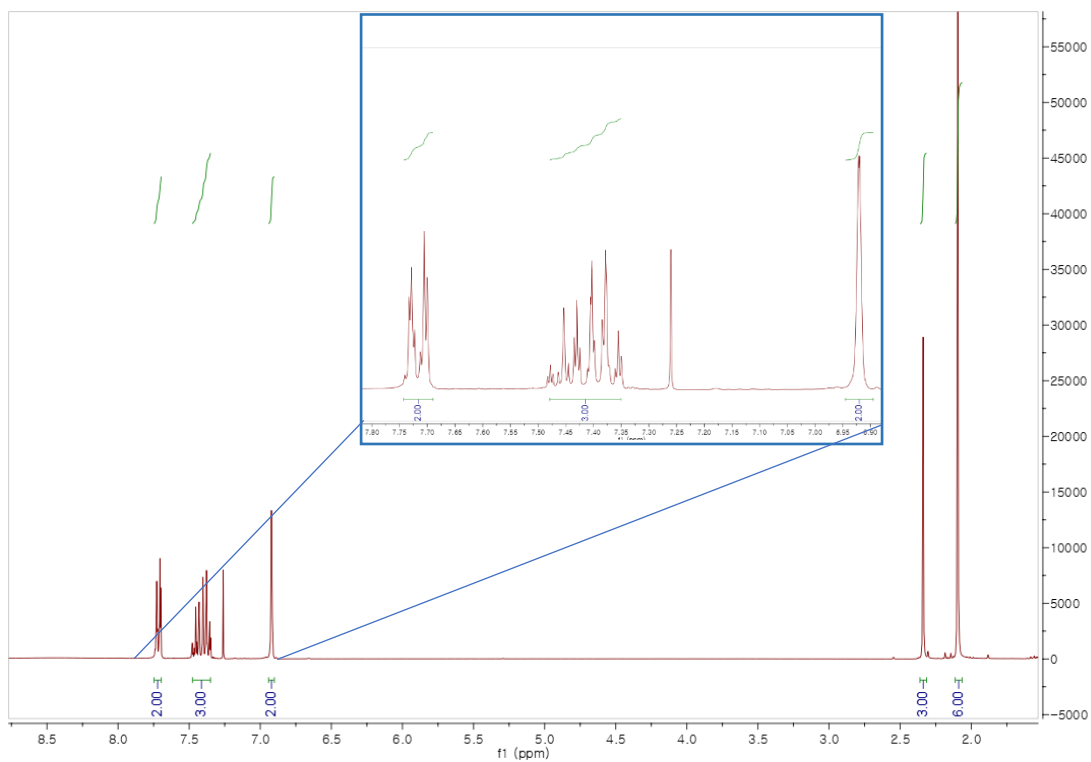


Figure 4.2. ^1H NMR data of the mesityl(phenyl)methanone **10**.

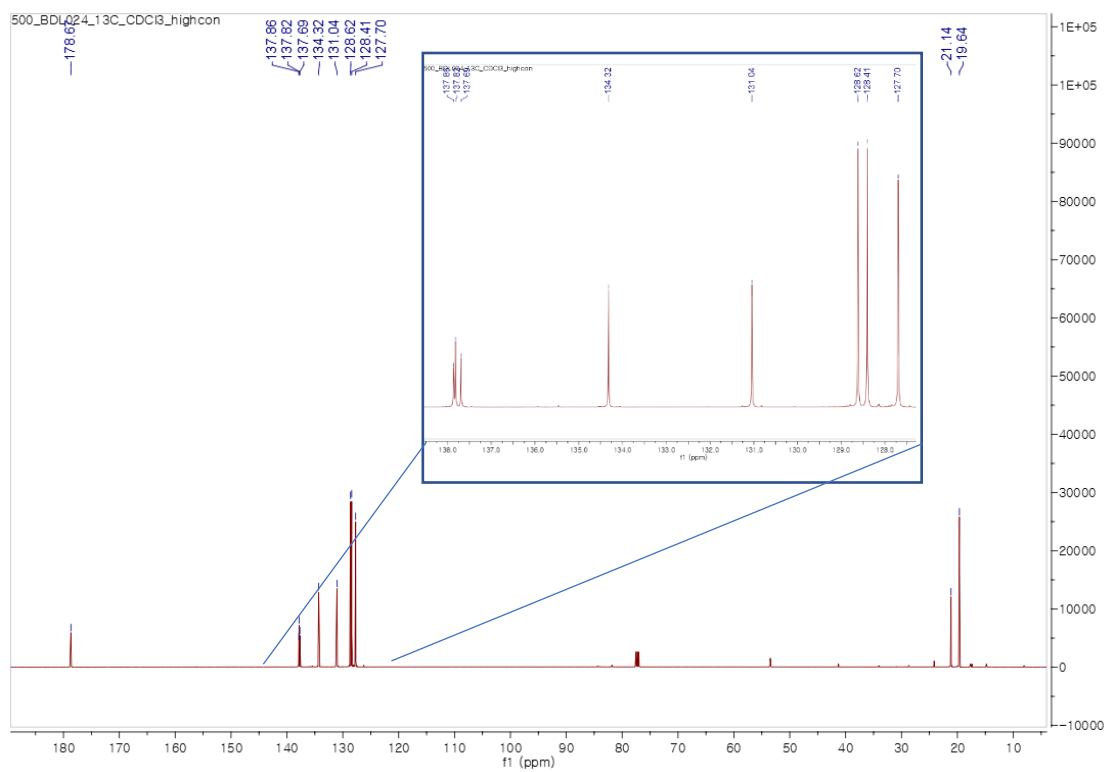


Figure 4.3. ^{13}C NMR data of the mesityl(phenyl)methanone **10**.

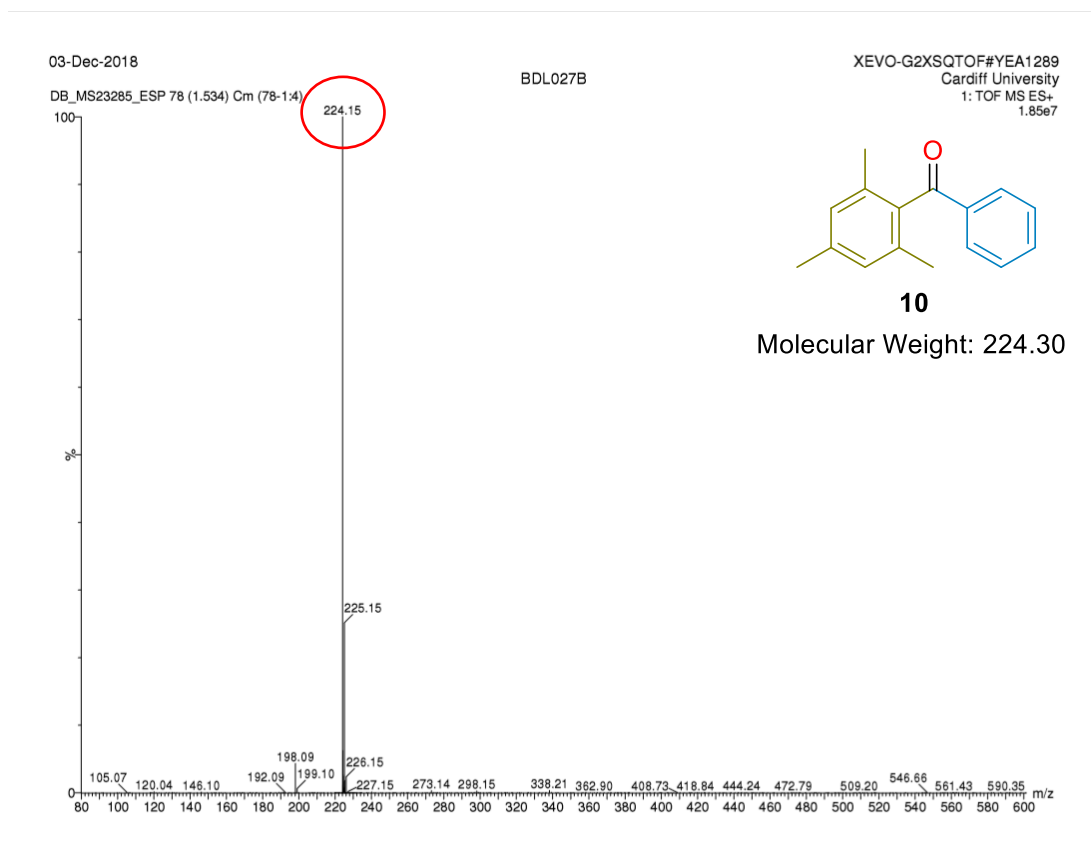
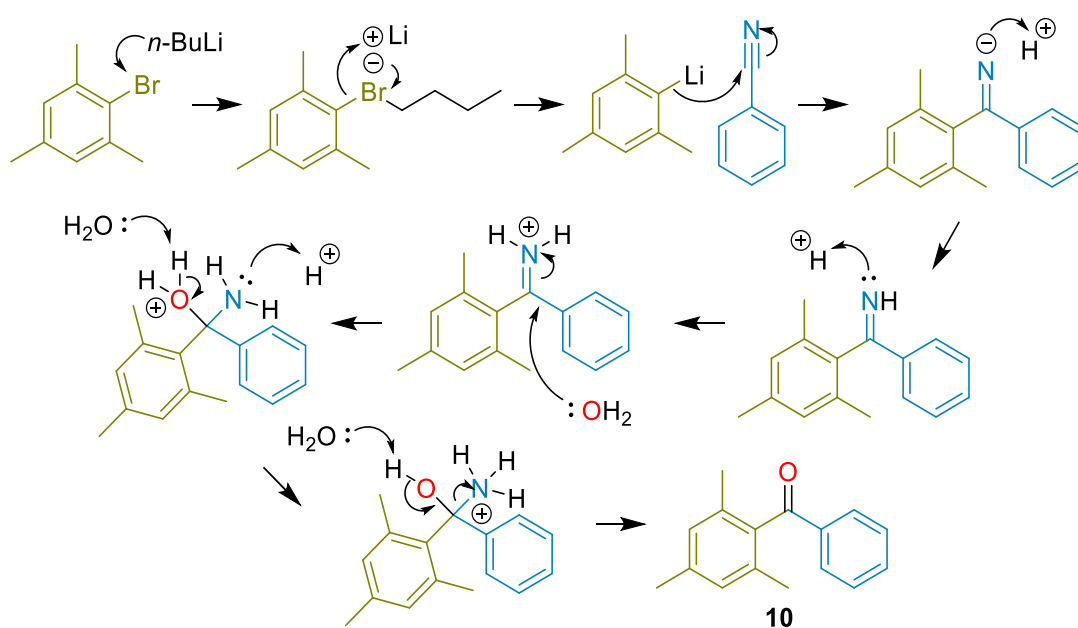


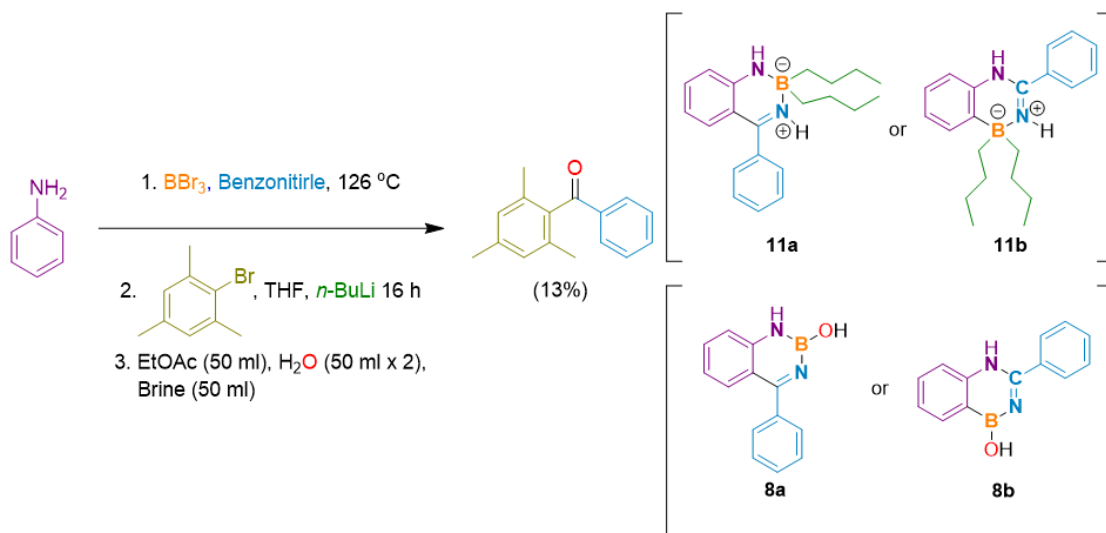
Figure 4.4. Mass spectrometry data of the mesityl(phenyl)methanone **10**.

The mesityl (phenyl) methanone was formed by the reaction of MesLi and benzonitrile, as outlined in scheme 4.4.



Scheme 4.4. Proposed mechanism for the mesityl(phenyl)methanone **10** synthesis.

In the first step the imine was formed by a nucleophilic attack of MesLi onto the nitrile carbon, this was then hydrolysed by water during the work up step resulting in the formation of ketone **10**. According to this mechanism, we can conclude that the formation of this product is due to the fact that benzonitrile had not been completely removed before the addition of MesLi. Therefore, we repeated the reaction under the same conditions but tried to remove benzonitrile completely by distillation before the addition of MesLi. (Scheme 4.5)



Scheme 4.5. The repeated reaction of scheme 4.3.

As a result, two major products were collected by column chromatography. One of them is mesityl(phenyl)-methanone **10**, although this time it was isolated in a lower amount (13%) in comparison to the previous attempt (36%, scheme 4.4). This means that even though more benzonitrile had been removed from the reaction mixture, some was still present. The target product **9a** or **9b** could not be found. However, the ^1H NMR (Figure 4.5) and ^{13}C NMR spectra of the isolated product indicated the presence of either dibutyl phenyl dihydro diazaborinine **11a** or **11b**. However, it was difficult to establish from the data what the actual structure of the obtained product was. In the mass spectrum, the masses of dihydro diazaborinine **11a** or **11b** could be observed as shown in figure 4.6. In addition, those of the hydrolysed diazaborinine **8a** or **8b** could be detected meaning that these had formed and had not been separated by column chromatography from the other product. Therefore, the yield of reaction could not be calculated.

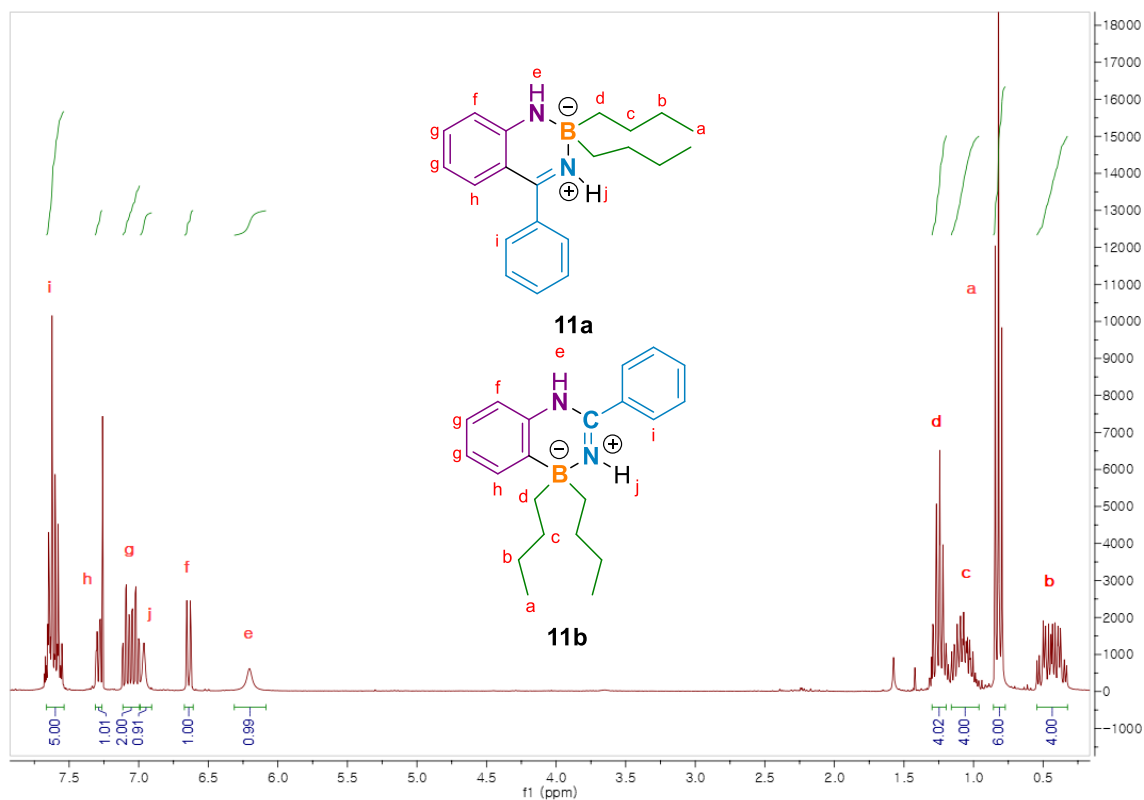


Figure 4.5. ¹H NMR of the dibutyl phenyl dihydro diazaborinine **11a** or **11b** in CDCl₃ (Solvent residual peak: 7.26 ppm).

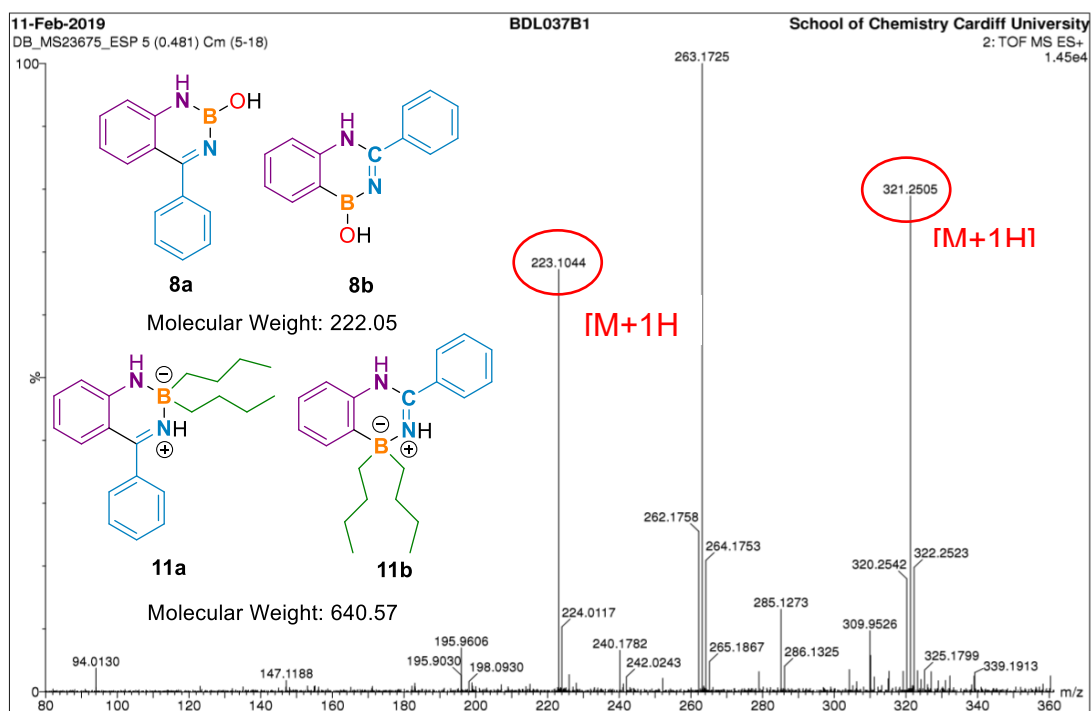
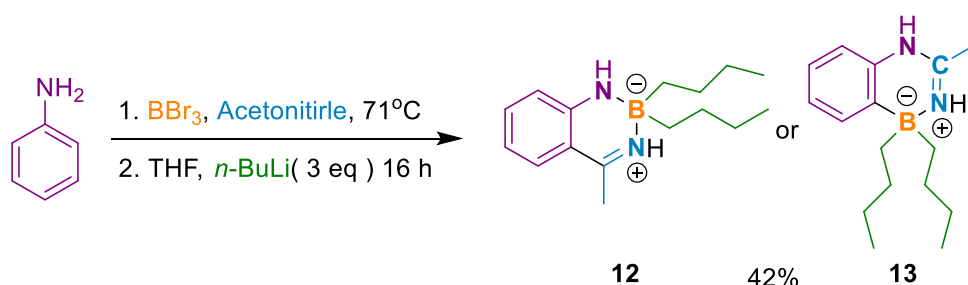


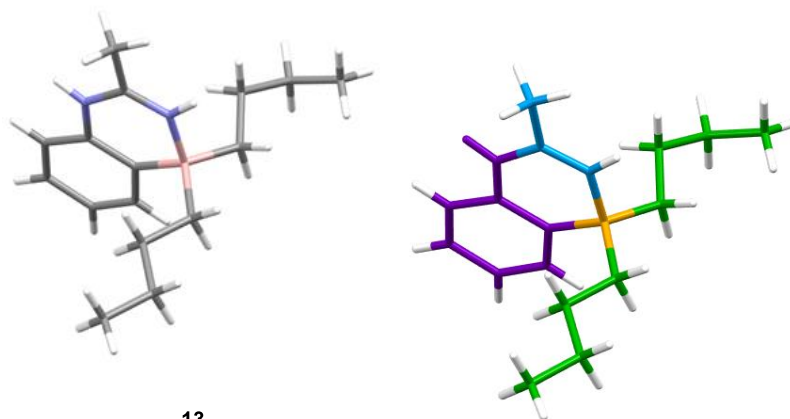
Figure 4.6. Mass spectrum of the hydrolysed diazaborinine **8a** or **8b** and dibutyl phenyl dihydro diazaborinine **11a** or **11b**

Although the NBN or NCNB heterocyclic compound was formed, the yield of the reaction mentioned before was low. To increase the yield, the same reaction was carried out using CH₃CN instead of benzonitrile. This choice was made because the boiling point of CH₃CN (82 °C) is much lower than that of benzonitrile (191 °C). Therefore, complete removal of the solvent by distillation should be much easier. This complete elimination of the solvent should avoid the formation of the side product that would otherwise form by reaction of CH₃CN with MesLi. In addition, we considered the possibility that the high distillation temperature needed for removing benzonitrile. This could have induced some thermal decomposition of the newly formed heterocyclic ring (NBN or NCNB). Instead, the distillation using CH₃CN would be performed at a lower temperature due to its lower boiling point. Therefore, avoiding the potential decomposition of the heterocyclic products (NBN or NCNB) should they form. Besides, since MesLi seems to not react with the intermediate, it was decided to use an excess of BuLi as the organometallic nucleophile. When these changes were applied to the reaction, the observed yield in the product increased. However, the exact structure was still unknown at this stage being either the NBN heterocycle **12** or the NCNB heterocycle **13**.



Scheme 4.6. Preparation of the dibutyl methyl dihydro diazaborinine **12**, **13**.

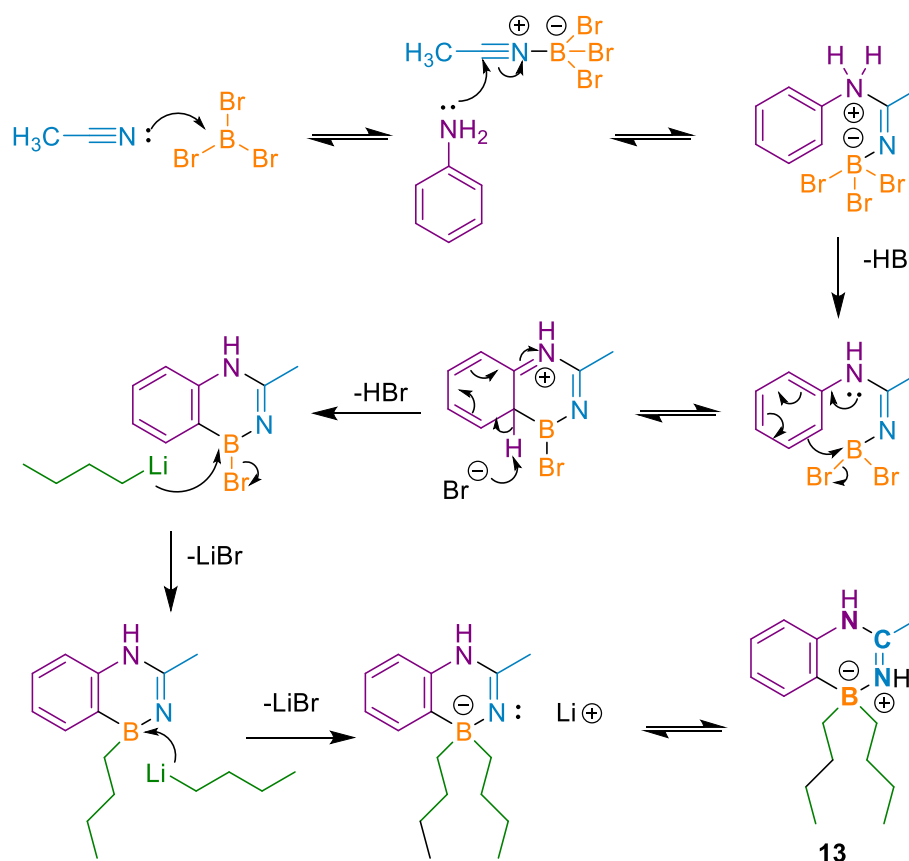
The product **12** or **13** of the scheme 4.6 reaction was isolated by column chromatography with a 42% yield. In addition, single crystals of the product were easily obtained by slow solvent evaporation of a petroleum ether solution and the molecular structure was determined by X-ray diffraction analysis (Figure 4.8).



13

Figure 4.7. A capped sticks style representation of the molecular crystal structure of the dibutyl methyl dihydro diazaborinine **13**. Space group P21/n, R-Factor = 8.66%.

As is clearly visible from the molecular structure in Figure 4.7, the non-planar structure of the crystal shows the obtained product alongside its a Zwitterion. This Zwitterion includes a quadruple bonded negatively charged boron atom.

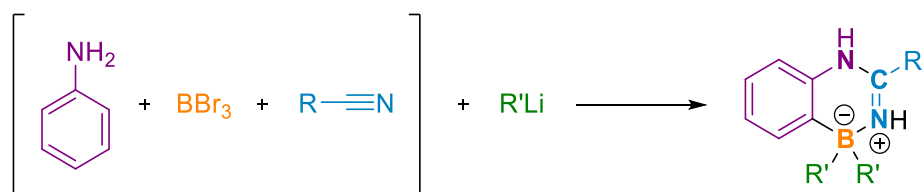


Scheme 4.7. Proposed pathway B '1,4-azaborinine' mechanism for the formation of the dibutyl methyl dihydro diazaborinine **13**.

Considering the confirmed structure, we can assume that the reaction followed the mechanism as discussed at the beginning of *chapter 3*. As shown in scheme 4.7, the CH_3CN reacts with BBr_3 , forming a Lewis adduct that then undergoes a nucleophilic attack by aniline. This mixture is refluxed and produces HBr gas. The nitrogen atom of aniline begins the cyclisation process by attacking the electrophilic boron, resulting in the formation of a quadruple bonded bromide anion. The bromide anion then takes the proton from the positively charged azaborine derivative, restabilising the aromaticity of the aniline ring.

4.3. Overall results and conclusion

Further investigation of the proposed multicomponent reaction led to some successful results. We discovered that by a new multicomponent reaction involving aniline as the Lewis base, BBr_3 as the Lewis acid, nitrile derivatives and $n\text{-BuLi}$; we could obtain NCNB heterocyclic compounds. The crystal of the dibutyl methyl dihydro diazaborinine **13** was obtained; this confirmed its NCNB heterocyclic structure. Based on the described results, the general multicomponent reaction can be described as shown in scheme 4.8.



Scheme 4.8. The new discovered multicomponent reaction.

Chapter 5 – Third stage: Exploration of the multicomponent reaction

The previous stage, led to the discovery of the one-pot NCNB Zwitterion formation process. Starting from the observed results, several experiments with different starting materials were subsequently explored. This section reports these experiments, carried out to evaluate the reaction scope. For our study, the components of the reaction, Lewis bases, nitrile substituted reagents and lithiation reagents were changed one at the time, and the results are described separately. Since we have already established that BBr_3 led to a better result than other Lewis acids, such as $PhBCl_2$ or BCl_3 , it was not changed in the following investigation described in this chapter.

5.1. Exploring the reaction with different amino nucleophiles

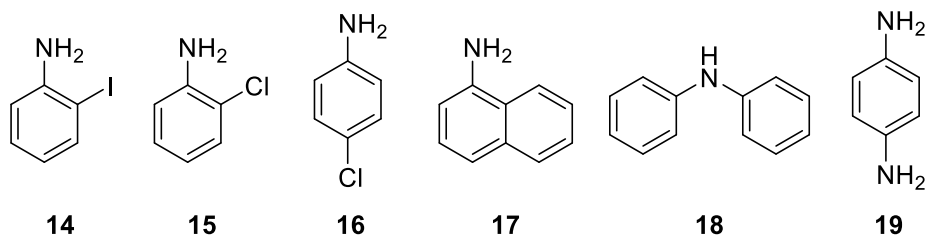
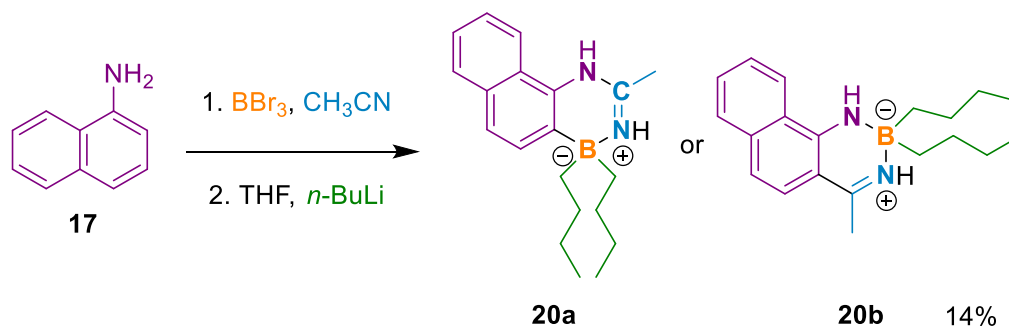


Figure 5.1. The aniline derivatives considered in this stage.

The reactivity of six different amino nucleophiles with BBr_3 , CH_3CN and butyllithium (Figure 5.1) was tested in the new multicomponent reaction. For the 2-iodoaniline **14**, 2-chloroaniline **15**, diphenylamine **18** and *p*-phenylenediamine **19** reactions, the resulting product could not be purified completely due to the a lot of mixtures was included. In addition, according to ^{11}B NMR, Boron was not found in the mixture product. Therefore, they would not perform the targeted heterocyclic product of multicomponent reaction. This was assumed by two observations. First of all, This represents that the major would have strong non-polar character and it is not correspond with other . For 4-chloroaniline **16**, no reaction took place, and the most of starting materials recollectd by the column. This might have been due to the drying process of 4-chloroaniline **16**, meaning

the reagent was not perfectly anhydrous.

However, naphthalen-1-amine **17** proved to be an exception among the different studied anilines and the formation of the expected dibutyl methyl dihydro naphthodiazaborinine **20a** or **20b** could be observed (Scheme 5.1).



Scheme 5.1. Preparation of the dibutyl methyl dihydro naphthodiazaborinine **20a** or **20b** from naphthalen-1-amine **17**.

The product was analysed by ^1H , ^{13}C , ^{11}B NMR and MS and all the data confirmed the presence of naphthodiazaborinine **20a** or **20b**. This was especially evident in the MS spectrum (Figure 5.2).

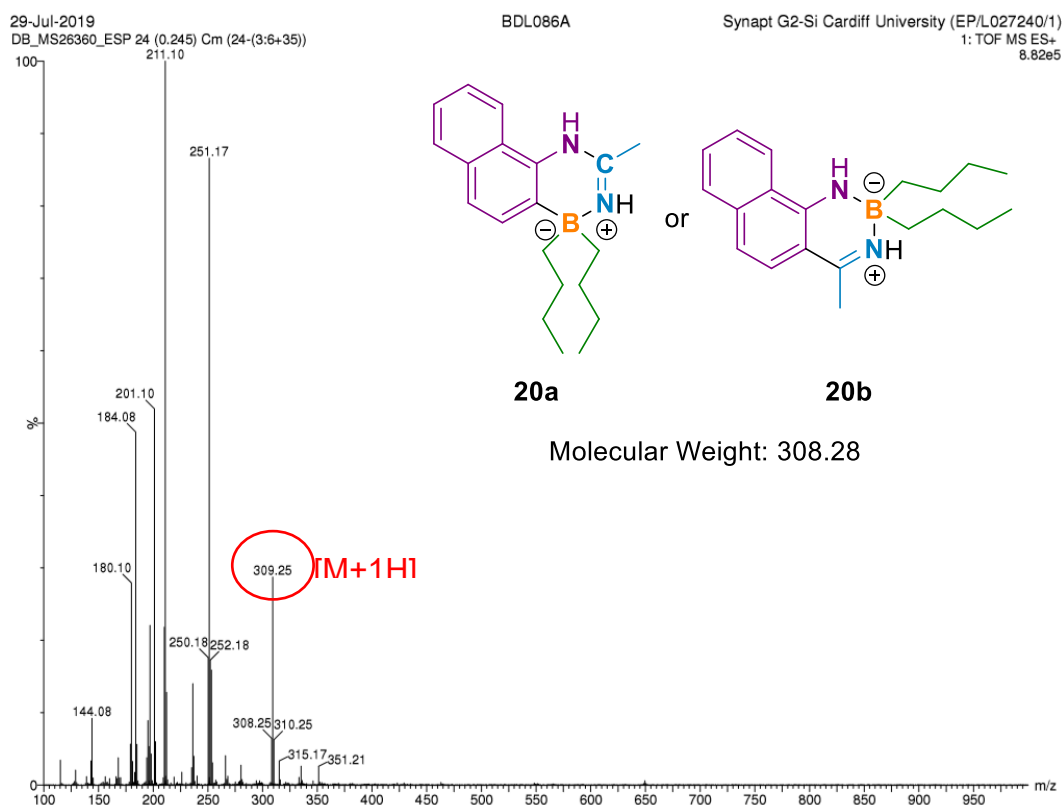


Figure 5.2. Mass spectrometry data of the naphthodiazaborinine **20a** or **20b**.

In the case of NMR data, also the peak for dibutyl methyl dihydro naphthodiazaborinine **20a** or **20b** was found clearly (Figure 5.3).

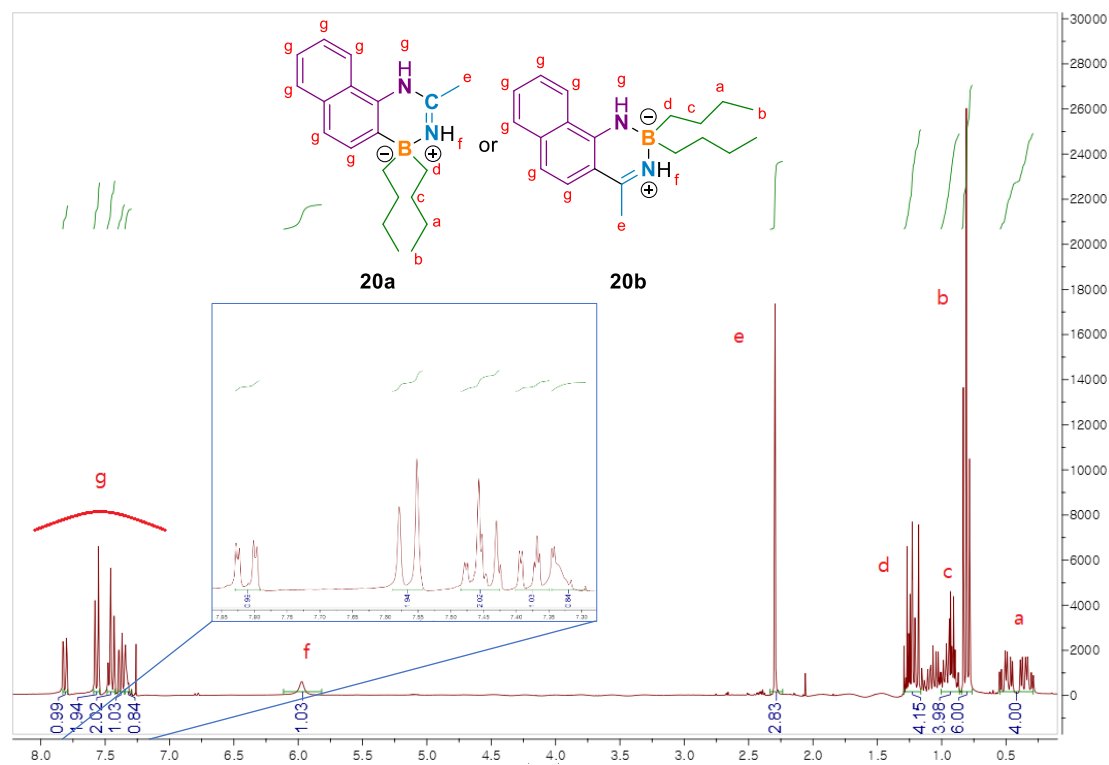


Figure 5.3. ^1H NMR of the dibutyl methyl dihydro naphthodiazaborinine **20a** or **20b** in CDCl_3 (Solvent residual peak: 7.26 ppm).

However, the purification of the product could not be easily achieved and therefore peaks of impurities were also observed. The crystallisation of the dibutyl dihydro methyl naphthodiazaborinine **20a** or **20b** was attempted in the same way as for dibutyl dihydro methyl diazaborinine **13** (Figure 4.5) but the formation of crystals was not observed. Additional crystallisation experiments by slow solvent evaporation from solution were also tried with different solvents such as DCM, CHCl_3 , EtOAc and MeOH. Despite the attempts, the crystallisation could not be achieved. Therefore, we could not confirm the product structure via x-ray analysis. Furthermore, due to the low yield of the reaction, the low amount of the obtained product did not allow us to try further analytical experiments aimed at understanding which one of the two isomers had formed.

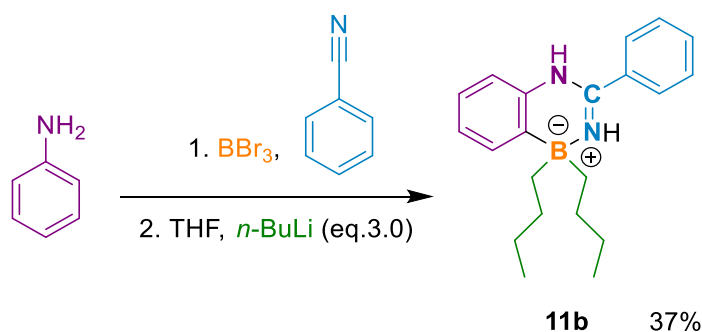
5.2. Exploring the reaction with different types of nitrile substituted reagents

Two types of nitrile reagents were analysed for our multicomponent reaction. (Figure 5.4)



Figure 5.4. Nitrile substituted compounds considered in this stage.

In chapter 4.2 (scheme 4.5), we had already established that PhCN worked to some extent in forming diazaborinine compounds. However, the exact structure of the product could not be identified with only MS analysis. The yield of the reaction was also very low. Hence, at this stage, the first step is achieving a higher yield of the product. This experiment was also more focused on identifying what combination of heterocycle was formed during the reaction. This will be determined by trying to obtain crystals of the product to establish its molecular structure.



Scheme 5.2. Preparation of the dibutyl phenyl dihydro diazaborinine **11b** from the benzonitrile.

This time dibutyl phenyl dihydro diazaborinine **11b** could be isolated with a 37% yield and a single crystal was obtained from a petroleum ether solution by slow evaporation of the solvent (Figure 5.5).

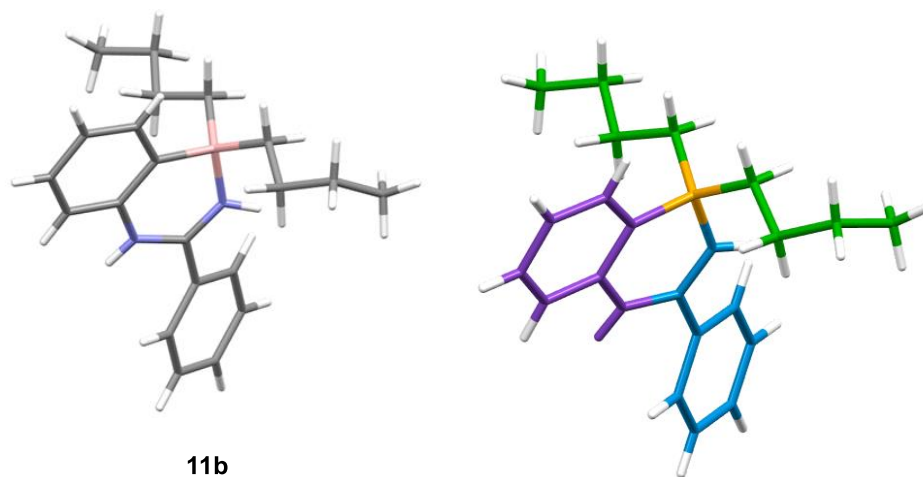
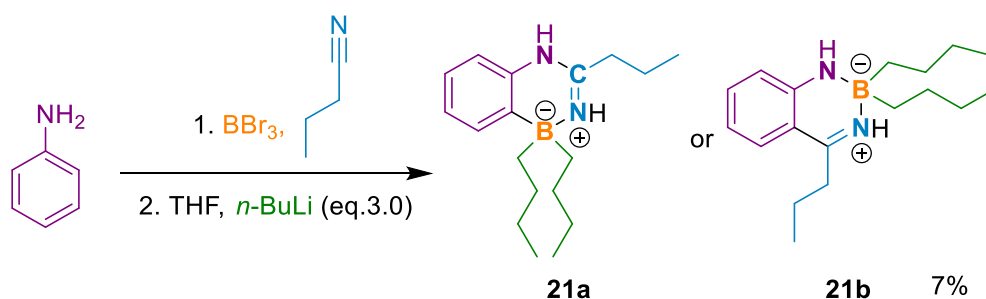


Figure 5.5. Crystal structure of the dibutyl phenyl dihydro diazaborinine **11b** in capped sticks style representation. Space group $Pbca$, R-Factor = 7.95%.

The crystal structure of the phenyl diazaborinine **11b** confirmed the formation of a NCNB heterocyclic ring as previously observed when CH_3CN was used (Scheme 4.6). Along with a phenyl substituent, it derived from PhCN instead of the methyl. According to the crystal structure, a Zwitterion with a quadruple bonded negatively charged boron atom is observed. The nitrogen atom next to the boron atom also has four bonds and is positively charged.



Scheme 5.3. Preparation of the dibutyl propyl dihydro diazaborinine **21a** or **21b** from the butyronitrile.

Only one product could be isolated via column chromatography when using PrCN as the starting material (Scheme 5.3). The ^1H NMR and ^{13}C NMR of the product were measured, but the results were challenging to interpret. For example, in the ^1H NMR spectrum (Figure 5.6), there were peaks at 1.6. and 2.4 ppm which could not be attributed to any of the protons found in the possible products. All the other peaks, however, seem to match the protons in the structures of both possible dibutyl propyl dihydro diazaborinine products (**21a**

and **21b**). The only difference between them being the order of heteroatoms in the newly formed ring.

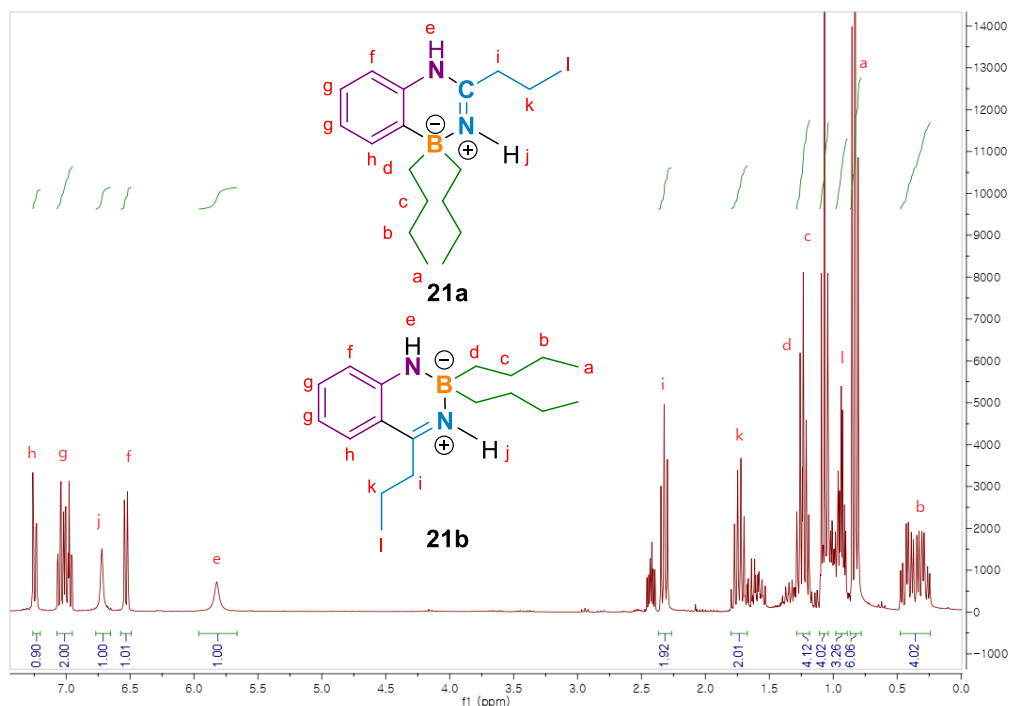


Figure 5.6. ^1H NMR of the dibutyl propyl dihydro diazaborinine **21a** or **21b** in CDCl_3 (Solvent residual peak: 7.26 ppm).

The MS of the collected product was also measured. The spectrum includes the peak corresponding to the mass of possible products **21a** or **21b** (Figure 5.7). This confirms that the reaction afforded one of the expected heterocyclic products. However, we failed to identify the sequence of the heteroatoms in the ring, and therefore failed to determine the structure. This was due to the fact that only a small amount of product could be collected after purification, meaning crystals could not be obtained.

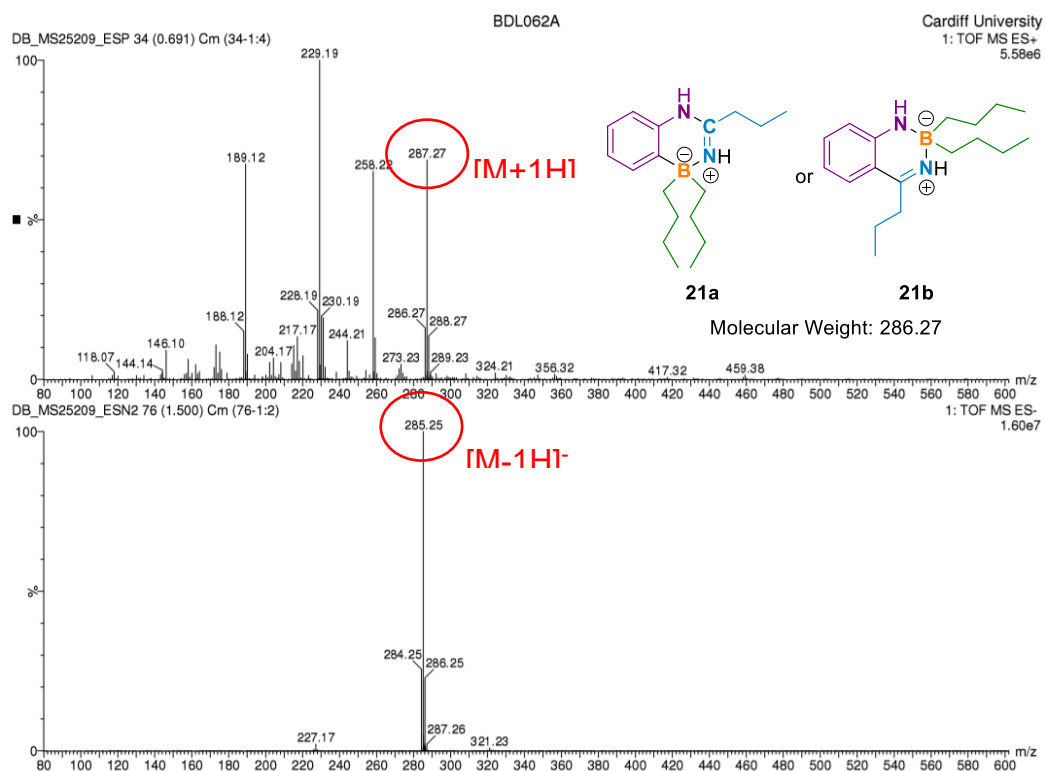
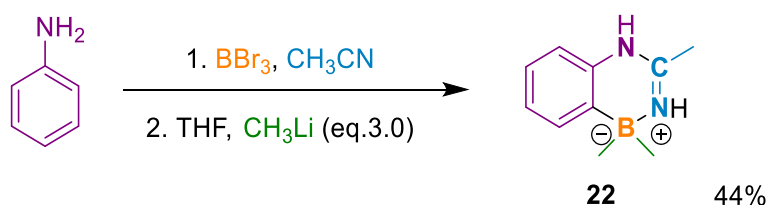


Figure 5.7. Mass spectrum of dibutyl propyl dihydro diazaborinine **21a** or **21b**.

5.3. Exploring the reaction with different types of lithiation reagents

Lastly, two lithiation reagents: MeLi and phenyl lithium, were tested under the same reaction conditions instead of *n*-BuLi.

Firstly, MeLi was used for the reaction and trimethyl dihydro diazaborinine **22** formed with a 44% yield (Scheme 5.4).



Scheme 5.4. Diazaborinine **22** formation from the MeLi.

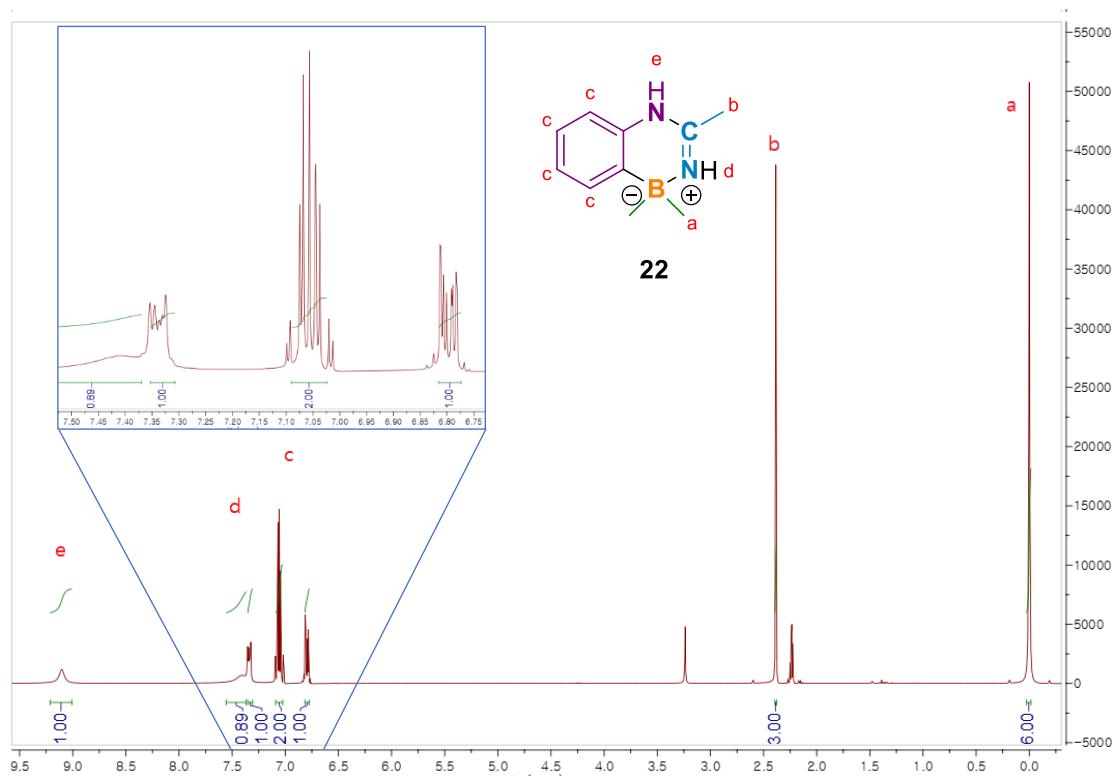


Figure 5.8. ¹H NMR of the trimethyl dihydro diazaborinine **22** in CDCl₃ (Solvent residual peak: 7.26 ppm).

The mass spectrum showed peaks for masses corresponding to possible products **22** and **22a**, with the latter most probably due to fragmentation of **22** during mass analysis (Figure 5.9).

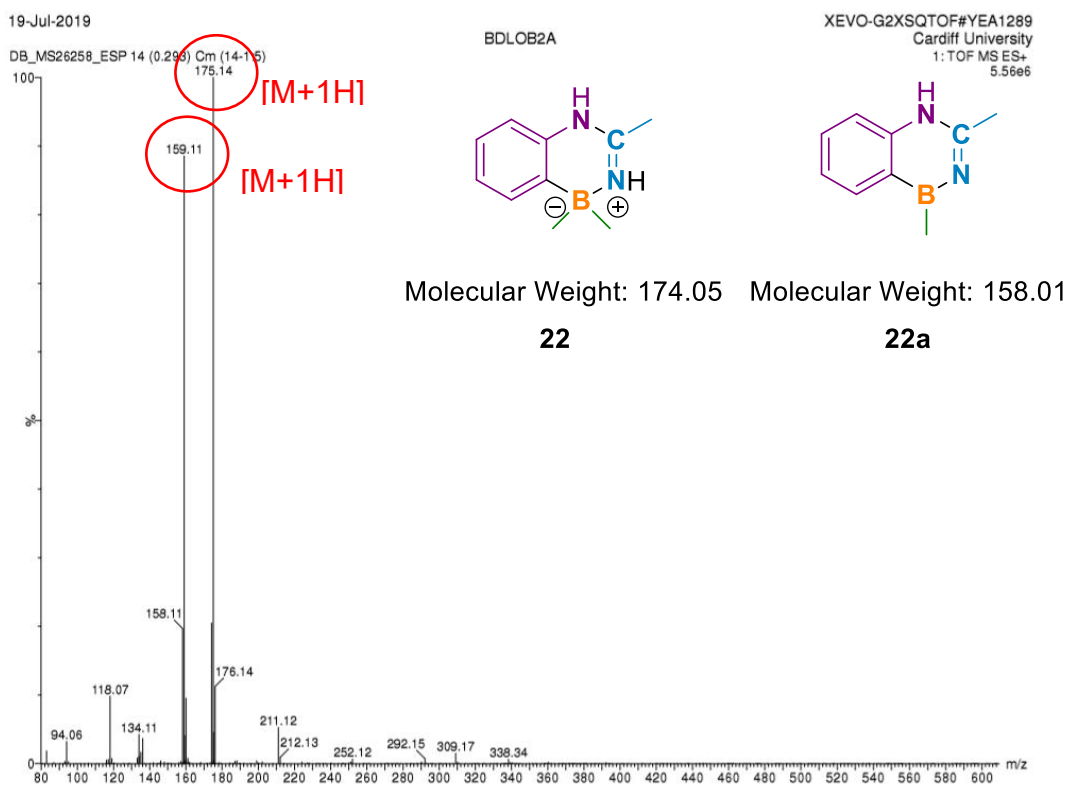


Figure 5.9. Mass spectrometry data of the trimethyl dihydro diazaborinine **22** and dimethyl hydro diazaborinine **22a**.

The crystallisation of product **22** by slow solvent evaporation from a petroleum ether solution afforded crystals suitable for single crystal analysis. This crystal structure confirmed that trimethyl dihydro diazaborinine **22** containing an NCNB heterocycle had been obtained as shown in figure 5.10.

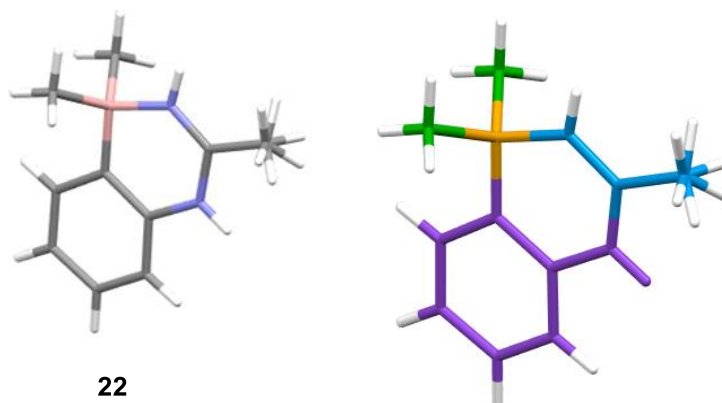
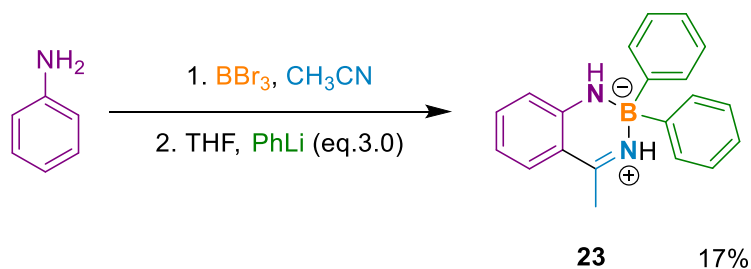


Figure 5.10. Crystal structure of the product **22** in a capped sticks interpretation. Space group Pnma, R-Factor = 4.94%.

The reaction was then tried with PhLi (Scheme 5.5.) and the purified product was isolated by column chromatography with a 17% yield, which is considerably lower than that obtained with MeLi (44%). The ^1H NMR, ^{13}C NMR and MS (Figure 5.12) of the collected product were measured and the formation of the heterocyclic ring was confirmed.



Scheme 5.5. Diazaborinine **23** formation from the phenyl lithium.

According to the ^1H NMR result (Figure 5.11), the peak of hydrogen on aromatic ring (**a**) was observed in between 6.77 and 7.25 ppm. In the case of the peak for hydrogen of the NH (**b** and **c**) and the methyl (**d**), they were identified clearly on 9.39, 7.90 and 2.38 ppm.

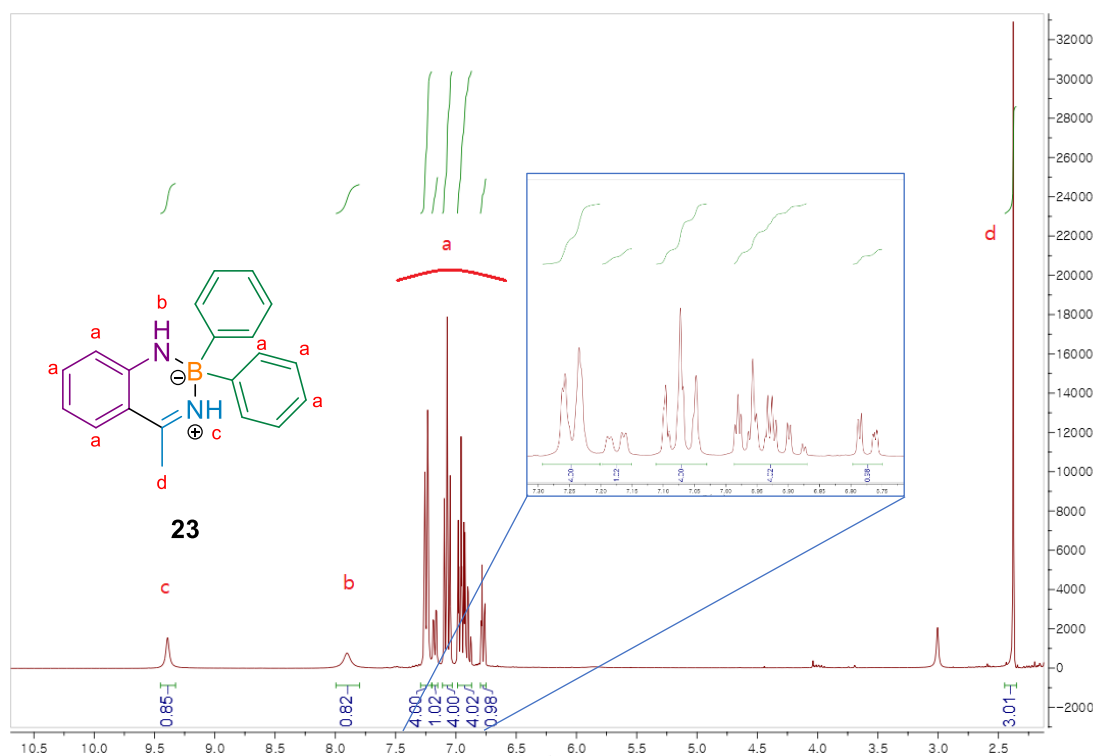


Figure 5.11. ^1H NMR of the methyl diphenyl dihydro diazaborinine **23** in Acetone (Solvent residual peak: 2.05 ppm).

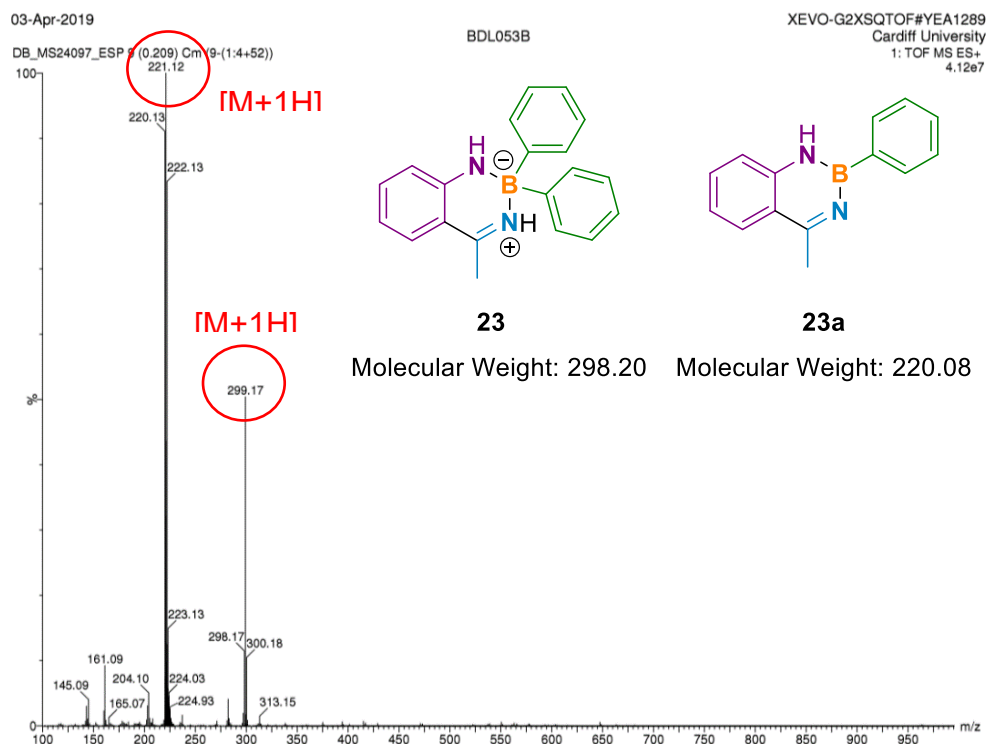


Figure 5.12. Mass spectrometry data for the methyl diphenyl dihydro diazaborinine **23** and methyl phenyl hydro diazaborinine **23a**.

Crystals of the product could be obtained by slow solvent evaporation and the crystal structure was determined by X-ray analysis. A remarkable change from the previous results could be observed, as the NBN heterocyclic ring (Figure 5.13) had formed instead of that observed for NCNB ring.

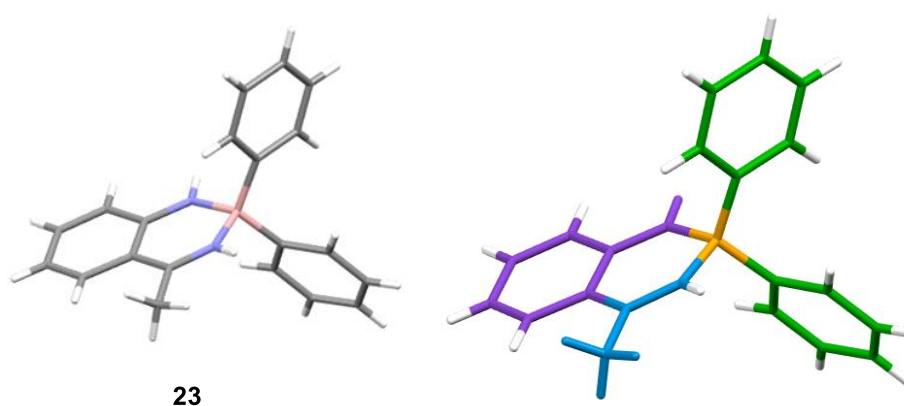


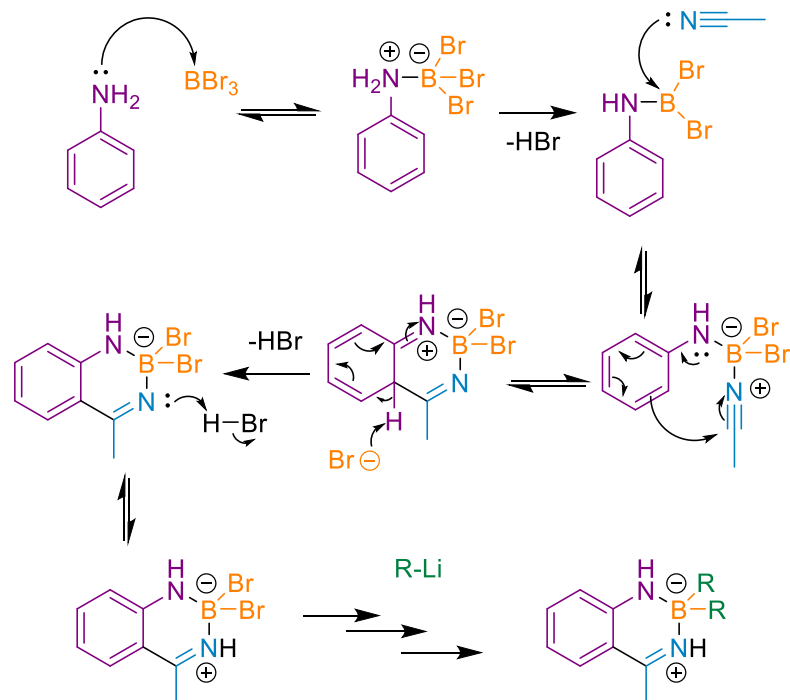
Figure 5.13. Crystal structure of product **23** in a capped sticks interpretation. Space group P1, R-Factor = 5.11%.

In order to interpret this exception, we have to answer two significant questions regarding this reaction. The first one is why the yield of the methyl diphenyl dihydro diazaborinine **23** is relatively low. The second one is why the methyl diphenyl dihydro diazaborinine **23** formed the NBN combination. In table 5.1, the two possible pathways for the reaction are indicated, as shown the order in which the starting materials reacts changes the outcome of the reaction leading to a different heterocycle.

Table 5.1. Interpretation of the different heterocyclic combinations from a mechanistic point of view.

| | Initial reaction | Second reaction | | Product |
|--------------------------------------|--|---------------------------|---|---|
| Pathway A (Sugasawa like pathway) | Amino nucleophile + Electrophile (BBr_3) | Nitrile polarised reagent | ➔ | NBN heterocyclic ring 1,2-azaborinine |
| Pathway B | Nitrile polarised reagent + Electrophile (BBr_3) | Amino nucleophile | | NCNB heterocyclic ring 1,4-azaborinine |

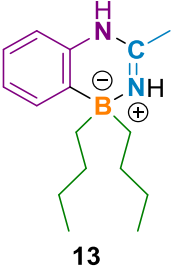
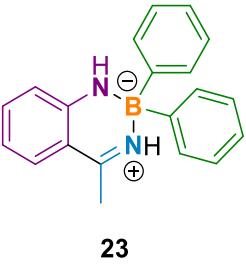
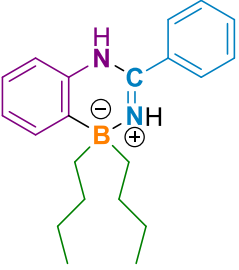
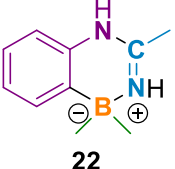
We already know that depending on the reaction order, rings with a different order of heteroatoms (NBN and NCNB) can be formed, as was discussed at the beginning of chapter 3. Obviously, the possible heterocyclic products (NBN and NCNB) are formed before the lithiation quenching step, which means, that the difference in yield would depend on this first stage. If amino nucleophile react with electrophile initially, then it would perform ‘Sugasawa like Pathway A’ (Table 5.1) as below scheme 5.6 and form NBN 1,2-azaborine.



Scheme 5.6. Proposed mechanism for the formation of the NBN 1,2-azaborine product via the Sugasawa like Pathway A.

However, according to a summary of the yields of the obtained heterocyclic products, NCNB formation is more favourable than NBN formation. (Table 5.2) On the other hand, since nitrile polarised reagent was employed not only as reactant but also as the solvent, we used an excess of the nitrile polarised reagent. This chemical environment would push the electrophile to react with the nitrile polarised reagent rather than the amino nucleophile (Pathway B, Table 5.1). As a result, the final product would form NCNB 1,4-azaborinine.

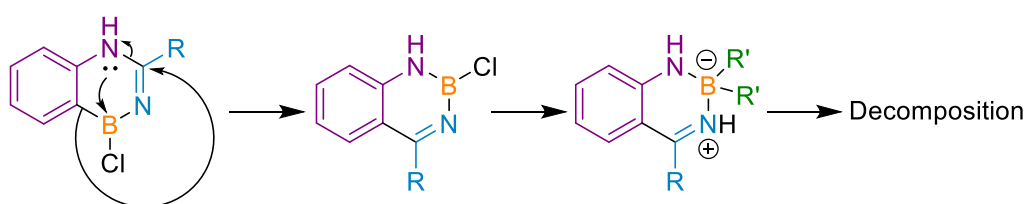
Table 5.2. A summary of the yields of the heteroatomic cyclic ring products.

| NCNB combination | | NBN combination | |
|--|----------------------|---|----------------------|
| Crystal structure of the product | Yield of the product | Crystal structure of the product | Yield of the product |
|  13 | 42% |  23 | 17% |
|  11b | 37% | | |
|  22 | 44% | | |

The only exception to this is product **23**, despite the fact this reaction also used an excess of nitrile reagent. Considering the obtained yield of the heteroatomic ring product is 44%, it is possible that both rings are formed during the first stage. However, the NBN cycle formation should be less favourable due to the excess of nitrile derivative in the solution before the addition of the lithiated reagents. After that, during the last stage, the reaction favours one over the other, leading to a major product. This hypothesis cannot be confirmed as we were always only able to isolate one single product for each reaction. In the case of the methyl diphenyl dihydro diazaborinine **23**, both the NCNB and NBN diazaborinine may have formed. However, considering the phenyl group has a much larger steric hinderance when compared to the linear butyl chain, the

reaction resulting in a NCNB heterocycle will be less favourable than the NBN combination. Indeed, only the NBN product was isolated and with a lower yield than the NCNB products obtained in the other reactions. This suggests that the formation of the NBN cycles might be less favoured under the employed conditions. Although it is quite strange that not even the hydrolysed NCNB product was found, therefore the possible formation of both cycles in the first step remains a hypothesis.

Another possibility is the rearrangement from the NCNB product to the NBN product. (Scheme 5.7)



Scheme 5.7. Rearrangement reaction from NCNB product to NBN product.

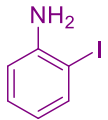
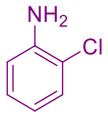

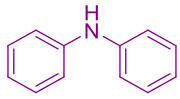

The two phenyl groups in methyl diphenyl dihydro diazaborinine **23** have a large steric hindrance in both NBN and NCNB combinations. This steric hindrance means a halogen-organolithium exchange reaction with PhLi would be less favoured. Thus, this rearrangement reaction could proceed immediately after it fails to react with PhLi. With the rearrangement leading to the NBN combination product becoming the major product and being available for collection. After this rearrangement, the NBN product could be decomposed that could explain relatively lower yield of the NBN product.

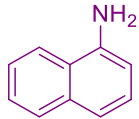
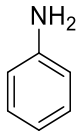
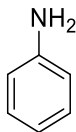
5.4. Conclusion of the exploration stage

In conclusion, we could observe that a NCNB heterocyclic compound could be obtained by the proposed multicomponent reaction when aniline and CH₃CN with either butyllithium or methyllithium were used; or alternatively when aniline, benzonitrile and butyllithium were used. When aniline and CH₃CN were reacted under the same conditions using PhLi, a NBN heterocycle was obtained. The products of these reactions could be crystallised by the slow evaporation

technique using petroleum ether as the solvent, and thus their molecular structure was confirmed by X-ray analysis. From the multicomponent reaction with butyllithium of naphthalen-1-amine and CH₃CN, or aniline and butyronitrile, heterocyclic compounds were formed, as determined by MS analysis, however, they could not be easily isolated, and their structure was not determined. As an interpretation, we hypothesised that both NCNB and NBN heterocycles might be formed in the first stage, however, after the quenching step with lithiated reagents, one of the products is more dominant and can be isolated from the mixture. However, this interpretation still needs to be proved. Furthermore, the rest of the tested reagents, which failed to give the expected heteroatom ring products need to be explored more to understand this new multicomponent reaction better.

Table 5.3. Summary table of reactions in Chapter 5.

| 5.1. Exploring the reaction with different amino-nucleophiles | | | | | |
|---|------------------|-------------------|--------------------|--------------------------|----------------|
| Nucleophiles | Electrophile | Polarised reagent | Lithiation reagent | Heterocyclic ring formed | Crystal formed |
|  | BBr ₃ | MeCN | <i>n</i> -BuLi | No | - |
|  | | | | No | - |
|  | | | | No | - |
|  | | | | No | - |
|  | | | | No | - |

|  | | | | Yes | No |
|---|------------------|--------------------|--------------------|--------------------------|----------------|
| 5.2. Exploring the reaction with different types of nitrile substituted reagents | | | | | |
| Nucleophile | Electrophile | Polarised reagents | Lithiation reagent | Heterocyclic ring formed | Crystal formed |
|  | BBr ₃ | PhCN | <i>n</i> -BuLi | Yes | Yes |
| | | PrCN | | Yes | No |
| 5.3. Exploring the reaction with different types of lithiation reagents | | | | | |
| Nucleophile | Electrophile | Polarised reagents | Lithiation reagent | Heterocyclic ring formed | Crystal formed |
|  | BBr ₃ | MeCN | <i>n</i> -BuLi | Yes | Yes |
| | | | PhLi | Yes | Yes |
| | | | MeLi | Yes | Yes |

References

- 1 S. Park and R. S. Ruoff, *Nat. Nanotechnol.*, 2009, **4**, 217–224.
- 2 F. Schwierz, *Nat. Nanotechnol.*, 2010, **5**, 487–496.
- 3 E. Vessally, S. Soleimani-Amiri, A. Hosseinian, L. Edjlali and A. Bekhradnia, *Appl. Surf. Sci.*, 2017, **396**, 740–745.
- 4 B. Guo, L. Fang, B. Zhang and J. R. Gong, *Insciences J.*, 2011, **1**, 80–89.
- 5 R. Lv and M. Terrones, *Mater. Lett.*, 2012, **78**, 209–218.
- 6 H. Liu, Y. Liu and D. Zhu, *J. Mater. Chem.*, 2011, **21**, 3335–3345.
- 7 X. Wang, G. Sun, P. Routh, D. H. Kim, W. Huang and P. Chen, *Chem. Soc. Rev.*, 2014, **43**, 7067–7098.
- 8 T. Miletić, A. Fermi, I. Orfanos, A. Avramopoulos, F. De Leo, N. Demitri, G. Bergamini, P. Ceroni, M. G. Papadopoulos, S. Couris and D. Bonifazi, *Chem. - A Eur. J.*, 2017, **23**, 2363–2378.
- 9 D. Bonifazi, F. Fasano, M. M. Lorenzo-Garcia, D. Marinelli, H. Oubaha and J. Tasseroul, *Chem. Commun.*, 2015, **51**, 15222–15236.
- 10 J. Dosso, D. Marinelli, N. Demitri and D. Bonifazi, *ACS Omega*, 2019, **4**, 9343–9351.
- 11 T. Saupe, M. A. Zirnstein, H. A. Staab, M. R. Bryce, N. C. Goode, N. Miller, J. Owen, C. Krieger, H. A. Staab, A. M. Malte, W. S. Matthews, Y. Meyers, G. J. Mccollum and J. C. Branca, *Chem. Int. Ed.*, 1989, **1**, 88–90.
- 12 J. Dosso, J. Tasseroul, F. Fasano, D. Marinelli, N. Biot, A. Fermi and D. Bonifazi, *Angew. Chem. Int. Ed.*, 2017, **56**, 4483–4487.
- 13 O. Allemann, S. Duttwyler, P. Romanato, K. K. Baldrige and J. S. Siegel, *Science.*, 2011, **332**, 574–577.
- 14 M. J. S. Dewar and P. A. Marr, *J. Am. Chem. Soc.*, 1962, **84**, 3782–3782.
- 15 A. Stock and E. Pohland, *Chem. Soc.*, 1926, **59**, 2215–2223.

- 16 X.-Y. Wang, J.-Y. Wang and J. Pei, *Chem. - A Eur. J.*, 2015, **21**, 3528–3539.
- 17 G. A. Jeffrey, J. R. Ruble, R. K. McMullan and J. A. Pople, *Proc. R. Soc. A Math. Phys. Sci.*, 1987, **414**, 47–57.
- 18 W. Harshbarger, G. Lee, R. F. Porter and S. H. Bauer, *Inorg. Chem.*, 1969, **8**, 1683–1689.
- 19 D. C. Frost, F. G. Herring, C. A. McDowell and I. A. Stenhouse, *Chem. Phys. Lett.*, 1970, **5**, 291–292.
- 20 J. Zhou, W. Yang, B. Wang and H. Ren, *Angew. Chem. Int. Ed.*, 2012, **51**, 12293–12297.
- 21 L. Ci, L. Song, C. Jin, D. Jariwala, D. Wu, Y. Li, A. Srivastava, Z. F. Wang, K. Storr, L. Balicas, F. Liu and P. M. Ajayan, *Nat. Mater.*, 2010, **9**, 430–435.
- 22 M. Kawaguchi, T. Kawashima and T. Nakajima, *Chem. Mater.*, 1996, **8**, 1197–1201.
- 23 T. P. Kaloni, R. P. Joshi, N. P. Adhikari and U. Schwingenschlögl, *Appl. Phys. Lett.*, 2014, **104**, 73-116.
- 24 M. Haji, *Beilstein J. Org. Chem.*, 2016, **12**, 1269–1301.
- 25 I. Ugi, *Angew. Chem. Int. Ed.*, 1962, **1**, 8–21.
- 26 I. Kanizsai, Z. Szakonyi, R. Sillanpää and F. Fülöp, *Tetrahedron Lett.*, 2006, **47**, 9113–9116.
- 27 U. Kusebauch, B. Beck, K. Messer, E. Herdtweck and A. Dömling, *Org. Lett.*, 2003, **5**, 4021–4024.
- 28 I. Ugi and K. Offermann, *Angew. Chem. Int. Ed.*, 1963, **2**, 624–624.
- 29 I. Ugi and S. Heck, *Comb. Chem.*, 2012, **4**, 1–34.
- 30 C. Iacobucci, S. Reale, J. F. Gal and F. De Angelis, *Org. Chem. - A Eur. J.*, 2014, **14**, 7087–7090.

- 31 A. Dömling, *Chem. Rev.*, 2006, **106**, 17–89.
- 32 C. B. Gilley, M. J. Buller and Y. Kobayashi, *Org. Lett.*, 2007, **9**, 3631–3634.
- 33 R. E. Dolle, B. Le Bourdonnec, G. A. Morales, K. J. Moriarty and J. M. Salvino, *J. Comb. Chem.*, 2006, **8**, 597–635.
- 34 F. Bonnaterre, M. Bois-Choussy and J. Zhu, *Org. Lett.*, 2006, **8**, 4351–4354.
- 35 P. Biginelli and P. Gazz, *Chem.*, 1893, **23**, 360–413.
- 36 C. O. Kappe, *J. Org. Chem.*, 1997, **62**, 7201–7204.
- 37 K. Folkers and T. B. Johnson, *J. Am. Chem. Soc.*, 1933, **55**, 3784–3791.
- 38 F. Sweet and J. D. Fissekis, *J. Am. Chem. Soc.*, 1973, **95**, 8741–8749.
- 39 P. A. Wender, *Nat. Prod. Rep.*, 2014, **31**, 433–440.
- 40 R. O. M. A. De Souza, E. T. Da Penha, H. M. S. Milagre, S. J. Garden, P. M. Esteves, M. N. Eberlin and O. A. C. Antunes, *Chem. - A Eur. J.*, 2009, **15**, 9799–9804.
- 41 T. Sugasawa, T. Toyoda, M. Adachi and K. Sasakura, *J. Am. Chem. Soc.*, 1978, **100**, 4842–4852.
- 42 A. W. Douglas, N. L. Abramson, I. N. Houpis, S. Karady, A. Molina, L. C. Xavier and N. Yasuda, *Tetrahedron Lett.*, 1994, **35**, 6807–6810.
- 43 K. Prasad, G. T. Lee, A. Chaudhary, M. J. Girgis, J. W. Stremke and O. Repič, *Org. Process Res. Dev.*, 2003, **7**, 723–732.
- 44 G. T. Lee, K. Prasad and O. Repič, *Tetrahedron Lett.*, 2002, **43**, 3255–3257.
- 45 A. Neu, T. Mennekes, P. Paetzold, U. Englert, M. Hofmann and P. von Ragué Schleyer, *Inorg. Chem. Acta.*, 2002, **289**, 58–69.

Chapter 6 - Experimental section

6.1. General remarks

Due to the COVID-19 pandemic situation, University of Cardiff was shut down since 23rd of March 2020. Therefore, before start this chapter, I need to inform that there was a limitation for some characterisation of this project.

6.1.1 Instrumentation

Nuclear magnetic resonance (NMR) ^1H , ^{13}C and ^{11}B spectra were obtained on a Bruker Fourier 300 MHz spectrometer equipped with a dual (^{13}C , ^1H) probe, Bruker DPX 400 MHz with (^{11}B , ^{13}C , ^1H) or a Bruker AVANCE III HD 500 MHz NMR spectrometer equipped with a Broadband multinuclear (BBFO) SmartProbe™. ^1H spectra were obtained at 300 MHz or 400 MHz, ^{13}C spectra were obtained at 400 MHz and ^{11}B spectra were obtained at 400MHz and 500MHz. All spectra were measured at room temperature (r.t.). Chemical shifts were reported in ppm according to tetramethylsilane (TMS) using the solvent residual signal as an internal reference (CDCl_3 : $\delta_{\text{H}} = 7.26$ ppm, $\delta_{\text{C}} = 77.16$ ppm, Acetone: $\delta_{\text{H}} = 2.05$ ppm, $\delta_{\text{C}} = 29.9, 206.7$ ppm). Coupling constants (J) were given in Hz. Resonance multiplicity was described as s (singlet), d (doublet), t (triplet), dd (doublet of doublets) and m (multiplet). Carbon and boron spectra were measured with a complete decoupling for the proton.

Infrared spectra (IR) could not be measured as the laboratories were closed due to the Coronavirus-19 emergency.

Mass spectrometry (MS) (i) High-resolution ESI mass spectra (HRMS) were performed on a Waters LCT HR TOF mass spectrometer in the positive or negative ion mode.

Thin-layer chromatography (TLC) was conducted on a pre-coated aluminium sheet with 0.20 mm Merk Millipore Silica gel 60 with fluorescent indicator F254.

Column chromatography was carried out using Merck Gerduran silica gel 60 (particle size 40-63 μm)

Melting point (mp) could not be measured as the laboratories were closed due to the Coronavirus-19 emergency.

X-ray diffraction

Crystallographic studies were undertaken on single crystal mounted in paratone and studied on an Agilent SuperNova Dual three-circle diffractometer using Cu-K α ($\lambda = 1.540598 \text{ \AA}$) or Mo-K α ($\lambda = 0.7093187 \text{ \AA}$) radiation and a CCD detector. Measurements were typically made at 150(2) K with temperatures maintained using an Oxford Cryostream unless otherwise stated. Data was collected, integrated and corrected for absorption using a numerical absorption correction based on gaussian integration over a multifaceted crystal model within CrysAlisPro. The structures were solved by direct methods and refined against F^2 within SHELXL-2013.

6.1.2 Material and methods

Chemicals were purchased from *Sigma Aldrich*, *Acros Organics*, *TCI* and *Alfa Aesar* and used as received. Solvents were purchased from *Fluorochem* and *Sigma Aldrich*, while deuterated solvents were from *Eurisotop* and *Sigma Aldrich*. THF and toluene were dried on a Braun MB SPS-800 solvent purification system and further dried over activated 4 \AA molecular sieves.

Low-temperature baths were prepared using different solvent mixtures depending on the desired temperature: -84 $^{\circ}\text{C}$ with Ethyl acetate/liq. N $_2$, and 0 $^{\circ}\text{C}$ with ice/H $_2\text{O}$.

Anhydrous conditions were achieved by putting all glassware in the oven at 140 $^{\circ}\text{C}$ for at least 12 h before allowing it to cool down under vacuum, followed by drying Schlenk tubes and two neck flasks by a flame with a heat gun under vacuum and purging with nitrogen.

The inert atmosphere was maintained using Nitrogen-filled balloons equipped with a syringe and needle that was used to penetrate the silicon stoppers used to close the flask's necks.

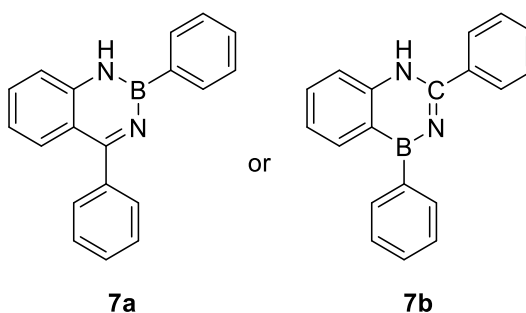
Additions of liquid reagents were performed using dried plastic or glass syringes.

Degassing of solutions was performed using the *Freeze-pump-thaw* (fpt) procedure: solutions were frozen using liquid nitrogen and kept under vacuum for 10 min before thawing.

Molecular sieves (3 and 4 Å) were activated by heating at 180 °C under vacuum overnight and by further heating with a heat gun under vacuum immediately before use.

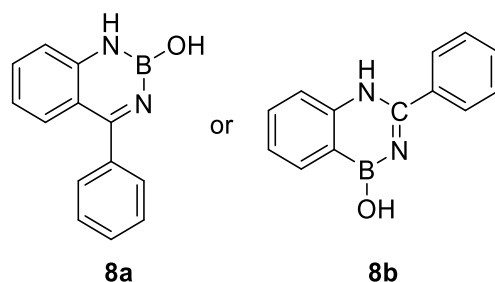
6.2. Experiment details

6.2.1. Synthesis of the diphenyl diazaborinine 7a or 7b



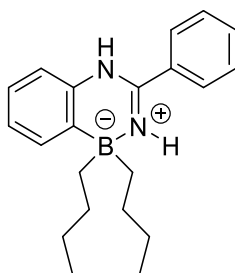
All the steps of this reaction were performed under an inert atmosphere. In a flame dried Schlenk tube, 0.3 g (3.22 mmol) of aniline was dissolved in dry PhCN (4 ml) and the resulting solution cooled to 0 °C using an ice bath. PhBCl₂ (3.86 ml, 3.86 mmol, 1M in DCM) was added dropwise and the resulting suspension stirred at the same temperature for 10 min. The Schlenk tube was then equipped with a condenser and the solution refluxed for 16 h. After refluxing, the reaction mixture cooled down and diluted in EtOAc (50 ml) and the organic layer was washed with H₂O (50 mL × 2) and brine (50 ml). The obtained crude product was purified by silica gel column chromatography (Petroleum ether /EtOAc, 8:2). ¹¹B NMR (400 MHz, CDCl₃) δ: 29.6.

6.2.2. Synthesis of the phenyl diazaborininol 8a or 8b



All the steps of this reaction were performed under an inert atmosphere. In a flame dried Schlenk tube, 0.3 g (3.22 mmol) of aniline and 0.37 ml (3.54 mmol) of PhCN were dissolved in dry toluene (4 ml) and the resulting solution cooled to 0 °C using an ice bath. BCl₃ (3.86 ml, 3.86 mmol, 1M in heptane) was added dropwise and the resulting suspension stirred at the same temperature for 10 min. The Schlenk tube was then equipped with a condenser and the solution refluxed for 16 h. After refluxing, the reaction mixture cooled down and diluted in EtOAc (50 ml) and the organic layer was washed with H₂O (50 mL × 2) and brine (50 ml). The obtained crude product was purified by silica gel column chromatography (Petroleum ether /EtOAc, 8:2). ¹¹B NMR (500 MHz, CDCl₃) δ: 18.9.

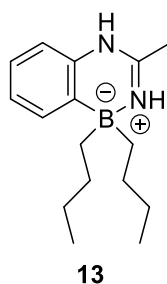
6.2.3. Synthesis of the dibutyl phenyl dihydro diazaborinine 11b



11b

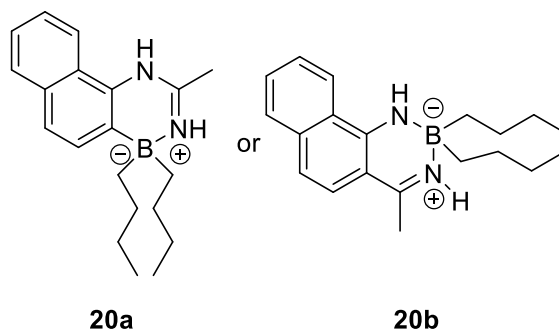
All the steps of this reaction were performed under an inert atmosphere. In a flame dried Schlenk tube, 0.3 g (3.22 mmol) of aniline was dissolved in dry PhCN (4 ml) and the resulting solution cooled to 0 °C using an ice bath. BBr₃ (3.86 ml, 3.86 mmol, 1M in DCM) was added dropwise and the resulting suspension stirred at the same temperature for 10 min. The Schlenk tube was then equipped with a condenser and the solution refluxed for 16 h. After the reflux, the remained PhCN solvent was removed completely by distillation. In parallel, dry THF (6 ml) was added to a flame dried Schlenk tube and the solution cooled to -84 °C using an EtOAc/N₂ bath. *n*-BuLi (2 ml, 3.2 mmol, 1.6 M in hexane) was added, and the reaction stirred at the same temperature for 10 min. The solution containing the organolithium derivative was cannulated into the diazaborinine crude and the resulting mixture stirred for 30 min at -84 °C, 30 min at 0 °C and for 16 h at r.t. The reaction was diluted in EtOAc (50 ml) and the organic layer washed with H₂O (50 mL × 2) and brine (50 ml). The obtained crude product was purified by silica gel column chromatography (Petroleum ether /EtOAc, 8:2). The organic layer was evaporated under vacuum then a colourless liquid was obtained (381.6 mg, 37%). ¹H NMR (300 MHz, CDCl₃) δ: 7.60 (m, 5H), 7.29 (dd, *J* = 7.1, 1.7 Hz, 1H), 7.06 (dtd, *J* = 16.6, 7.3, 1.5 Hz, 1H), 6.94 (s, *J* = 16.0 Hz, 1H), 6.64 (dd, *J* = 7.6, 1.0 Hz, 1H), 6.20 (s, 1H), 1.26 (m, 4H), 1.05 (m, 4H), 0.82 (t, *J* = 7.2 Hz, 6H), 0.43 (m, 4H). ¹³C NMR (400 MHz, CDCl₃) δ: 157.7, 137.0, 133.0, 132.5, 132.5, 129.8, 125.9, 125.3, 124.6, 113.7, 29.7, 27.1, 14.5. ¹¹B NMR (500 MHz, CDCl₃) δ: -6.5.

6.2.4. Synthesis of the dibutyl methyl dihydro diazaborinine 13



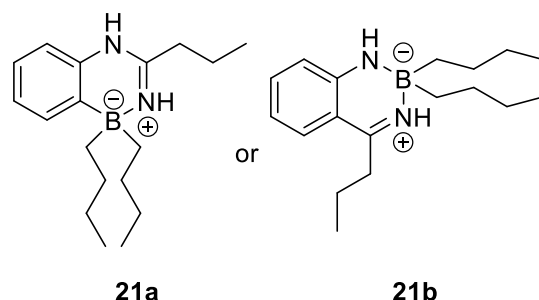
All the steps of this reaction were performed under an inert atmosphere. In a flame dried Schlenk tube, 0.3 g (3.22 mmol) of aniline was dissolved in dry CH₃CN (4 ml) and the resulting solution cooled to 0 °C using an ice bath. BBr₃ (3.86 ml, 3.86 mmol, 1M in DCM) was added dropwise and the resulting suspension stirred at the same temperature for 10 min. The Schlenk tube was then equipped with a condenser and the solution refluxed for 16 h. After the reflux, the remained CH₃CN solvent was removed completely by distillation. In parallel, dry THF (6 ml) was added to a flame dried Schlenk tube and the solution cooled to -84 °C using an EtOAc/N₂ bath. *n*-BuLi (6 ml, 9.6 mmol, 1.6 M in hexane) was added, and the reaction stirred at the same temperature for 10 min. The solution containing the organolithium derivative was cannulated into the diazaborinine crude and the resulting mixture stirred for 30 min at -84 °C, 30 min at 0 °C and for 16 h at r.t. The reaction was diluted in EtOAc (50 ml) and the organic layer washed with H₂O (50 mL × 2) and brine (50 ml). The obtained crude product was purified by silica gel column chromatography (Petroleum ether /EtOAc, 8:2). The organic layer was evaporated under vacuum then a colourless liquid was extracted (349 mg, 42%). ¹H NMR (300 MHz, CDCl₃) δ: 7.24 (dd, *J* = 7.1, 1.6 Hz, 1 H), 7.01 (dtd, *J* = 16.6, 7.3, 1.4 Hz, 2H), 6.59 (s, 1 H), 6.51 (dd, *J* = 7.6, 1.1 Hz, 1 H), 5.82 (s, 1 H), 1.21 (m, 4 H), 1.00 (m, 4 H), 0.82 (t, *J* = 7.3 Hz, 6 H), 0.34 (dtd, *J* = 25.1, 13.4, 4.8 Hz, 4H). ¹³C NMR (500 MHz, CDCl₃) δ: 156.1, 136.8, 132.5, 129.4, 124.9, 124.4, 115.2, 113.1, 29.6, 27.1, 22.1, 14.5. ¹¹B NMR (500 MHz, CDCl₃) δ: -7.0.

6.2.5. Synthesis of the dibutyl methyl dihydro naphthodiazaborinine 20a or 20b



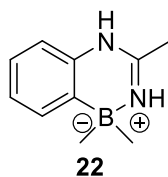
All the steps of this reaction were performed under an inert atmosphere. In a flame dried Schlenk tube, 0.461 g (3.22 mmol) of naphthalen-1-amine was dissolved in dry CH₃CN (4 ml) and the resulting solution cooled to 0 °C using an ice bath. BBr₃ (3.86 ml, 3.86 mmol, 1M in DCM) was added dropwise and the resulting suspension stirred at the same temperature for 10 min. The Schlenk tube was then equipped with a condenser and the solution refluxed for 16 h. After the reflux, the remained CH₃CN solvent was removed completely by distillation. In parallel, dry THF (6 ml) was added to a flame dried Schlenk tube and the solution cooled to -84 °C using an EtOAc/N₂ bath. *n*-BuLi (6 ml, 9.6 mmol, 1.6 M in hexane) was added, and the reaction stirred at the same temperature for 10 min. The solution containing the organolithium derivative was cannulated into the diazaborinine crude and the resulting mixture stirred for 30 min at -84 °C, 30 min at 0 °C and for 16 h at r.t. The reaction was diluted in EtOAc (50 ml) and the organic layer washed with H₂O (50 mL × 2) and brine (50 ml). The obtained crude product was purified by silica gel column chromatography (Petroleum ether /EtOAc, 8:2). The organic layer was evaporated under vacuum then a colourless liquid was extracted (139 mg, 14%) ¹H NMR (300 MHz, CDCl₃) δ: z 7.81 (m, 1H), 7.57 (m, 2H), 7.48 (m, 2H), 7.37 (m, 1H), 7.32 (s, *J* = 6.2 Hz, 1H), 5.91 (d, *J* = 39.5 Hz, 1H), 2.30 (d, *J* = 0.5 Hz, 3H), 1.22 (m, 4H), 0.93 (m, 4H), 0.81 (t, *J* = 7.3 Hz, 6H), 0.42 (m, 4H). ¹³C NMR (500 MHz, CDCl₃) δ: 171.31, 156.42, 132.16, 130.97, 129.93, 129.10, 125.40, 124.04, 123.83, 121.01, 116.99, 29.77, 27.04, 22.27, 14.41. ¹¹B NMR (500 MHz, CDCl₃) δ: -6.52.

6.2.6. Synthesis of the dibutyl propyl dihydro diazaborinine 21a or 21b



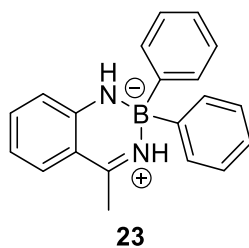
All the steps of this reaction were performed under an inert atmosphere. In a flame dried Schlenk tube, 0.3 g (3.22 mmol) of aniline was dissolved in dry PrCN (4 ml) and the resulting solution cooled to 0 °C using an ice bath. BBr₃ (3.86 ml, 3.86 mmol, 1M in DCM) was added dropwise and the resulting suspension stirred at the same temperature for 10 min. The Schlenk tube was then equipped with a condenser and the solution refluxed for 16 h. After the reflux, the remained PrCN solvent was removed completely by distillation. In parallel, dry THF (6 ml) was added to a flame dried Schlenk tube and the solution cooled to -84 °C using an EtOAc/N₂ bath. *n*-BuLi (6 ml, 9.6 mmol, 1.6 M in hexane) was added, and the reaction stirred at the same temperature for 10 min. The solution containing the organolithium derivative was cannulated into the diazaborinine crude and the resulting mixture stirred for 30 min at -84 °C, 30 min at 0 °C and for 16 h at r.t. The reaction was diluted in EtOAc (50 ml) and the organic layer washed with H₂O (50 mL × 2) and brine (50 ml). The obtained crude product was purified by silica gel column chromatography (Petroleum ether /EtOAc, 8:2). The organic layer was evaporated under vacuum then a colourless liquid was extracted (64.5 mg, 7%). ¹H NMR (300 MHz, CDCl₃) δ: 7.24 (m, 1H), 7.01 (dtd, *J* = 16.6, 7.3, 1.5 Hz, 2H), 6.72 (s, 1H), 6.53 (dd, *J* = 7.5, 1.1 Hz, 1H), 5.82 (s, 1H), 2.32 (m, 2H), 1.72 (m, 2H), 1.23 (m, 4H), 1.07 (m, 4H), 0.93 (m, 3H), 0.82 (t, *J* = 7.4 Hz, 6H), 0.35 (m, 4H). ¹³C NMR (500 MHz, CDCl₃) δ: 159.7, 137.0, 132.4, 124.8, 124.4, 113.2, 44.8, 42.7, 37.4, 29.7, 27.1, 26.1, 22.4, 20.1, 17.4, 14.5, 13.9, 13.8, 13.3. ¹¹B NMR (500 MHz, CDCl₃) δ: -7.1.

6.2.7. Synthesis of the trimethyl dihydro diazaborinine 22



All the steps of this reaction were performed under an inert atmosphere. In a flame dried Schlenk tube, 0.3 g (3.22 mmol) of aniline was dissolved in dry CH₃CN (4 ml) and the resulting solution cooled to 0 °C using an ice bath. BBr₃ (3.86 ml, 3.86 mmol, 1M in DCM) was added dropwise and the resulting suspension stirred at the same temperature for 10 min. The Schlenk tube was then equipped with a condenser and the solution refluxed for 16 h. After the reflux, the remained CH₃CN solvent was removed completely by distillation. In parallel, dry THF (6 ml) was added to a flame dried Schlenk tube and the solution cooled to -84 °C using an EtOAc/N₂ bath. MeLi (6 ml, 9.6 mmol, 1.6 M in diethyl ether) was added, and the reaction stirred at the same temperature for 10 min. The solution containing the organolithium derivative was cannulated into the diazaborinine crude and the resulting mixture stirred for 30 min at -84 °C, 30 min at 0 °C and for 16 h at r.t. The reaction was diluted in EtOAc (50 ml) the organic layer washed with H₂O (50 mL × 2) and brine (50 ml). The obtained crude product was purified by silica gel column chromatography (Petroleum ether /EtOAc, 8:2). The organic layer was evaporated under vacuum then a colourless liquid was extracted (246 mg, 44%). ¹H NMR (300 MHz, Acetone) δ: 9.01 (s, 1 H), 7.41 (s, *J* = 9.3, 5.3 Hz, 1 H), 7.33 (m, 1 H), 7.06 (m, 2 H), 6.79 (m, 1 H), 2.39 (d, *J* = 0.6 Hz, 3 H), 0.00 (s, 6 H) ¹³C NMR (500 MHz, Acetone) δ: 156.4, 137.3, 131.8, 124.0, 123.9, 113.3, 19.8 ¹¹B NMR (500 MHz, Acetone) δ: -9.7.

6.2.8. Synthesis of the methyl diphenyl dihydro diazaborinine 23



All the steps of this reaction were performed under an inert atmosphere. In a flame dried Schlenk tube, 0.3 g (3.22 mmol) of aniline was dissolved in dry CH₃CN (4 ml) and the resulting solution cooled to 0 °C using an ice bath. BBr₃ (3.86 ml, 3.86 mmol, 1M in DCM) was added dropwise and the resulting suspension stirred at the same temperature for 10 min. The Schlenk tube was then equipped with a condenser and the solution refluxed for 16 h. After the reflux, the remained CH₃CN solvent was removed completely by distillation. In parallel, dry THF (6 ml) was added to a flame dried Schlenk. The Schlenk tube was cooled to -84 °C using an EtOAc/N₂ bath. PhLi (5 ml, 9.6 mmol, 1.9 M in dibutyl ether) was then added carefully, and the reaction was stirred at the same temperature for 10 min. The solution containing the lithiated derivative was annulated in the diazaborinine crude and the resulting mixture stirred for 30 min at -84 °C, 30 min at 0 °C and for 16 h at r.t. The reaction was diluted in EtOAc (50 ml) and the organic layer washed with H₂O (50 mL × 2) and brine (50 ml). The obtained crude product was purified by silica gel column chromatography (Petroleum ether /EtOAc, 8:2). The organic layer was evaporated under vacuum then a colourless liquid was extracted (163 mg, 17%). ¹H NMR (300 MHz, Acetone) δ: 9.39 (s, 1H), 7.90 (s, 1H), 7.25 (m, 4H), 7.17 (dd, *J* = 7.0, 1.7 Hz, 1H), 7.07 (m, 4H), 6.93 (m, 4H), 6.77(m, 1H), 2.38 (d, *J* = 0.5 Hz, 3H) ¹³C NMR (500 MHz, Acetone) δ: 157.4, 137.6, 134.3, 133.3, 126.5, 125.0, 124.0, 123.9, 114.0, 19.8. ¹¹B NMR (500 MHz, Acetone) δ: -6.6.

6.3. NMR-HRMS spectroscopic characterization (^1H , ^{13}C , ^{11}B , LRMS, HRMS)

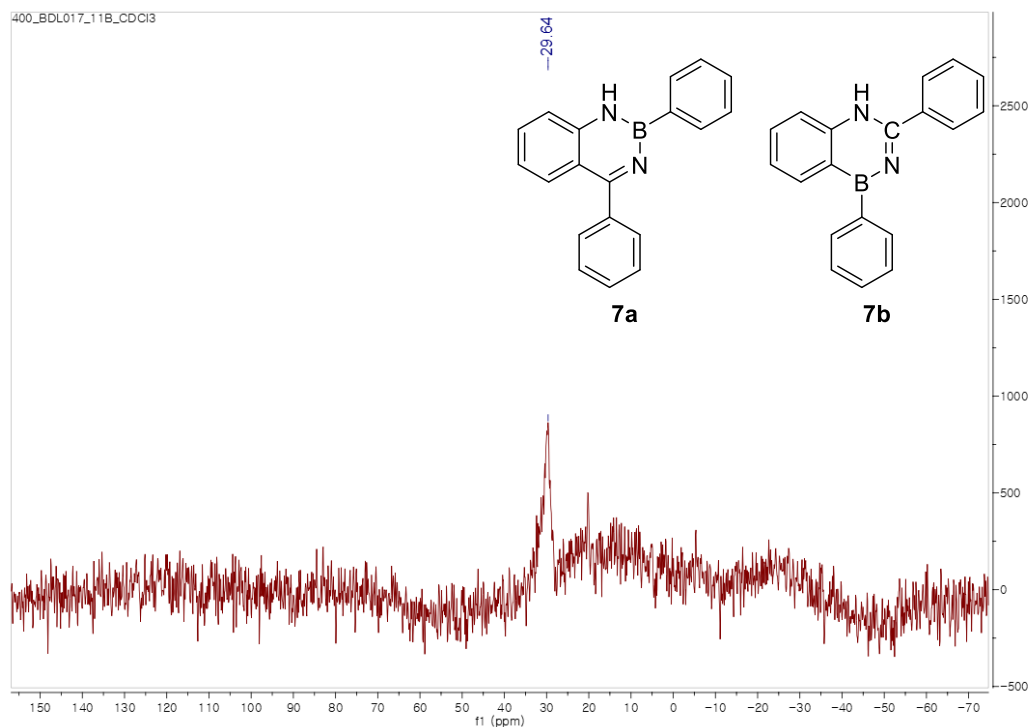


Figure 6.1. ^{11}B NMR of the diphenyl diazaborinine **7a** or **7b**.

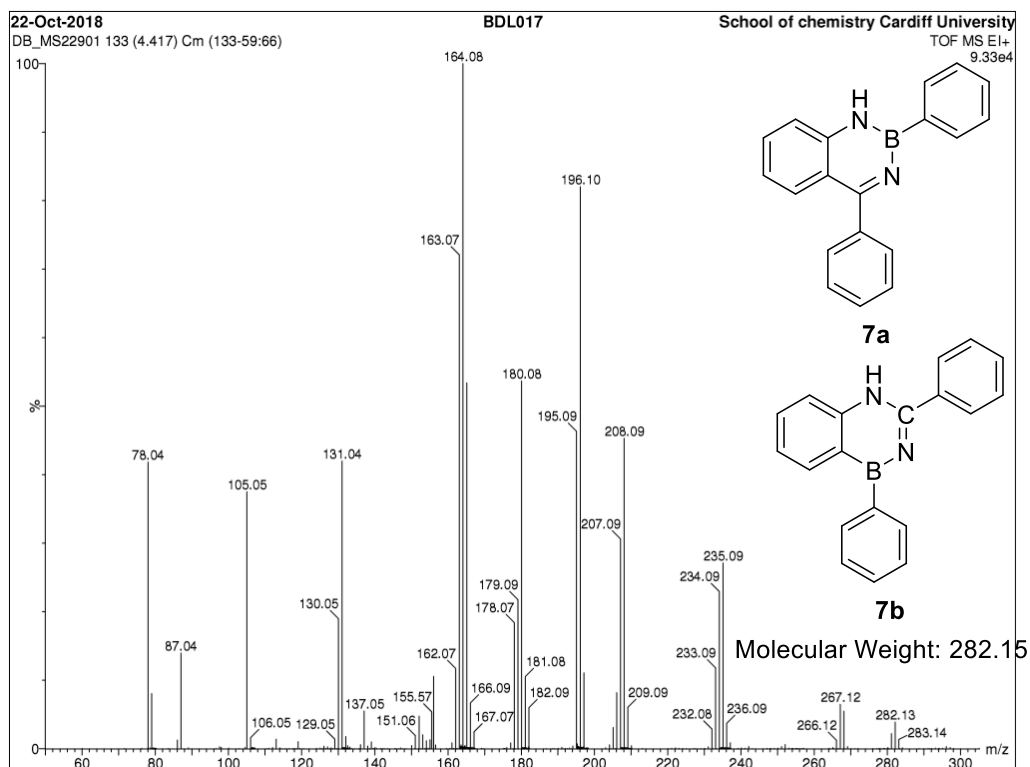


Figure 6.2. MS spectrometry data of the diphenyl diazaborinine **7a** or **7b**.

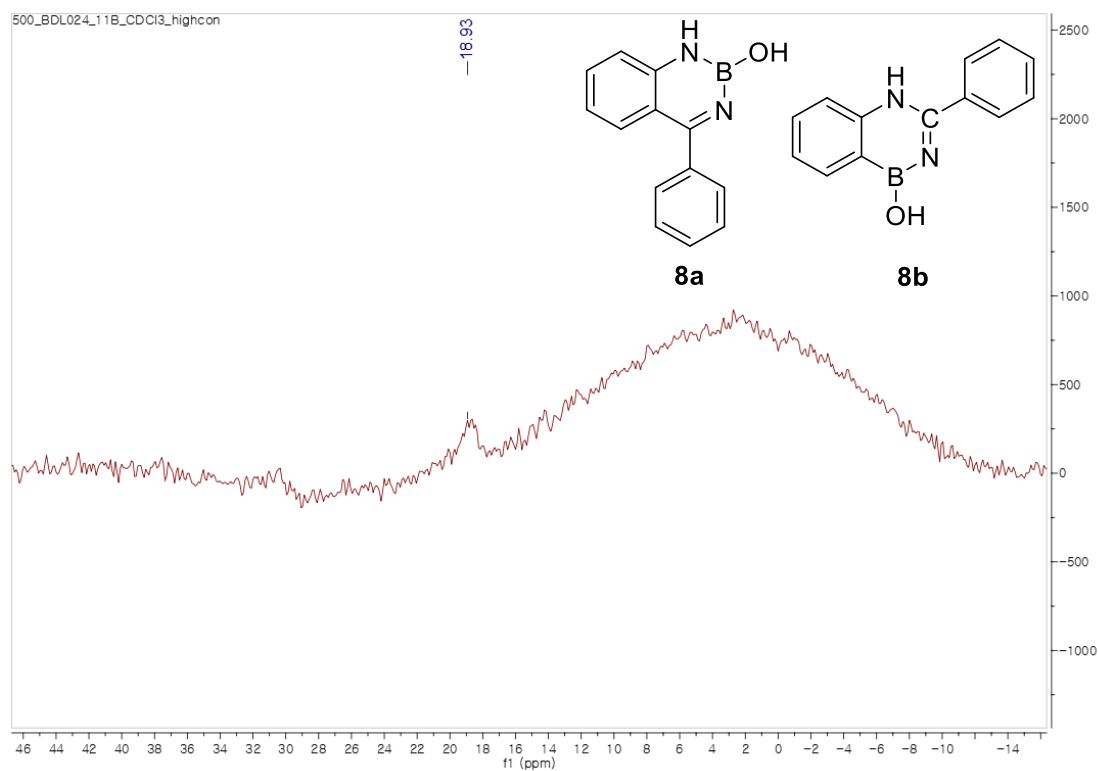


Figure 6.3. ^{11}B NMR of the hydrolysed diazaborinine **8a** or **8b**.

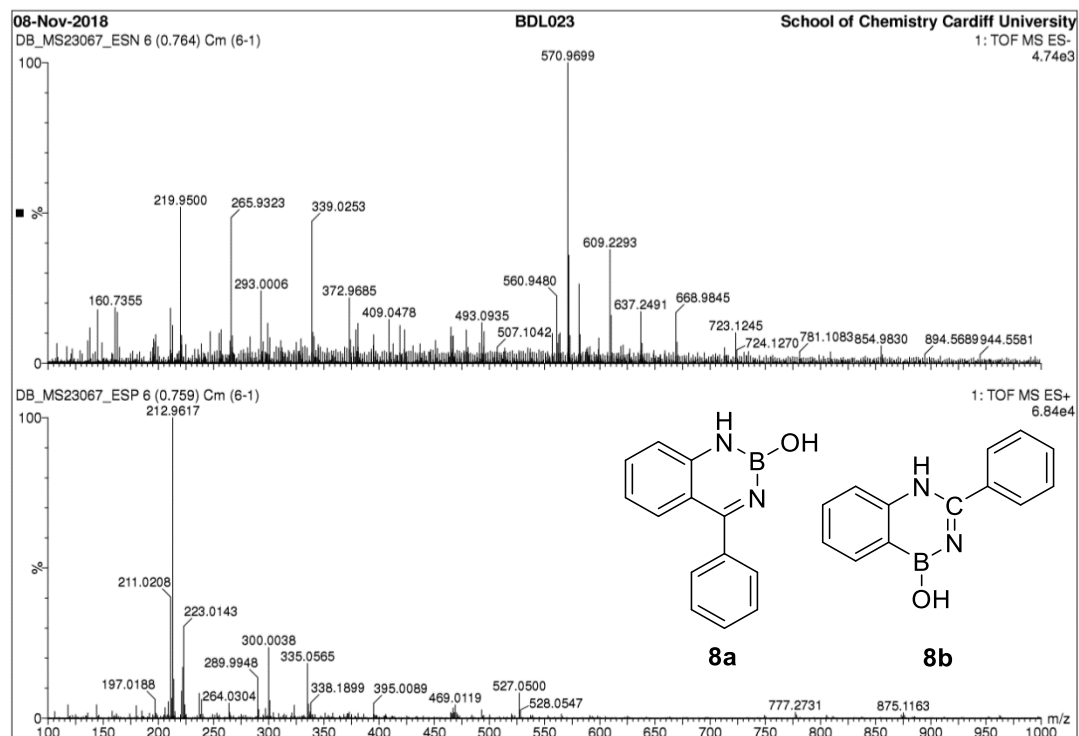


Figure 6.4. MS spectrometry data of the hydrolysed diazaborinine **8a** or **8b**.

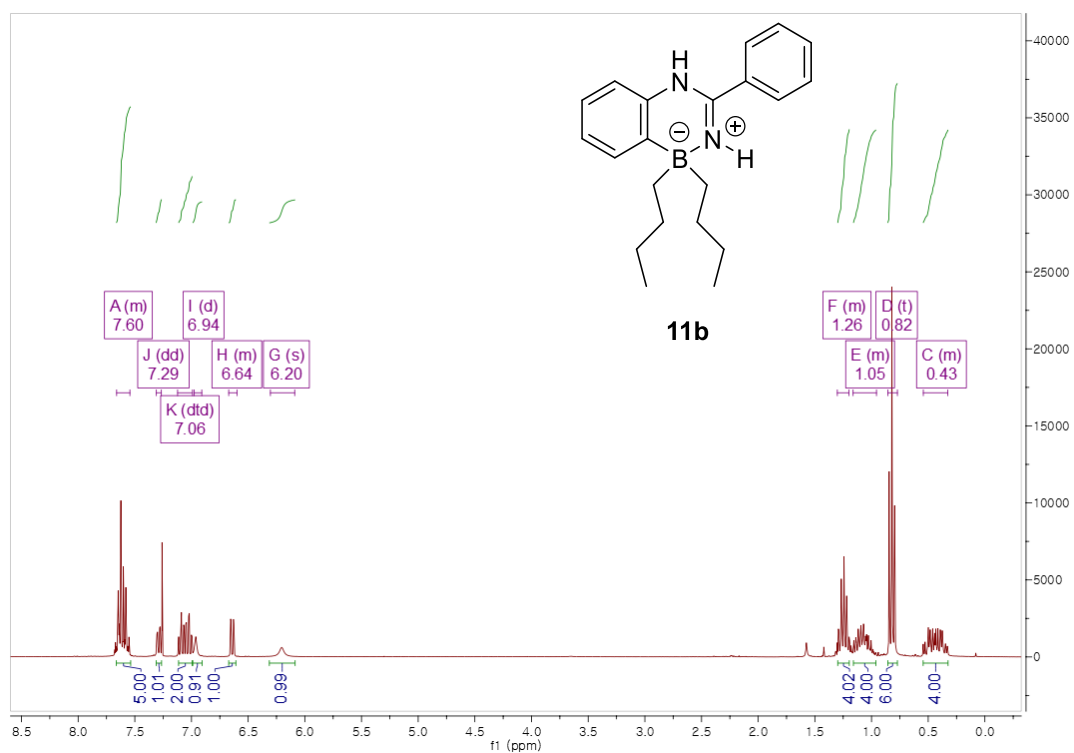


Figure 6.5. ^1H NMR data of the dibutyl phenyl dihydro diazaborinine **11b** in CDCl_3 (Solvent residual peak: 7.26 ppm).

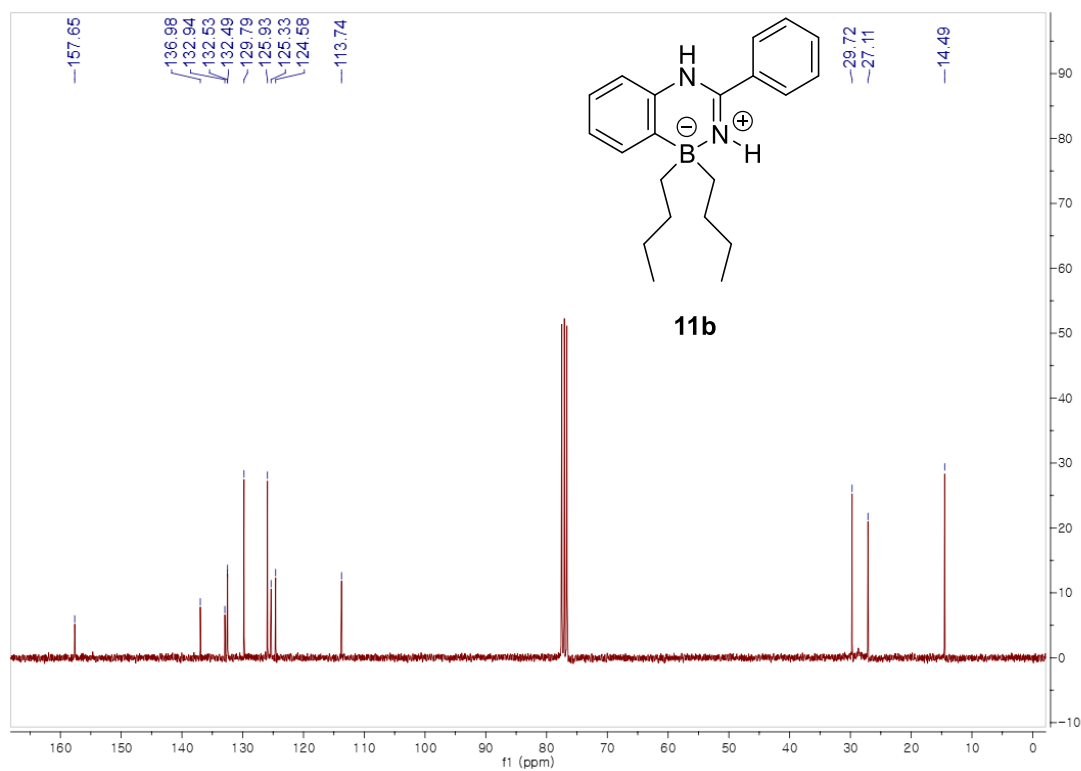


Figure 6.6. ^{13}C NMR data of the dibutyl phenyl dihydro diazaborinine **11b** in CDCl_3 (Solvent residual peak: 77.2 ppm).

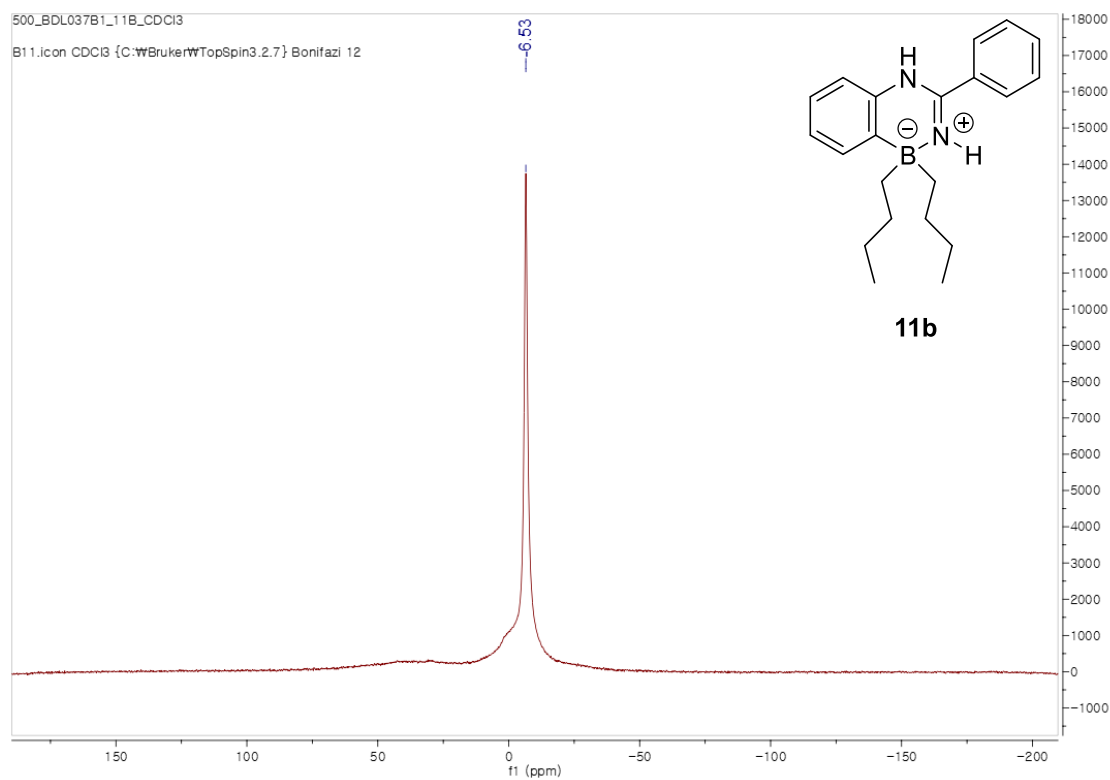


Figure 6.7. ^{11}B NMR data of the dibutyl phenyl dihydro diazaborinine **11b**.

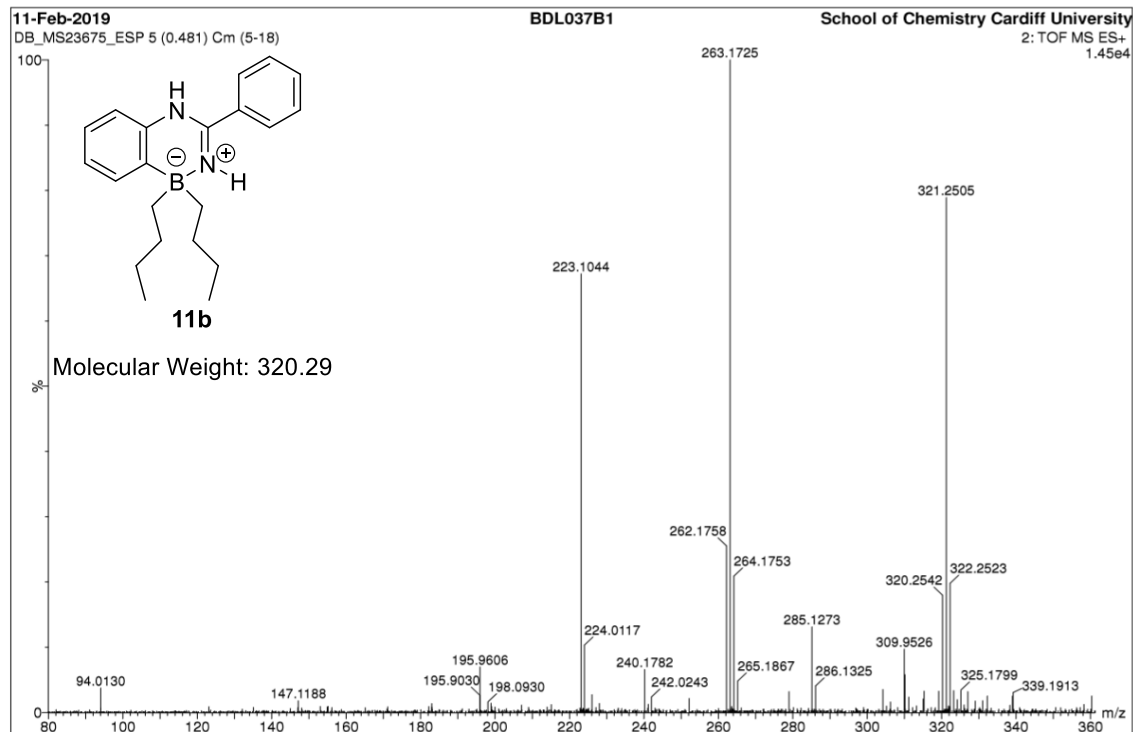


Figure 6.8. MS spectrometry data of the dibutyl phenyl dihydro diazaborinine **11b**.

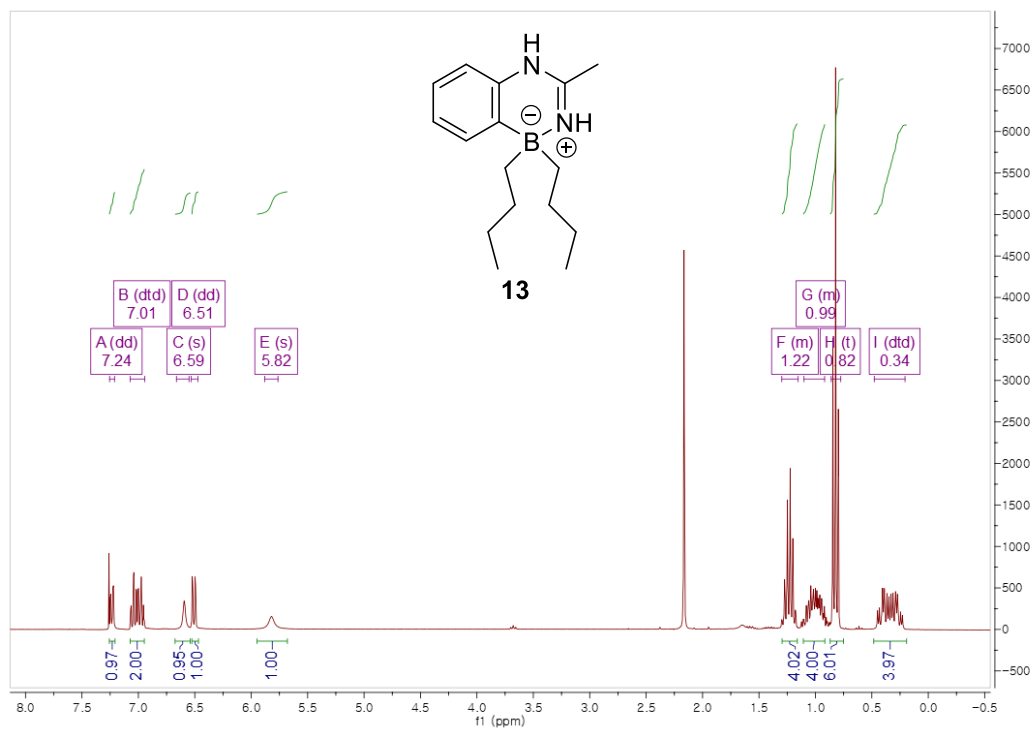


Figure 6.9. ^1H NMR data of the dibutyl methyl dihydro diazaborinine **13** in CDCl_3 (Solvent residual peak: 7.26 ppm).

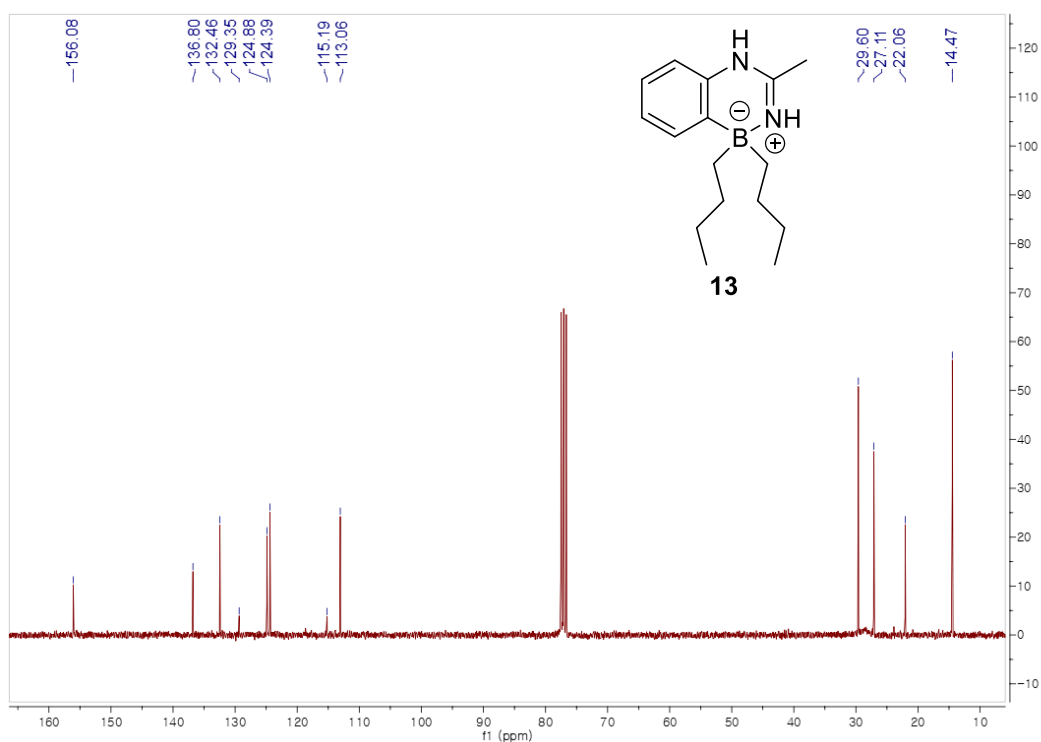


Figure 6.10. ^{13}C NMR data of the dibutyl methyl dihydro diazaborinine **13** in CDCl_3 (Solvent residual peak: 77.2 ppm).

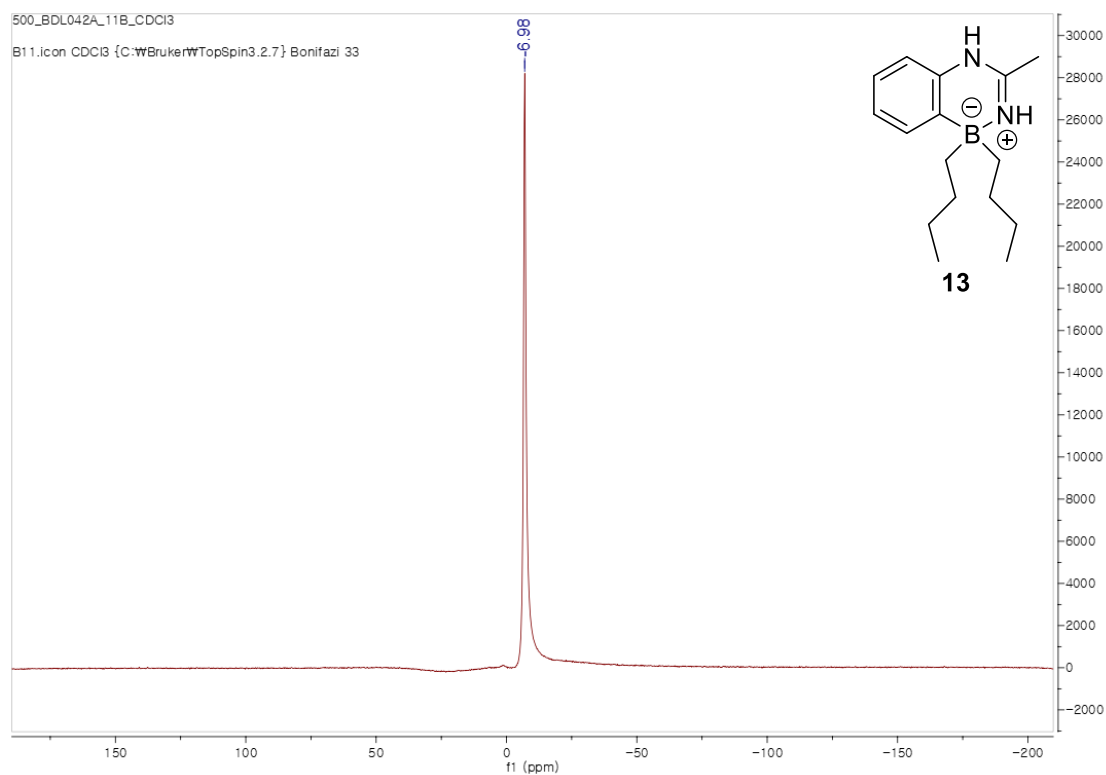


Figure 6.11. ^{11}B NMR data of the dibutyl methyl dihydro diazaborinine **13**.

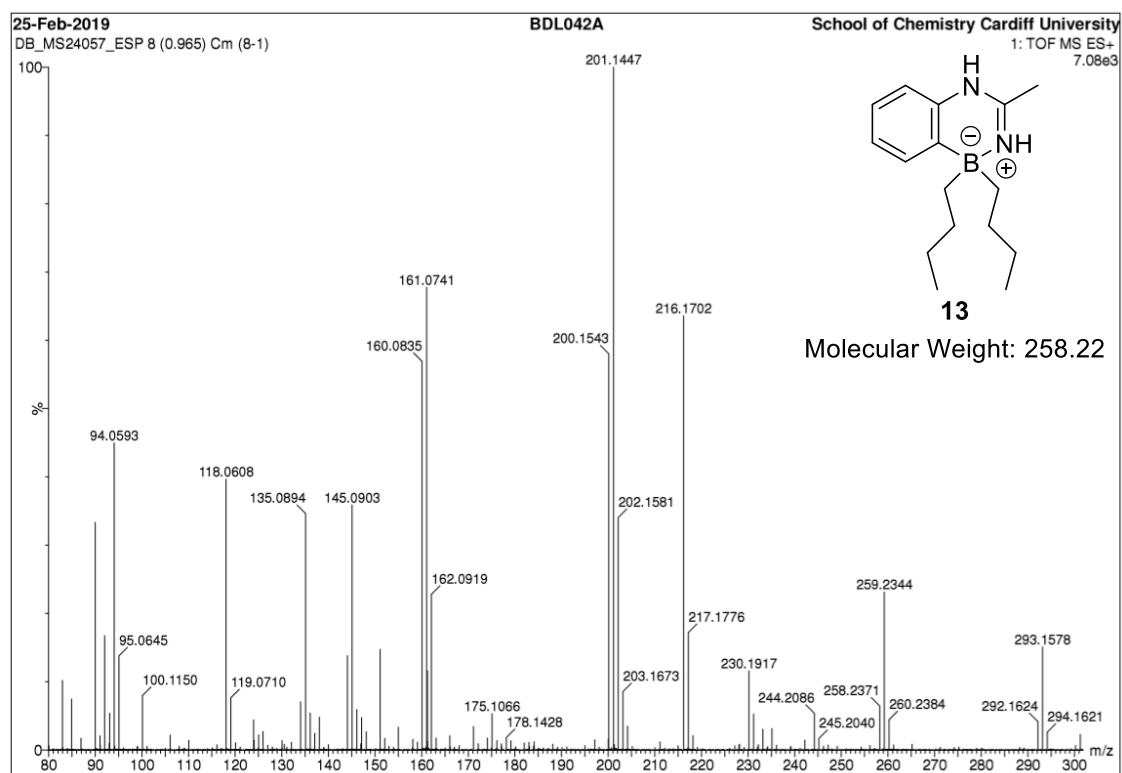


Figure 6.12. MS spectrometry data of the dibutyl methyl dihydro diazaborinine **13**.

Single Mass Analysis

Tolerance = 5.0 PPM / DBE: min = -1.5, max = 100.0

Element prediction: Off

Number of isotope peaks used for i-FIT = 9

Monoisotopic Mass, Even Electron Ions

4 formula(e) evaluated with 1 results within limits (up to 50 best isotopic matches for each mass)

Elements Used:

C: 0-16 H: 0-28 N: 0-2 11B: 0-1

25-Feb-2019

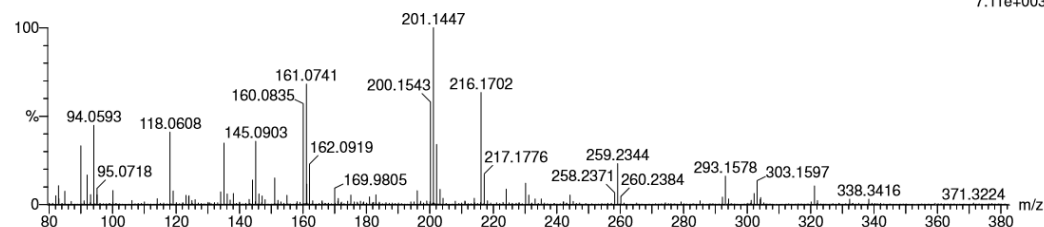
BDL042A

School of Chemistry Cardiff University

DB_MS24057_ESP 8 (0.965)

1: TOF MS ES+

7.11e+003



Minimum:

Maximum: 5.0 5.0 -1.5

Mass Calc. Mass mDa PPM DBE i-FIT i-FIT (Norm) Formula

| Mass | Calc. Mass | mDa | PPM | DBE | i-FIT | i-FIT (Norm) | Formula |
|----------|------------|------|------|-----|-------|--------------|----------------|
| 259.2344 | 259.2346 | -0.2 | -0.8 | 4.5 | 325.7 | 0.0 | C16 H28 N2 11B |

Figure 6.13. Single Mass analysis for elemental composition report of the dibutyl methyl dihydro diazaborinine **13**.

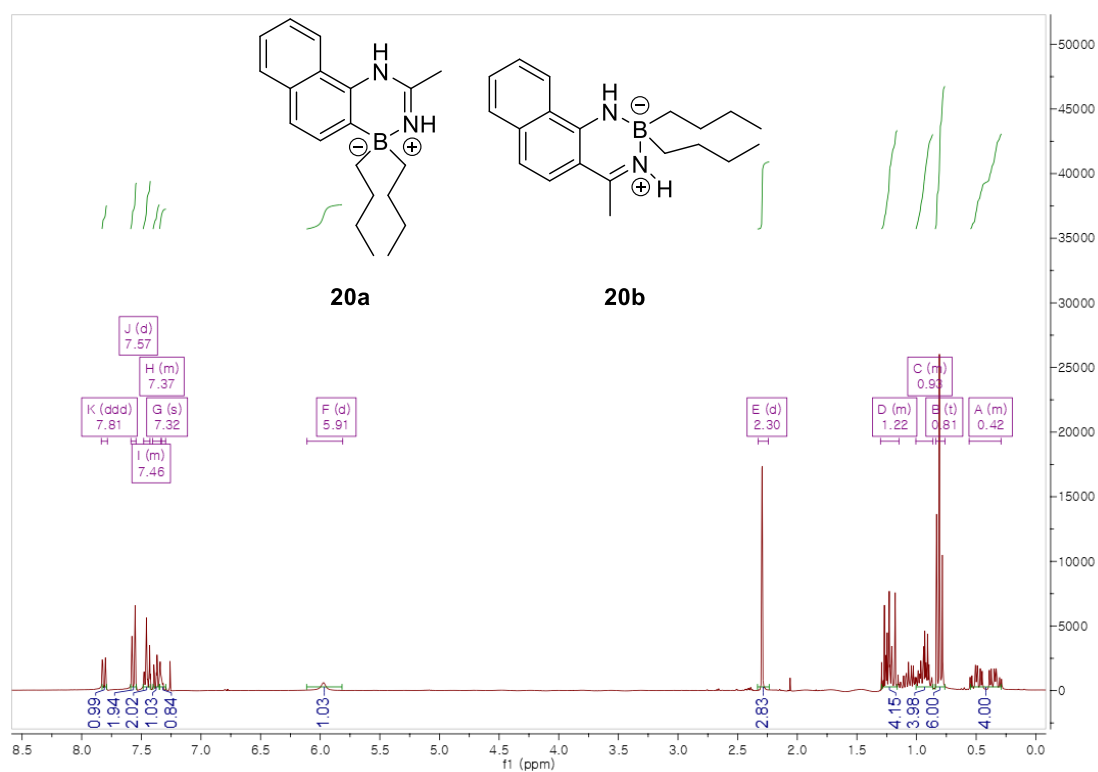


Figure 6.14. ^1H NMR data of the naphthodiazaborinine **20a** or **20b**.in CDCl_3 (Solvent residual peak: 7.26 ppm).

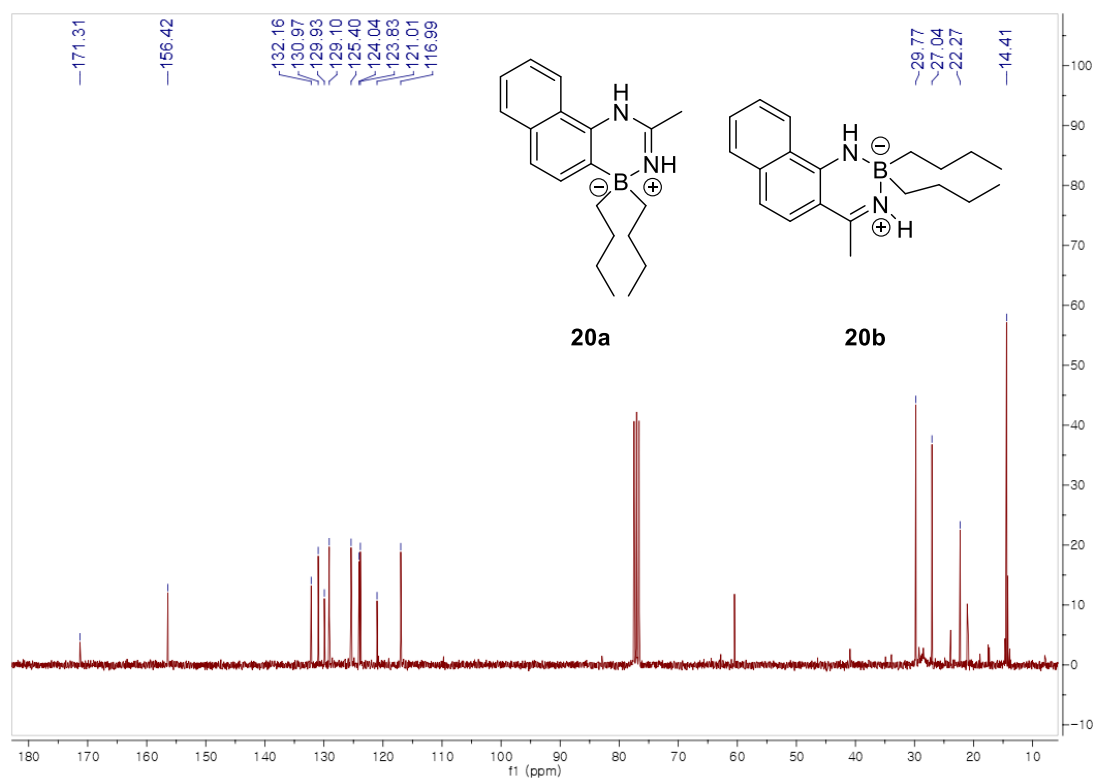


Figure 6.15. ^{13}C NMR data of the naphthodiazaborinine **20a** or **20b**.in CDCl_3 (Solvent residual peak: 77.2 ppm).

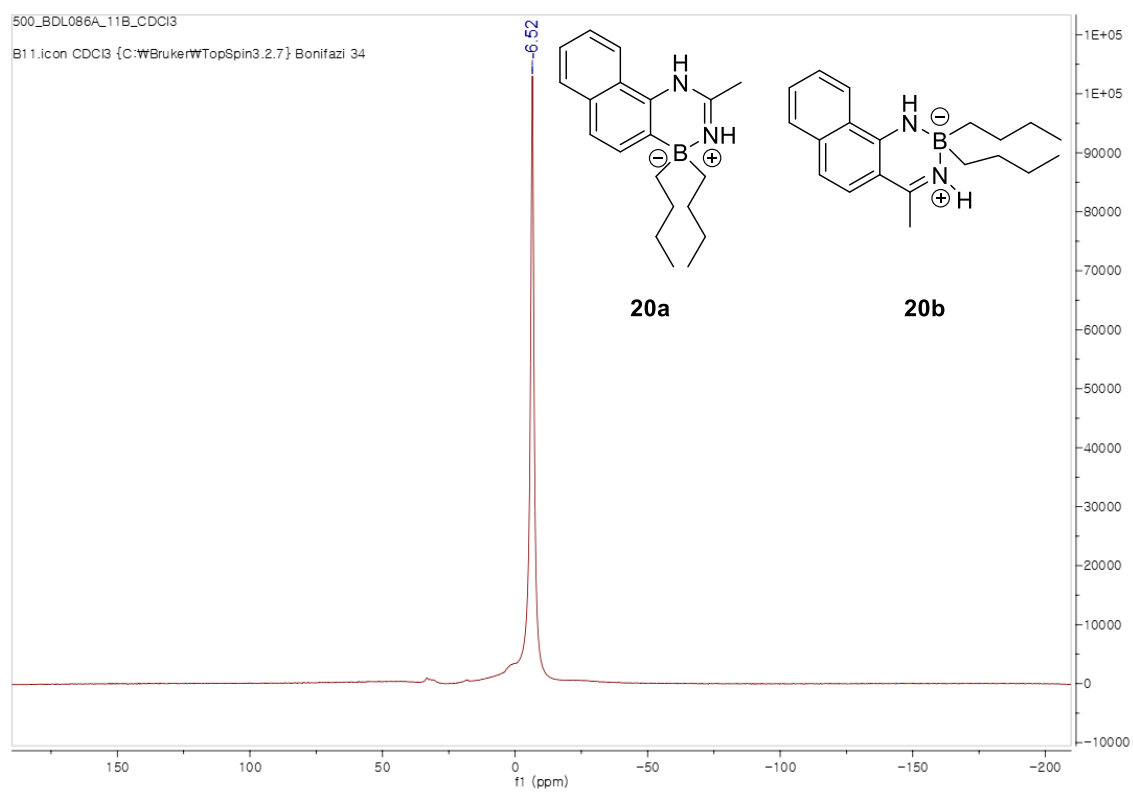


Figure 6.16. ^{11}B NMR data of the naphthodiazaborinine **20a** or **20b**.in CDCl_3

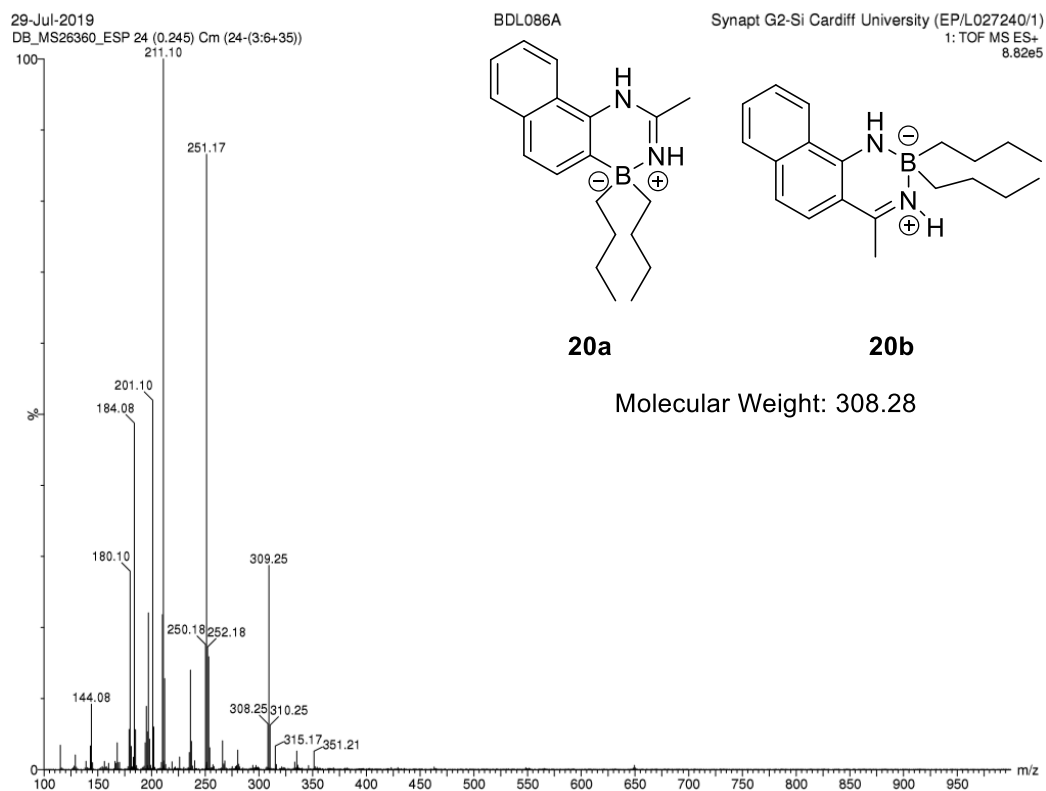


Figure 6.17. MS spectrometry data of the naphthodiazaborinine **20a** or **20b**.

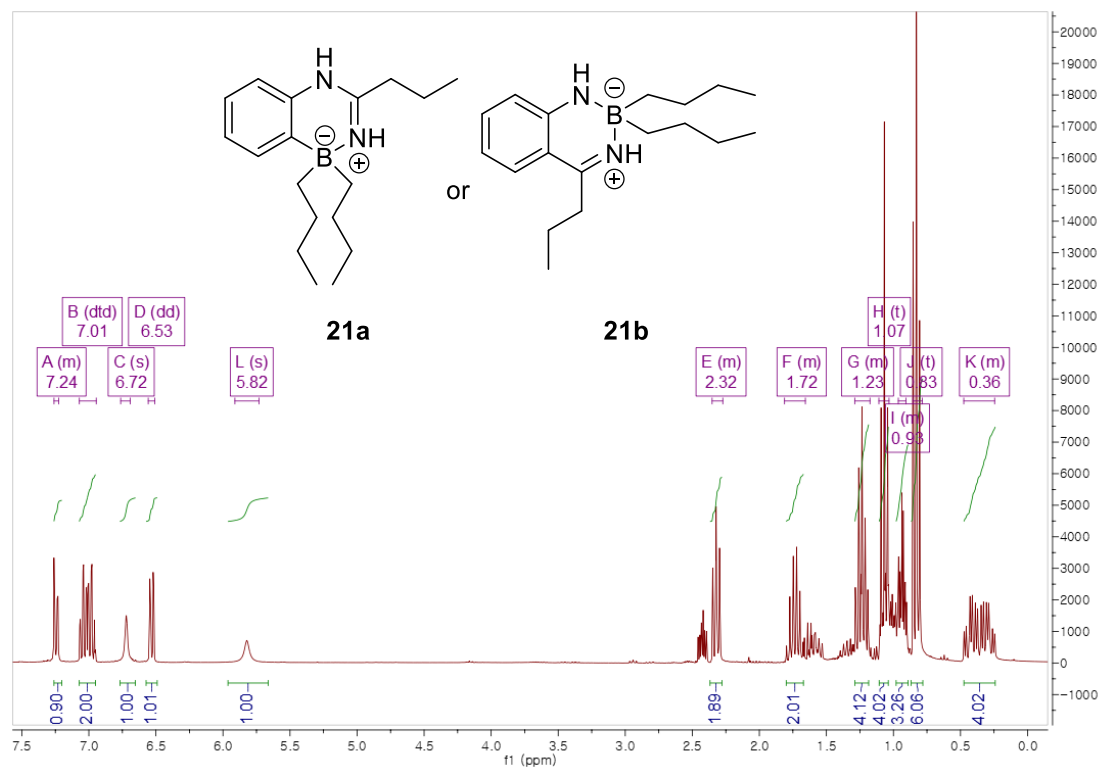


Figure 6.18. ^1H NMR of the dibutyl propyl dihydro diazaborinine **21a** or **21b** in CDCl_3 (Solvent residual peak: 7.26 ppm).

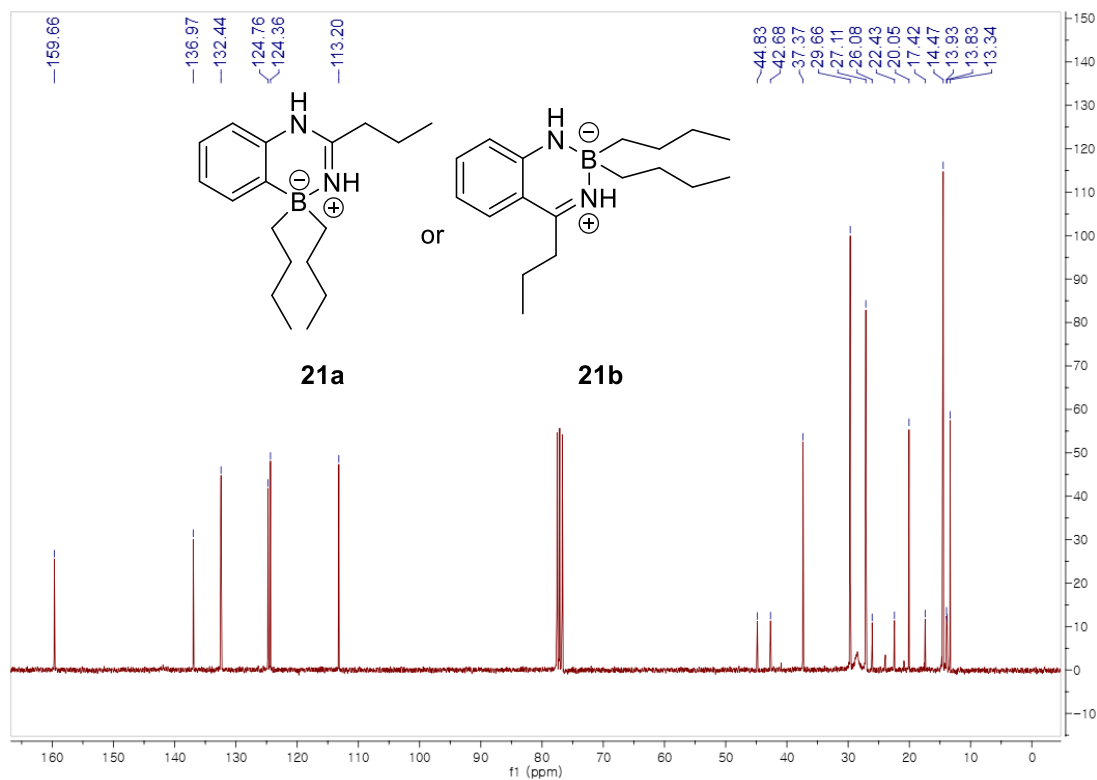


Figure 6.19. ^{13}C NMR of the dibutyl propyl dihydro diazaborinine **21a** or **21b** in CDCl_3 (Solvent residual peak: 77.2 ppm).

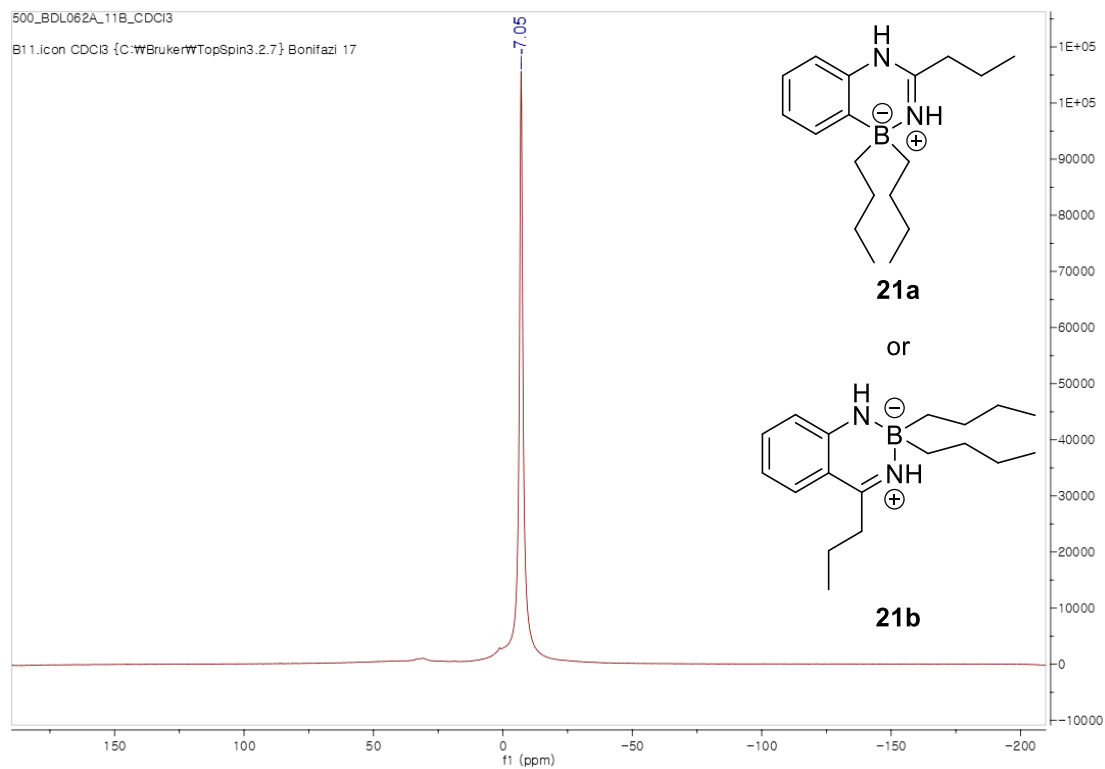


Figure 6.20. ^{11}B NMR of the dibutyl propyl dihydro diazaborinine **21a** or **21b**.

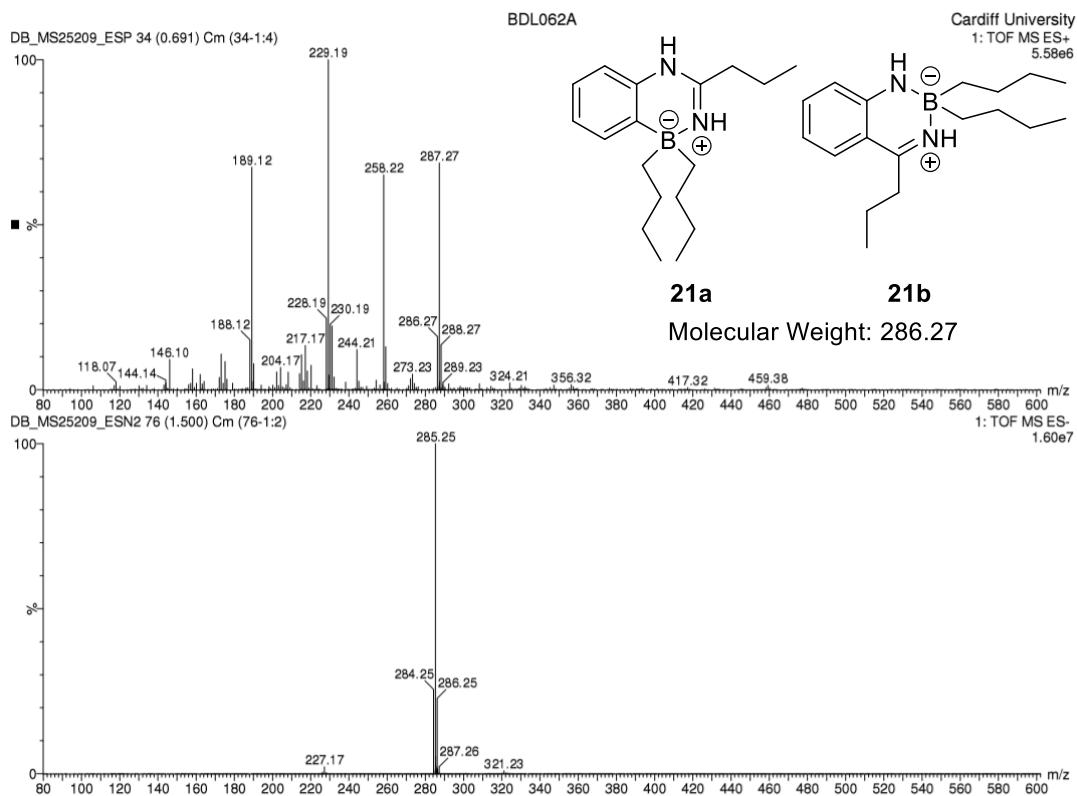


Figure 6.21. MS spectrometry data of the dibutyl propyl dihydro diazaborinine **21a** or **21b**.

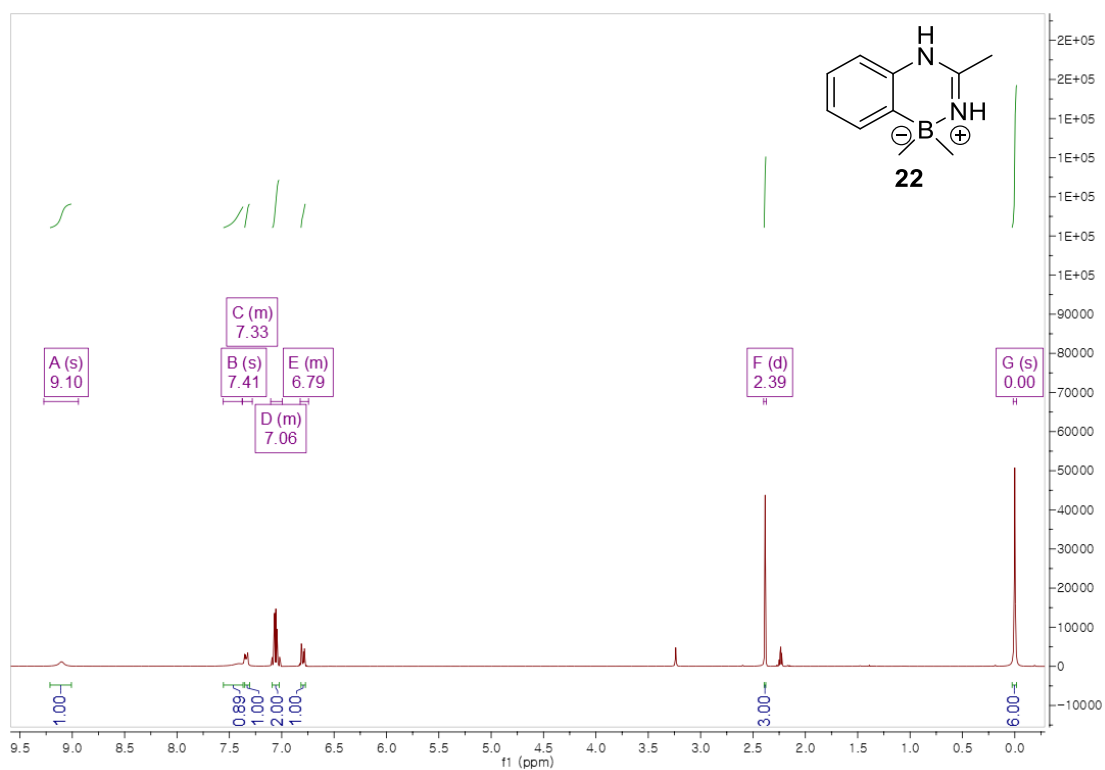


Figure 6.22. ^1H NMR of the trimethyl dihydro diazaborinine **22** in acetone (Solvent residual peak: 2.05 ppm).

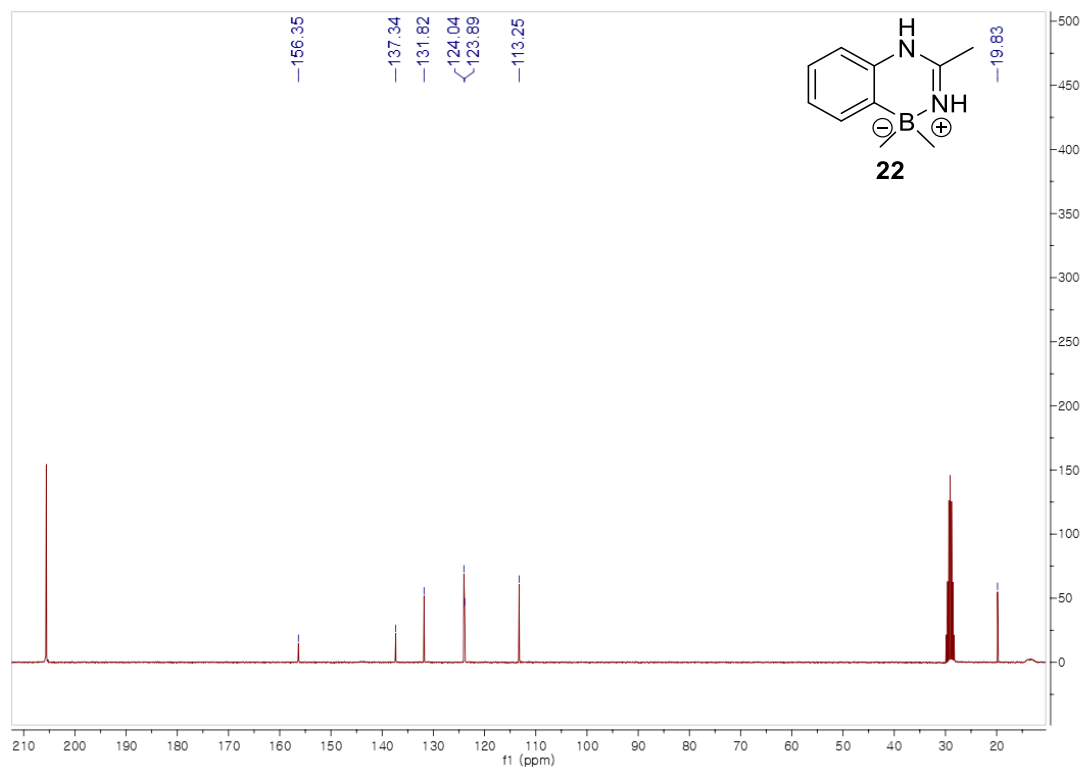


Figure 6.23. ^{13}C NMR of the trimethyl dihydro diazaborinine **22** in acetone (Solvent residual peak: 29.9 and 206.7 ppm).

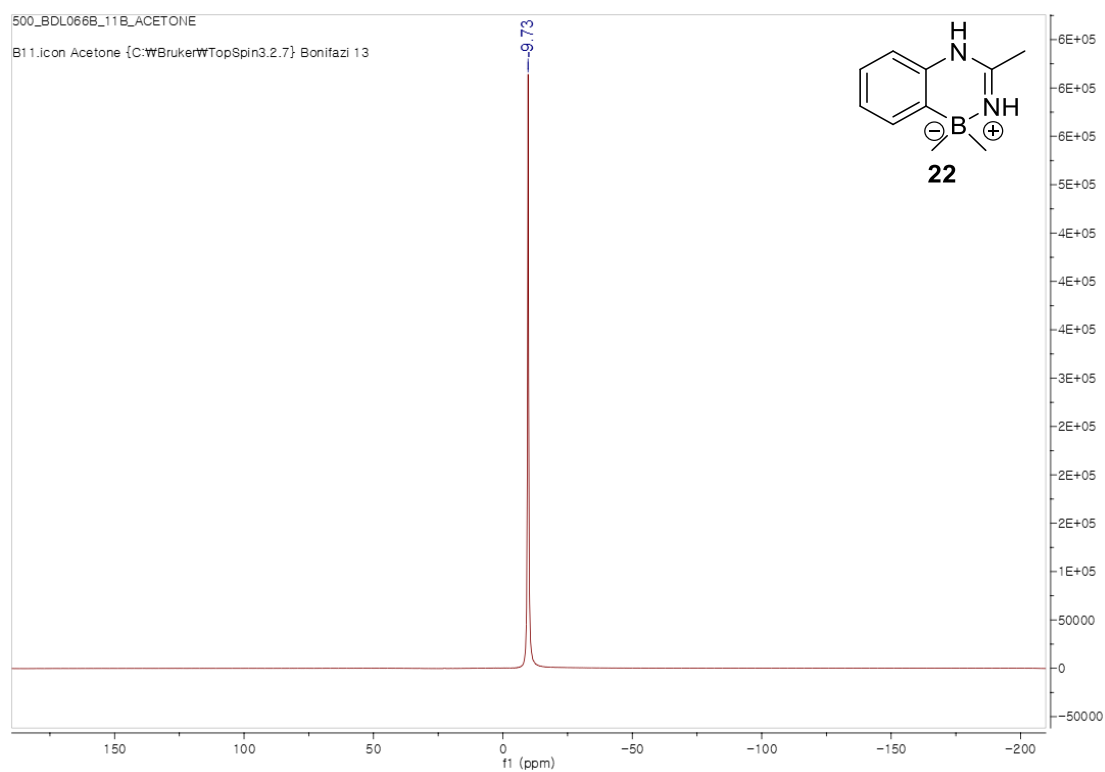


Figure 6.24. ^{11}B NMR of the trimethyl dihydro diazaborinine **22**.

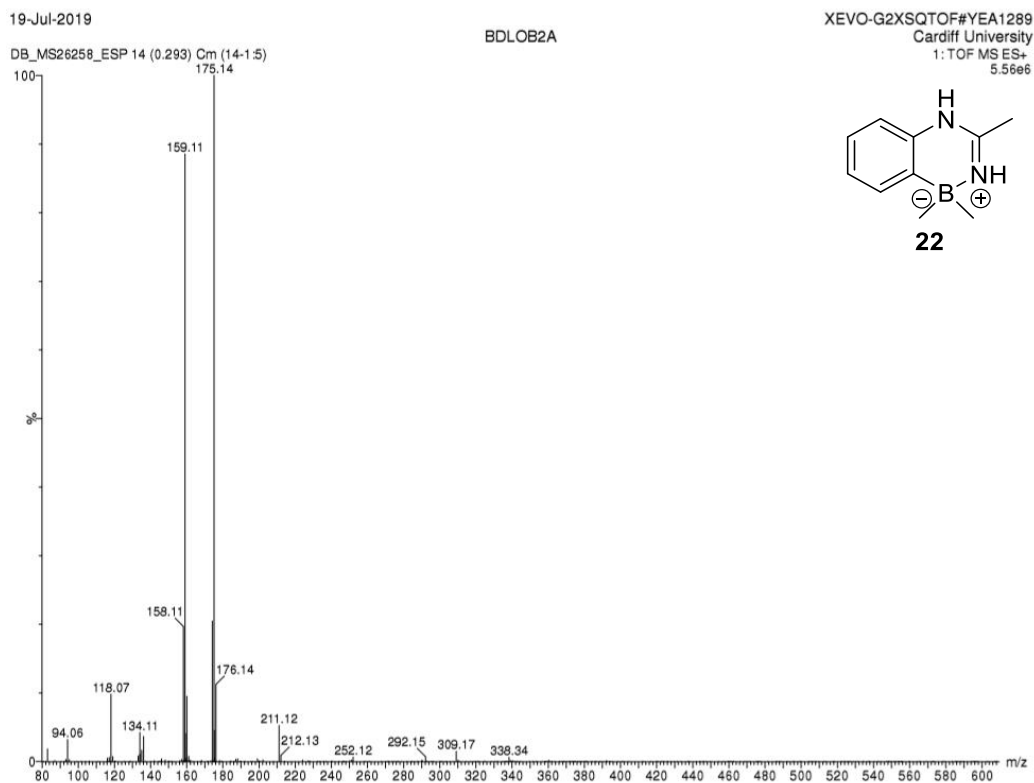


Figure 6.25. MS spectrometry data of the trimethyl dihydro diazaborinine **22**.

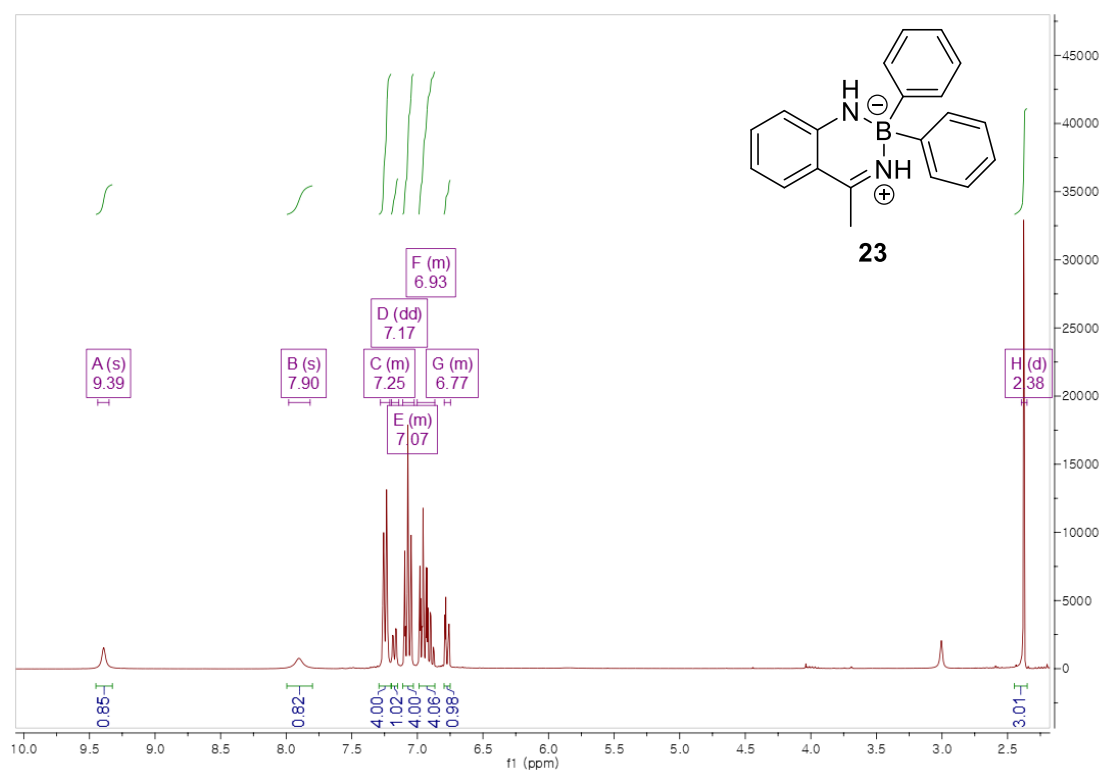


Figure 6.26. ^1H NMR of the methyl diphenyl dihydro diazaborinine **23** in acetone (Solvent residual peak: 2.05 ppm).

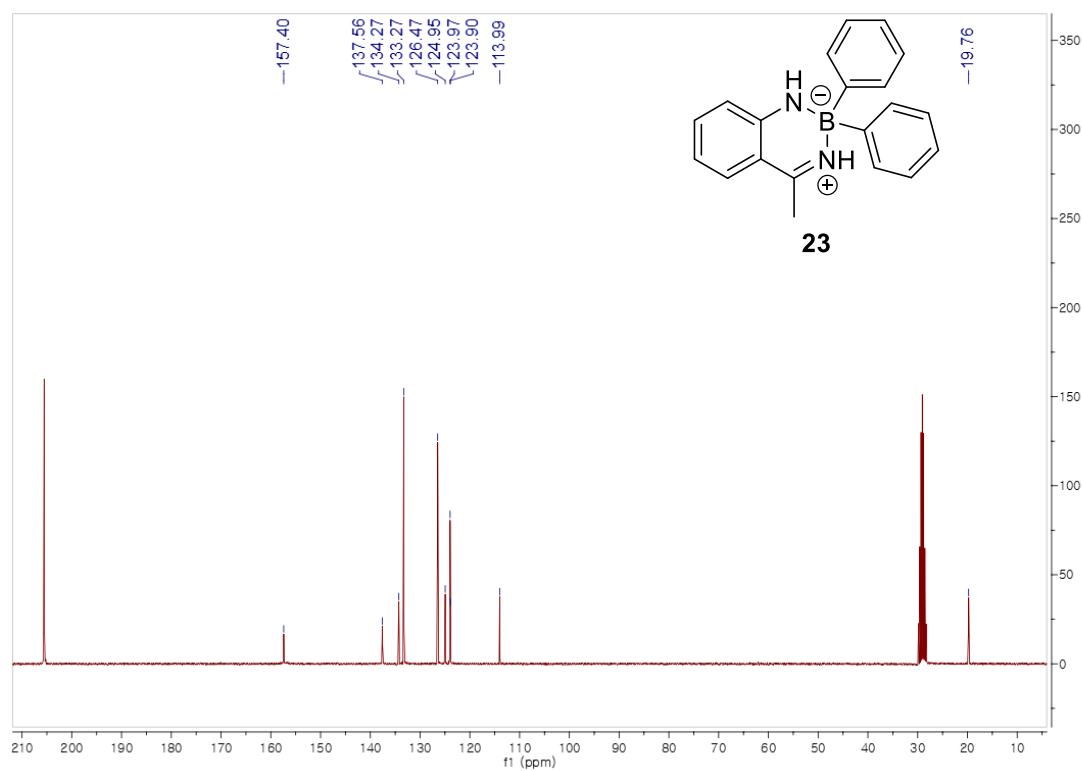


Figure 6.27. ^{13}C NMR of the methyl diphenyl dihydro diazaborinine **23** in acetone (Solvent residual peak: 29.9 and 206.7 ppm).

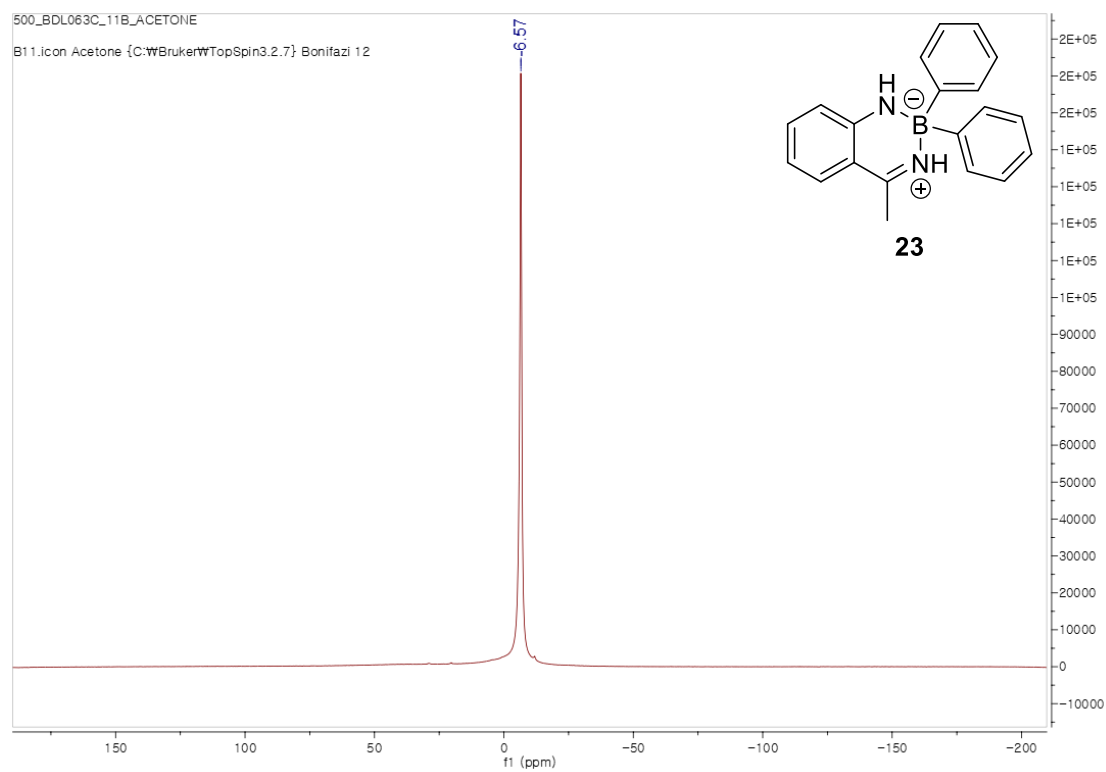


Figure 6.28. ^{11}B NMR of the methyl diphenyl dihydro diazaborinine **23**.

03-Apr-2019

BDL053B

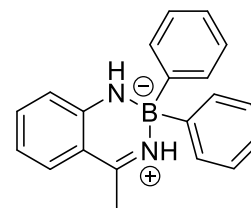
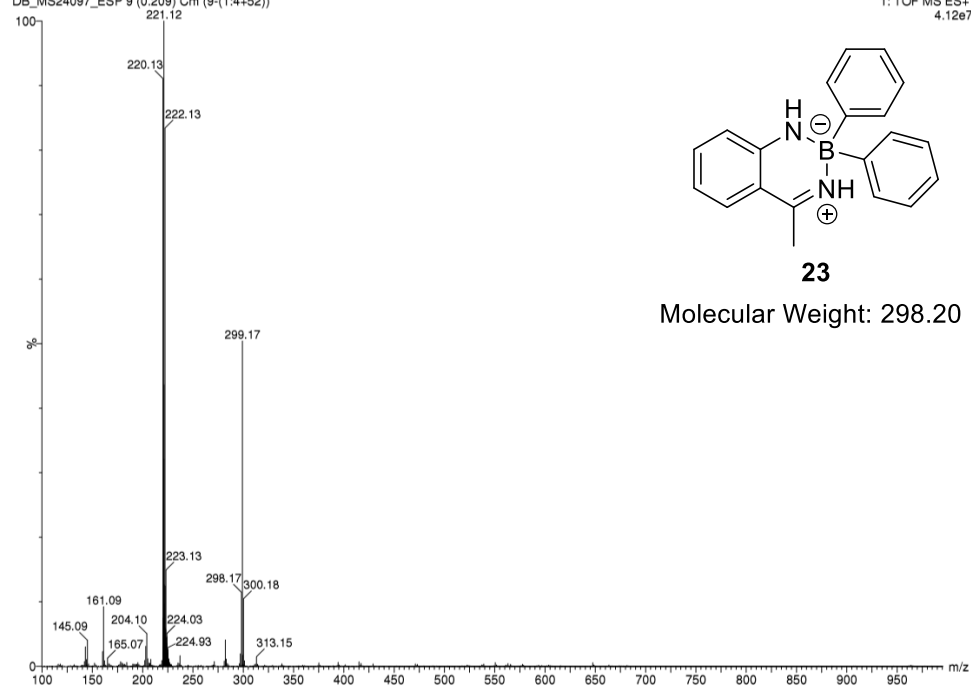
XEVO-G2XSQTOF#YEA1289

Cardiff University

1: TOF MS ES+

4.12e7

DB_MS24097_ESP 9 (0.209) Cm (9-(1.4+52))



23

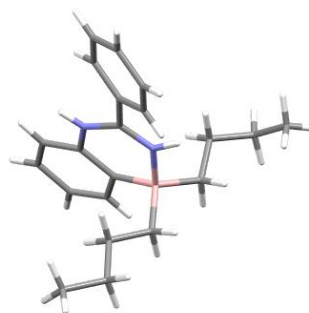
Molecular Weight: 298.20

Figure 6.29. MS spectrometry data of the methyl diphenyl dihydro diazaborinine **23**.

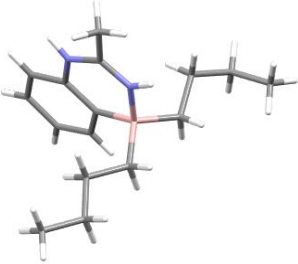
6.4. X-ray data

Crystal data and structure refinement of **11b**

| | | |
|-----------------------------------|--|-----------------|
| Identification code | shelx | |
| Empirical formula | C ₂₀ H ₁₉ B N ₂ | |
| Formula weight | 298.18 | |
| Temperature | 298(2) K | |
| Wavelength | 1.54184 Å | |
| Crystal system | Triclinic | |
| Space group | P -1 | |
| Unit cell dimensions | a = 9.1743(12) Å | a = 4.887(13)°. |
| | b = 9.7173(10) Å | b = 3.805(12)°. |
| | c = 11.0047(18) Å | g = 9.804(11)°. |
| Volume | 832.8(2) Å ³ | |
| Z | 2 | |
| Density (calculated) | 1.189 Mg/m ³ | |
| Absorption coefficient | 0.528 mm ⁻¹ | |
| F(000) | 316 | |
| Crystal size | 0.252 x 0.155 x 0.082 mm ³ | |
| Theta range for data collection | 4.442 to 72.847°. | |
| Index ranges | -10<=h<=11, -9<=k<=12, -13<=l<=12 | |
| Reflections collected | 5461 | |
| Independent reflections | 3173 [R(int) = 0.0202] | |
| Completeness to theta = 67.684° | 99.3 % | |
| Refinement method | Full-matrix least-squares on F ² | |
| Data / restraints / parameters | 3173 / 0 / 209 | |
| Goodness-of-fit on F ² | 1.054 | |
| Final R indices [I>2sigma(I)] | R1 = 0.0511, wR2 = 0.1475 | |
| R indices (all data) | R1 = 0.0661, wR2 = 0.1616 | |
| Extinction coefficient | n/a | |
| Largest diff. peak and hole | 0.193 and -0.229 e.Å ⁻³ | |

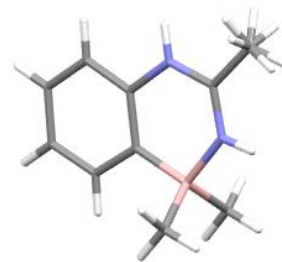


Crystal data and structure refinement of **13**

| | | |
|-----------------------------------|--|---|
| Identification code | shelx | |
| Empirical formula | C ₁₆ H ₂₇ B N ₂ |  |
| Formula weight | 258.20 | |
| Temperature | 150(2) K | |
| Wavelength | 0.71073 Å | |
| Crystal system | Monoclinic | |
| Space group | P 21/n | |
| Unit cell dimensions | a = 8.4152(6) Å | a = 90°. |
| | b = 10.2207(7) Å | b = 92.064(7)°. |
| | c = 18.4781(13) Å | g = 90°. |
| Volume | 1588.26(19) Å ³ | |
| Z | 4 | |
| Density (calculated) | 1.080 Mg/m ³ | |
| Absorption coefficient | 0.062 mm ⁻¹ | |
| F(000) | 568 | |
| Crystal size | 0.306 x 0.244 x 0.174 mm ³ | |
| Theta range for data collection | 3.296 to 29.660°. | |
| Index ranges | -10 ≤ h ≤ 11, -13 ≤ k ≤ 9, -25 ≤ l ≤ 18 | |
| Reflections collected | 8534 | |
| Independent reflections | 3790 [R(int) = 0.0480] | |
| Completeness to theta = 25.242° | 99.7 % | |
| Refinement method | Full-matrix least-squares on F ² | |
| Data / restraints / parameters | 3790 / 0 / 183 | |
| Goodness-of-fit on F ² | 1.059 | |
| Final R indices [I > 2σ(I)] | R1 = 0.0866, wR2 = 0.2349 | |
| R indices (all data) | R1 = 0.1264, wR2 = 0.2623 | |
| Extinction coefficient | n/a | |
| Largest diff. peak and hole | 0.369 and -0.265 e.Å ⁻³ | |

Crystal data and structure refinement of **22**

| | | |
|-----------------------------------|--|----------|
| Identification code | shelx | |
| Empirical formula | C ₁₀ H ₁₅ B N ₂ | |
| Formula weight | 174.05 | |
| Temperature | 200(2) K | |
| Wavelength | 1.54184 Å | |
| Crystal system | Orthorhombic | |
| Space group | P n m a | |
| Unit cell dimensions | a = 15.6474(11) Å | a = 90°. |
| | b = 6.9455(5) Å | b = 90°. |
| | c = 9.3322(7) Å | g = 90°. |
| Volume | 1014.21(13) Å ³ | |
| Z | 4 | |
| Density (calculated) | 1.140 Mg/m ³ | |
| Absorption coefficient | 0.511 mm ⁻¹ | |
| F(000) | 376 | |
| Crystal size | 0.423 x 0.307 x 0.117 mm ³ | |
| Theta range for data collection | 5.520 to 73.010°. | |
| Index ranges | -14 ≤ h ≤ 19, -8 ≤ k ≤ 8, -7 ≤ l ≤ 11 | |
| Reflections collected | 2351 | |
| Independent reflections | 1064 [R(int) = 0.0218] | |
| Completeness to theta = 67.684° | 99.5 % | |
| Refinement method | Full-matrix least-squares on F ² | |
| Data / restraints / parameters | 1064 / 0 / 78 | |
| Goodness-of-fit on F ² | 1.053 | |
| Final R indices [I > 2σ(I)] | R1 = 0.0494, wR2 = 0.1369 | |
| R indices (all data) | R1 = 0.0566, wR2 = 0.1464 | |
| Extinction coefficient | n/a | |
| Largest diff. peak and hole | 0.382 and -0.190 e.Å ⁻³ | |



Crystal data and structure refinement of **23**

| | | |
|-----------------------------------|--|-----------------|
| Identification code | shelx | |
| Empirical formula | C ₂₀ H ₁₉ B N ₂ | |
| Formula weight | 298.18 | |
| Temperature | 298(2) K | |
| Wavelength | 1.54184 Å | |
| Crystal system | Triclinic | |
| Space group | P -1 | |
| Unit cell dimensions | a = 9.1743(12) Å | a = 4.887(13)°. |
| | b = 9.7173(10) Å | b = 3.805(12)°. |
| | c = 11.0047(18) Å | g = 9.804(11)°. |
| Volume | 832.8(2) Å ³ | |
| Z | 2 | |
| Density (calculated) | 1.189 Mg/m ³ | |
| Absorption coefficient | 0.528 mm ⁻¹ | |
| F(000) | 316 | |
| Crystal size | 0.252 x 0.155 x 0.082 mm ³ | |
| Theta range for data collection | 4.442 to 72.847°. | |
| Index ranges | -10 ≤ h ≤ 11, -9 ≤ k ≤ 12, -13 ≤ l ≤ 12 | |
| Reflections collected | 5461 | |
| Independent reflections | 3173 [R(int) = 0.0202] | |
| Completeness to theta = 67.684° | 99.3 % | |
| Refinement method | Full-matrix least-squares on F ² | |
| Data / restraints / parameters | 3173 / 0 / 209 | |
| Goodness-of-fit on F ² | 1.054 | |
| Final R indices [I > 2σ(I)] | R1 = 0.0511, wR2 = 0.1475 | |
| R indices (all data) | R1 = 0.0661, wR2 = 0.1616 | |
| Extinction coefficient | n/a | |
| Largest diff. peak and hole | 0.193 and -0.229 e.Å ⁻³ | |

